Chemical and physical properties of iron(III)-oxide hydrate

CHEMICAL AND PHYSICAL PROPERTIES OF IRON (III)-OXIDE HYDRATE

A. A. van der GIESSEN

CHEMICAL AND PHYSICAL PROPERTIES OF IRON (III)-OXIDE HYDRATE

PROEFSCHRIFT

TER VERKRIJGING VAN DE GRAAD VAN DOCTOR IN DE TECHNISCHE WETENSCHAPPEN AAN DE TECHNISCHE HOGESCHOOL TE EINDHOVEN OP GEZAG VAN DE RECTOR MAGNIFICUS, DR. K. POSTHUMUS, HOOGLERAAR IN DE AFDELING DER SCHEIKUNDIGE TECHNOLOGIE, VOOR EEN COMMISSIE UIT DE SENAAT TE VERDEDIGEN OP DINSDAG 28 MEI 1968, DES NAMIDDAGS TE 4 UUR

DOOR

AART ANTONIE van der GIESSEN

SCHEIKUNDIG INGENIEUR

GEBOREN TE VLAARDINGEN

DIT PROEFSCHRIFT IS GOEDGEKEURD DOOR DE PROMOTOR
PROF. DR. G. C. A. SCHUIT

Aan mijn ouders
Aan Magda

CONTENTS

1. HYDROLYSIS IN SOLUTIONS OF IRON(III) NITRATE

1.1. Introduction

Precipitation of compounds in solutions usually leads to crystalline products with particles, of a shape and size depending upon the reaction conditions. A precipitate is formed when the solubility product is exceeded and when at the same time nuclei on which the crystals can grow are formed or are already present. Such a solution contains growing nuclei, together with the ions composing them. There are examples showing that precipitation in solutions does not lead to the formation of a crystalline product. For a number of ions such as Fe^{3+}, Al^{3+}, Cr^{3+}, the addition of OH^- ions to their aqueous solutions first gives rise to the formation of new products that remain in solution — in the case of Fe^{3+} ions this can already be derived from the darkening of the colour of the solution — and ultimately causes the formation of a gelatinous precipitate. Regarding the mechanism it was thought that a series of hydrolytic processes takes place, with the intermediate formation of polymeric ions, which finally unite to form the gelatinous precipitate. In the case of Fe^{3+} there is no general agreement in the literature with regard to the size and the composition of the polynuclear complexes.

According to various authors units of the type $Fe(OH)_n^{(3-n)+}$ are first formed which upon further addition of OH^- ions grow to larger complexes containing two or more Fe^{3+} ions. The size of the complex depends upon the hydrolysis conditions: both the concentration of the Fe(III) compound as well as that of OH^- ions are important. In very dilute solutions, with Fe(III) below 10^{-3} gion/l, only $Fe(OH)^{2+}$ complexes are formed as was concluded by Siddall and Vosburgh from spectrophotometric analysis [1-1]. In more concentrated solutions ($1\text{-}100.10^{-3}$ gion/l) dimers are also formed, according to Hedström [1-2]. The relation between the Fe^{3+} concentration (determined with the aid of redox-potential measurements of the system Fe^{3+}/Fe^{2+}) and the pH is such that the hydrolysis equilibria:

$$nFe^{3+} + mH_2O \rightleftarrows Fe_n(OH)_m^{(3n-m)+} + mH_3O^+$$

can be described with values for n equal to unity or two (formation of monomers and dimers). Mulay and Selwood investigated similar solutions by magnetic measurements [1-3]. These investigators found on increasing pH a considerable decrease in the magnetization (at constant field strength) between pH 1 and 2. Assuming a Curie law, a decrease in the magnetic moment per Fe^{3+} ion from 5·8 to 3·6 μ_B at pH = 1·5 was calculated. This was explained by the formation of a diamagnetic dimer (of zero moment) following the example of Hedström. These dimers, at the pH of precipitation, then unite to form the gelatinous precipitate.

The results of Selwood and Hedström are not in accordance with earlier results of Jander and Winkel [1-4]). These authors estimated the molecular weight of the particles present in hydrolyzed $Fe(ClO_4)_3$ solutions in the pH region 1-3, with the aid of measurements of the diffusion coefficient. In 0·1-molar solutions, at pH = 2, a considerable decrease in the diffusion velocity was observed, indicating the formation of larger particles. The molecular weights of these particles depend upon the pH. Assuming that, in solutions with pH < 1 only the ions $FeClO_4^{2+}$ are present (molecular weight about 250) and that the relation $D\sqrt{M}$ = constant is valid, they concluded that at pH = 3 polynuclear particles with a molecular weight of 5000 would be present. Recently Spiro et al., by ultracentrifuging partially hydrolyzed Fe^{3+} solutions, concluded the presence of even much larger particles with a size of 70 Å [1-5]).

There is apparently no consensus of opinion in the literature regarding the structure and the size of the species formed upon the hydrolysis. In our opinion this is not surprising as the measurements do not refer to equilibria: the results discussed are all obtained on supersaturated solutions. This immediately appears on checking the experimental conditions against the values of the solubility product of "$Fe(OH)_3$". The latter equals $10^{-38{\cdot}7}$, as determined by Biedermann and Schindler for solutions of $Fe(ClO_4)_3$ with the same ionic strength as those discussed above [1-6]). In view of this it is not surprising that a precipitate is formed in such supersaturated solutions in course of time. Feitknecht and Michaelis [1-7]) investigated such precipitates formed in solutions similar to those studied by Hedström, after the solution had stood at room temperature for a long time. The precipitates were isolated from the solution by ultracentrifugating and they appeared to consist of a mixture of needles of α-FeOOH and spherical particles of 50-70 Å.

Mechanism of hydrolysis

A summary of the literature in which possible mechanisms of the hydrolysis are discussed has been given by Rollinson [1-8]). In aqueous solution the Fe^{3+} ion is hydrated; the coordination sphere contains six H_2O molecules forming an octahedron. Strongly acidic solutions of Fe(III) salts contain the complexes $Fe(H_2O)_6^{3+}$. These complexes react as an acid by donation of a proton:

$$Fe(H_2O)_6^{3+} + H_2O \rightleftarrows [Fe(H_2O)_5(OH)]^{2+} + H_3O^+.$$

Addition of hydroxyl ions displaces this equilibrium to the right. The monomers can give dimers by the formation of OH bridges:

$$2\,[Fe(H_2O)_5(OH)]^{2+} \rightleftarrows \left[(H_2O)_4\,Fe\begin{matrix}\diagup\,H\,O\,\diagdown\\ \diagdown\,O\,H\,\diagup\end{matrix}Fe(H_2O)_4\right]^{4+} + 2\,H_2O.$$

This reaction is designated by the term olation. The dimer in turn can split off protons according to

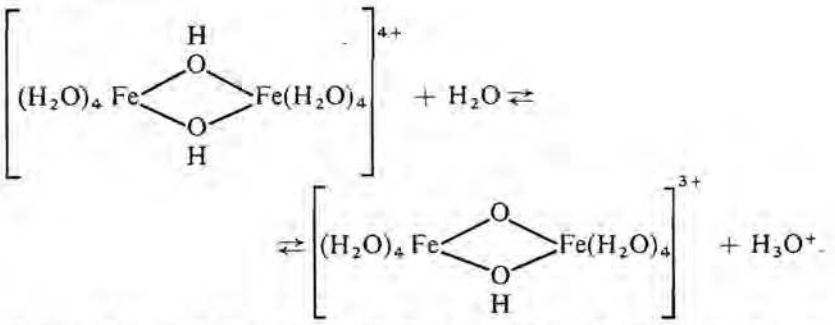

This is called oxolation; the Fe-O-Fe bond is called an oxo bridge. These reactions which give rise to a decrease of the pH proceed slowly. This applies especially to the oxolation reaction. The final result of these deprotonizing processes is the formation of polynuclear species, linear macromolecules (or ions) as well as chains with side branches (not depicted in the scheme). The reactions are reversible on decreasing pH but it is thought that it is particularly the oxo bridge that is difficult to break. As a consequence a precipitated oxide-hydroxide only very slowly redissolves upon the addition of acid.

According to the ideas discussed above the gels are the final products of hydrolytic processes and they consist of a network of polynuclear complexes linked up by -O- and -OH bridges.

Anions largely influence the process of hydrolysis. Anions, such as SO_4^{2-} which are able to give a coordination bond with the cation may replace H_2O as well as OH^-. This can be perceived from an increase in the pH on addition of Na_2SO_4 to a partially hydrolyzed solution of $Fe(NO_3)_3$. The addition of SO_4^{2-} ions also causes the formation of a precipitate, probably consisting of basic sulphates [1-9,10]; a precipitate is also observed [1-11] after addition of PO_4^{3-}.

Reaction rates and hydrolysis equilibria

It is stated repeatedly in the literature that after a rapid initial reaction the subsequent hydrolytic processes occurring in Fe^{3+} solutions are slow. At room temperature, after the addition of OH^- ions, it takes hundreds of hours before a constant pH value is reached. These slow pH changes are one of the main experimental facts underlying the olation-oxolation reactions mentioned above. It is not necessary, however, to assume the gradual formation of large polymers as the cause of these pH changes. Weiser and Milligan assume that, upon the hydrolysis of Fe(III) or Al(III) salts crystalline particles are formed, albeit of exceedingly small size compared to that of crystals formed in most other well-known precipitation reactions [1-12,13,14]. Their arguments, in favour

of crystallites, are, however, questionable. Yet the idea may be correct. It has been shown by Onoda and De Bruyn that in aqueous suspension coarse crystals of α-Fe_2O_3, after the addition of acid or base, also give rise to similar retarded changes in the pH, due to the slow diffusion of protons from the surface towards the inside of the crystals [1-15] (see also ref. 1–16). Hence the slow diffusion of protons from the inside of a crystalline material via its surface to the solution could also be a possible reason for the slow pH changes instead of the slowly proceeding olation-oxolation reactions. This mechanism only applies if indeed crystallites are formed upon hydrolysis. As no visible precipitate is formed as long as $OH^-/Fe^{3+} < 2{\cdot}5$ these then must be very small. A diminishing initially present disorder or a slow growth of these small particles could act as the driving forces of the donation of protons to the solution.

In the following sections a number of experiments will be discussed which have been carried out in order to obtain a better knowledge of the hydrolysis phenomena of Fe^{3+} ions. These experiments are all done with NO_3^--containing solutions. The reason for this is that NO_3^- (just as ClO_4^-) has only a weak affinity to the Fe^{3+} coordination shell (contrary to Cl^- and SO_4^{2-} ions) and thus secondary effects caused not by the OH^- ions but by the other ligands are avoided.

1.2. Reaction rates and hydrolysis equilibria

1.2.1. *Experimental*

The $Fe(NO_3)_3$ solutions are hydrolyzed by adding NaOH, 1 molar, from a burette at a rate of one drop per second with vigorous agitation, until the desired OH^-/Fe^{3+} ratio is reached. Solutions containing 0·10 mole/l $Fe(NO_3)_3$ (Merck, p.a.) and 2·8 mole/l $NaNO_3$ (U.C.B., p.a.) are prepared by dissolving the appropriate amounts of these compounds in distilled water. From this solution 100 ml is brought into a 250-ml beaker placed in a thermostat kept at 25 °C. The beaker is covered by a rubber plug in which the pH electrodes and the stirrer lead are fastened. The tap end of the burette protrudes into a spare hole lined with a glass tube. Through this also the nitrogen escapes which is bubbled through the solution at a rate of 100 ml/min. The pH is measured by means of a Philips G.A. 110 glass electrode and a saturated-calomel reference electrode.

For another series of experiments the amount of $Fe(NO_3)_3$ is varied so that $[Fe^{3+}]$ varies between 200.10^{-3} and 1 gion/l, whereas the pH is brought to the same value of 2·20. In order to obtain the same pH in all cases, either 0·1-molar NaOH or HNO_3 is added.

In a number of experiments, after establishing a certain OH^-/Fe^{3+} ratio, to 100 ml of the Fe^{3+} solution an equal volume of a 0·1-molar Na_2SO_4 solution is added which is brought to the same pH as the hydrolyzed Fe^{3+} solution, with H_2SO_4. After this addition the pH is measured again.

Determination of the hydrolysis equilibria is carried out with the aid of titrations of the Fe^{3+} ions with the disodium salt of ethylene diamine tetra-acetic acid, EDTA, using KCNS as an indicator. Of the solution to be examined, 25 ml is pipetted into a conical flask of 100 ml. This is titrated by adding an EDTA solution, 0·05 or 0·1 molar, dropwise from a burette until nearly the equivalent point is reached which is indicated by the appearance of a precipitate. When about half of the necessary amount of EDTA is added, a precipitate already appears; it intensifies near the equivalence point. This precipitate is removed by centrifuging, after which about 20 mg of KCNS indicator is added to the clear yellow solution. The solution is then further titrated with EDTA solution until the red colour of the Fe-(CNS) complex disappears; because of the interference of yellowish colour of the solution with the red colour of the Fe-(CNS) complex the equivalence point is difficult to determine and it is necessary first to make a rough estimation of the amount of EDTA required.

A number of viscosity measurements are done, at 25 °C, using an Ubbelohde viscosimeter.

1.2.2. *Results and discussion*

Titration of iron nitrate with a base

A comparison of the titration curve of a solution of $Fe(NO_3)_3$ with that of a HNO_3 solution shows that the $Fe(H_2O)_6^{3+}$ ion behaves as a fairly strong acid. Figure 1.1 shows a titration curve of a 0·1-molar $Fe(NO_3)_3$ solution together with that of a 0·3-molar HNO_3 solution. Upon addition of OH^- ions the Fe^{3+} solution becomes darker but no visible precipitate appears until about 2·5 OH^-

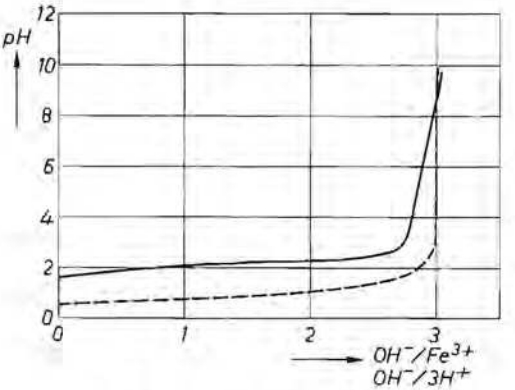

Fig. 1.1. Titration curves of
———— 0·1-molar $Fe(NO_3)_3$,
- - - - - - - - - 0·3-molar HNO_3.

ions are added per Fe^{3+} ion. Then the solution suddenly stiffens and a precipitate appears which forms a gelatinous mass. The fact that the gelatinous precipitate is formed in a small pH range can be demonstrated more precisely with measurements of the viscosity, as is shown in fig. 1.2. After the addition of OH^- ions the pH does not remain constant but slowly decreases until after several hundred hours a constant value is reached. Addition of alkali followed by an immediate back titration with HNO_3 gives hysteresis; even after several hours the pH of the solution does not regain the same value belonging to a certain ratio OH^-/Fe^{3+} when coming directly from the acid side (fig. 1.3). Evidently the reactions are slow.

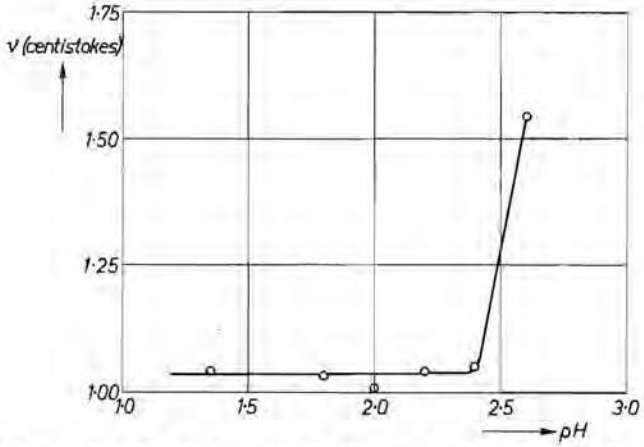

Fig. 1.2. The dependence of the viscosity on the pH of a solution containing 0·08 mole/l $Fe(NO_3)_3$ and 2·8 mole/l $NaNO_3$.

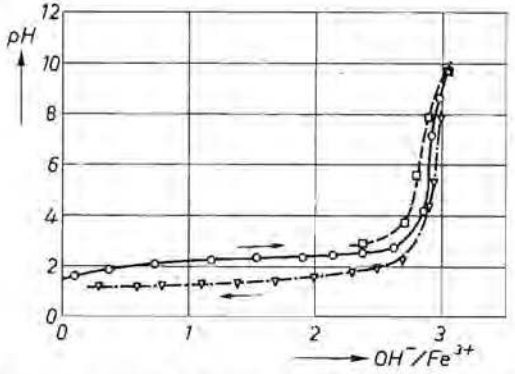

Fig. 1.3. Titration curves of a solution containing 0·1 mole/l $Fe(NO_3)_3$;
○ titration of Fe^{3+} with OH^-,
△ back titration with HNO_3,
□ pH after addition of a Na_2SO_4 solution.

The concentration of the NO_3^- ions is of only minor importance: the titration curve of a 0·1-molar $Fe(NO_3)_3$ solution which is 2·8 molar in $NaNO_3$ is only slightly shifted to the left for values of $OH^-/Fe^{3+} \approx 2{\cdot}5$ (fig. 1.4) compared to a solution of the same strength to which no $NaNO_3$ has been added. Nearly the same curves are obtained when two titrations are carried out, one by continuously dropping the NaOH into the solution and one by waiting four minutes after each ml NaOH added. When instead of 1-molar NaOH, 10-molar NaOH is used as a titrating agent the curve is shifted slightly to the left (not shown).

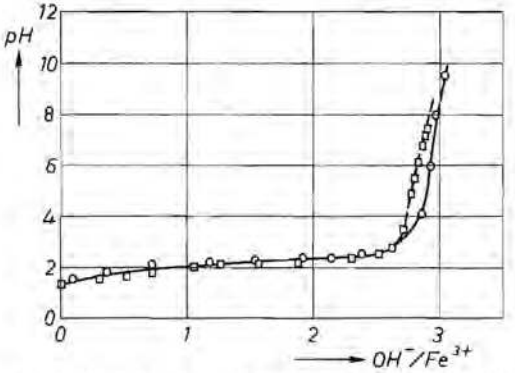

Fig. 1.4. A comparison of the titration curves of $Fe(NO_3)_3$;
○ 0·1-mole/l $(FeNO_3)_3$,
□ 0·1-mole/l $Fe(NO_3)_3$ + 3-mole/l $NaNO_3$.

Ligands which are able to form complexes with the Fe^{3+} ions, contrary to NO_3^- ions, influence the hydrolysis processes. Addition of a solution of Na_2SO_4 of the same pH as a hydrolyzed Fe^{3+} solution gives a marked increase in the pH (fig. 1.3) under the simultaneous formation of a precipitate. This proves that the SO_4^{2-} ions liberate OH^- ions from the species which are formed upon hydrolysis.

The sudden formation of a gel suggests that we are dealing here with the flocculation of a colloidal precipitate. This flocculate then consists of an agglomerate formed by either the polynuclear chains as described by the olation-oxolation theory or by small crystallites. In this study it will be shown that the latter possibility is the case: crystallites are formed on addition of OH^- ions and remain in colloidal solution until, due to a further addition of OH^- ions the point of electroneutrality is reached and flocculation occurs.

Determination of the hydrolysis equilibria

A chemical method has been used for the determination of the concentration of the Fe^{3+} ions in equilibrium with the larger units present in the solution as a result of the hydrolysis. It has been found that, under our experimental con-

ditions, the Fe^{3+} ions can be determined by the conventional titration with a solution of the disodium salt of ethylene diamine tetraacetic acid (EDTA); KCNS is used as an indicator. The titration of Fe^{3+} ions with the complexing agent is well known, see for instance ref. 1–17; a more detailed discussion regarding the theoretical background of this titration can be found in ref. 1–18. For the present case we used this method also for partially hydrolyzed solutions, under the assumption that at least all monomeric species of the type $Fe(OH)_n^{(3-n)+}$ react under the formation of a complex with the EDTA and that polynuclear ionic complexes or particles do not consume EDTA, an assumption justified by the results. This titration of Fe^{3+} in partly hydrolyzed solutions is possible due to the slow rate at which the hydrolysis processes occur: if the Fe^{3+} ions are removed from the solution by complexing them with EDTA, Fe^{3+} ions are only slowly liberated from the larger complexes.

It has been found that, in hydrolyzed solutions, the concentration of free Fe^{3+} ions is only a fraction of the total amount of iron present and independent of the total Fe(III) concentration at constant pH. This is illustrated with the data listed in table 1-I obtained with solutions of pH = 2·30. After one hour the equilibrium concentration is about 3.10^{-3} gion/l. This corresponds to a solubility product K_s of $3.10^{-3} \times 10^{-35.7} = 10^{-38.2}$ ($pK\ H_2O = 14{\cdot}22$). A solubility product of about the same numerical value can be calculated from Fe^{3+} titrations of about 0·08-molar $Fe(NO_3)_3$ solutions with different pH's, table 1-II. The results are related to solutions obtained after the addition of 0, 1, 2 and 2·6 OH^-/Fe^{3+}, respectively. The value of the solubility product is not entirely constant. The concentration of Fe^{3+} ions gradually decreases with

TABLE 1-I

Concentration (mgion/l) of Fe^{3+} ions which can be complexed with EDTA [Fe^{3+}]. All solutions contain 2·8 mole $NaNO_3$/l. One hour after the preparation the pH = 2·30. Determinations have been done 1, 24 and 200 hours after the preparation

[Fe(III)]	[Fe^{3+}] (mgion/l)		
(mmole/l)	1 h	24 h	200 h
220	—	2·0	—
80	3·0	2·5	0·6
45	2·0	2·4	—
25	2·4	1·5	0·6
5	3·8	1·9	—
1	0·5	0·5	0·4

TABLE 1-II

Concentration of Fe^{3+} ions, which can be complexed with EDTA in solutions containing about 0·08 mole/l Fe(III) as a function of the pH. All solutions contain 2·8 mole/l $NaNO_3$. Measurements are carried out one hour after precipitation

[Fe(III)] (mole/l)	[Fe^{3+}] (mgion/l)	pH	pK_s
100	100	1·24	—
91	71	1·68	38·8
83	21	1·89	38·7
80	3	2·32	38·2

the time and so does the pH: after 48 hours the pK_s value equals 39·2. This value lies intermediate between the pK_s values of freshly precipitated "$Fe(OH)_3$" as found by Biedermann, viz. 38·7, and that of the stable phase α-FeOOH, p$K_s = 41$, which after prolonged standing is formed in acid solutions, as found by Feitknecht et al. [1–19]). The existence of a constant solubility product, independent of the total Fe(III) concentration and pH, suggests that we are dealing with a solubility equilibrium in which the Fe^{3+} concentration is determined by a solid phase, in equilibrium with the solution. As the solutions under consideration contain no visible precipitate and can easily be poured through a filter, this second phase must consist of very small colloidal particles.

The titration experiments with EDTA give another indication for the presence of small colloidal particles: in partially hydrolized solutions, with $OH^-/Fe^{3+} > 1$, the addition of EDTA causes a precipitate. This precipitate contains one EDTA molecule per 10 to 30 Fe^{3+} ions if the solution is aged for one hour and one EDTA molecule per 50 to 100 Fe^{3+} ions after 24 hours. This can be understood by assuming that the addition of EDTA causes a flocculation of particles which were present in the solution. The EDTA present in the precipitate is then due to the fact that a small number of EDTA molecules will be adsorbed on the surface of the particle, the amount depending on the extent and the activity of the exposed surface. This is confirmed by an X-ray examination of such a precipitate ($OH^-/Fe^{3+} \approx 2$). It exhibits an X-ray diagram which has the same — albeit only the strongest — reflections as the gelatinous precipitate obtained on complete hydrolysis of the Fe^{3+} ions with OH^- ions, see chapter 4. From this the conclusion can be drawn that the EDTA-containing precipitate is crystalline. It is a further argument in favour of our thesis that the addition

of EDTA causes the flocculation of particles that are already present in the partially hydrolyzed solution.

1.3. Mechanism of the hydrolysis

1.3.1. *Introduction*

If the formation of a gel, as mentioned before, may be described as the flocculation of particles formed upon hydrolysis, a study of these particles can give some idea of the processes occurring when the $Fe(H_2O)_6^{3+}$ ions are deprotonized. Such a study can only be done provided that the particles can be isolated from the gel without changing their properties. This isolation necessarily involves a dehydration procedure; such a dehydration process, described in chapter 3, has been used for the study described in the next sections.

At this point we shall introduce the characterization with the aid of the magnetic susceptibility preceding a more detailed discussion in chapter 4. Ultrafine antiferromagnetic crystallites with a size below 50 Å — the type of material we are dealing with — are superparamagnetic. Powders composed of such particles have a magnetization which is linearly proportional to the field strength. The susceptibility is independent of the size of the particles as long as this is below 50 Å and depends only upon the disorder prevailing in the lattice. Based on this knowledge the data presented in the following can assist in a further elucidation of the hydrolysis mechanism and show in which respect Selwood's interpretation of the magnetic properties of hydrolyzed solutions fails.

1.3.2. *Experimental*

In series of experiments 0·1-molar solutions of $Fe(NO_3)_3$ are hydrolyzed with NaOH solutions varying in concentration (1·0, 3·7 and 9·7 molar) such that $OH^-/Fe^{3+} = 2{\cdot}41$, and kept at 25 °C under vigorous agitation for about half an hour, after which the hydrolyzed solutions are brought to pH = 7·5 with NaOH of the desired concentration again by addition at a rate of one drop per second and while stirring. The time between the addition of the first drop to the freshly prepared solution and the precipitation is 60 minutes. The resulting gel is kept for another five minutes in the precipitation vessel, with agitation, and afterwards the pH which has dropped slightly is readjusted. The gel is then placed on a filter, washed with one portion of water brought to pH = 7·5 with NH_4OH and further dehydrated in a manner described on page 21. The resulting oxide hydrate is dried on P_2O_5 to constant weight at room temperature which corresponds to a H_2O content of about 16%. The magnetic susceptibilities, measured according to a method described in ref. 1–20 are all reduced to water contents of 16·0%.

1.3.3. *Results and discussion*

A number of hydrolysis experiments have been done in such a way that a solution of NaOH is added dropwise to a solution of $Fe(NO_3)_3$ until $OH^-/Fe^{3+} = 2{\cdot}41$ (first stage). The solutions are then stirred for about half an hour (depending upon NaOH concentration) after which more base is added until pH = 7·5, which results in the formation of a gel. The experiments differ in that the concentration of the NaOH used in the second stage is different from that in the first stage. A number of precipitations have also been carried out in which in one run the pH is brought to pH = 7·5 without interruption. Measurements of the magnetic susceptibility of the samples thus prepared are made at room temperature using field strengths varying from 0 to 13 000 Oe. The results are collected in table 1-III. From the results it is clear that the concentration of the base influences the magnetic properties of the final products, but only in the first stage of the hydrolysis. Irrespective of the fact whether 9·7- or 1-molar NaOH is used for the flocculation, i.e. the second stage, when the hydrolysis in the first stage is carried out with 1-molar NaOH, the products have the same χ (samples B_1, B_4). The same value of the magnetization is found when the gel is precipitated directly (sample B_0). When NaOH solutions of varying strength are used in the first stage of the hydrolysis, even though 1-molar NaOH is used in all cases in the second stage, the χ values differ and are higher the higher the concentration of the NaOH used in the first stage (samples B_1, B_2 and B_3).

The differences in the magnetic properties of the precipitates related to the concentration of the NaOH used in the first stage are difficult to explain by assuming the formation of a series of polymers, or, as suggested by Selwood even of monomers and dimers only, the latter being diamagnetic. It could be that the dimers and perhaps also larger diamagnetic polynuclear complexes

TABLE 1-III

The magnetic susceptibility χ of iron(III)-oxide hydrate in relation to the concentration of NaOH used for the hydrolysis; $OH^-/Fe^{3+} = 2{\cdot}41$ in the first stage

sample	B_1	B_2	B_3	B_4	B_5	B_0
concentration of NaOH (mole/l)						
first stage	1	3·7	9·7	1	9·7	1
second stage	1	1	1	9·7	9·7	1
χ	75	82	89	73	91	75

do not reach their equilibrium distribution within the ageing period used, due to kinetic effects. But, in that case, too, the results are in conflict with the assumption. When a drop of NaOH falls into the solution there is a brief local high concentration of OH^- ions which could lead only to a higher degree of complexation than that corresponding to the equilibrium conditions. Hence, at higher NaOH concentrations a smaller χ value seems more probable than a larger one. A more satisfactory explanation is offered by the assumption that NaOH addition leads to the formation of particles with a higher degree of disorder the higher the concentration of the base added. The occurrence of this disorder together with the small particle size could well result from the extremely low solubility product of the material under study. Hence, on the addition of a drop of NaOH, there is a brief local excess of OH^- ions, giving an enormous supersaturation and thus causing a very rapid precipitation. This leads to crystallites which are not much larger than the critical nucleus and which may be expected to have a large number of stacking faults. The explanation of the different χ values as due to a high degree of disorder is also in accord with the observed slow decrease of the solubility mentioned in sec. 1.2.2. The latter could be attributed to growth of the particles or to an increasing ordering within the particles. In view of the foregoing it is most likely that both processes contribute to the decrease of the solubility.

1.4. Summary

The ideas advanced in the literature regarding the processes that occur on hydrolyzing solutions of Fe(III) salts generally explain the experimental results mainly as due to the formation of deprotonized monomers $Fe(H_2O)_{6-n}(OH)_n^{(3-n)+}$ at low degree of hydrolysis or, at higher ratios of OH^-/Fe^{3+}, as due to the formation of polynuclear complexes with a size distribution depending on the experimental conditions. Hysteresis effects are accounted for by assuming that the donation or the acceptance of protons of these complexes is rather slow. When, on average, more than 2·5 OH^- ions per Fe^{3+} ion are added, a gel is formed, which accordingly must be regarded as a network of interconnected chains of polynuclear complexes. Weiser and Milligan, however, have a different opinion. They consider the gel as a flocculated colloid composed of crystallites which have previously been formed in the solution.

The results presented in this chapter are in favour of the latter mechanism. As described, titrations with an agent that has strong complexing properties to Fe^{3+} ions (EDTA) lead to the idea that there is a solid, colloidally dispersed, phase in the hydrolyzed solutions, which has a constant solubility product.

On addition of a base to a Fe (III) solution a gel is formed when the ratio OH^-/Fe^{3+} exceeds 2·5. This formation of a gel in a rather short pH range can thus be considered as a flocculation of the colloidal particles present in the

solution. Measurements of the magnetic susceptibility χ give some idea of the mechanism of the reactions that take place, i.e. the addition of OH^- ions to the Fe^{3+} solution causes a rapid formation of crystallites with more defects in the lattice the higher the concentration of the base added. From the knowledge that there is a high degree of disorder, the slow and gradual decrease of the solubility of the products in partially hydrolyzed solutions can at least partly be attributed to an increased ordering within the particles.

The results mentioned thus far allow the provisional conclusion that the precipitation processes occurring in solutions of Fe^{3+} ions differ from the usually observed precipitation reactions only in that the size of the crystallites is extremely small. The number of iron ions composing them is probably not far beyond the number which is necessary for the formation of a critical nucleus. The experimental evidence presented in the next chapters will show that this supposition is justified.

REFERENCES

[1-1]) Th. H. Siddall and W. C. Vosburgh, J. Am. chem. Soc. **73**, 427, 1951.
[1-2]) B. A. O. Hedström, Arkiv f. Kemi **6**, 1, 1952.
[1-3]) L. N. Mulay, P. W. Selwood, J. Am. chem. Soc. **76**, 6207, 1954; **77**, 2693, 1955.
[1-4]) G. Jander and A. Winkel, Z. anorg. allg. Chem. **193**, 1, 1930.
[1-5]) G. Spiro, S. E. Allerton, J. Renner, A. Terzis, R. Bils and P. Saltman, J. Am. chem. Soc. **88**, 2721, 1966.
[1-6]) G. Biedermann and P. Schindler, Acta chem. Scand. **11**, 731, 1957.
[1-7]) W. Feitknecht and W. Michaelis, Helv. chim. Acta **45**, 212, 1962.
[1-8]) J. C. Bailar and D. H. Busch, The chemistry of the coordination compounds, Reinhold-Publ. Corp., 1956, p. 448.
[1-9]) T. V. Arden, J. chem. Soc. **1951**, 350, 1951.
[1-10]) S. R. Gupta and S. Ghosh, Z. anorg. allg. Chem. **279**, 212, 1955.
[1-11]) H. Galal-Gorchev, J. inorg. nucl. Chem. **25**, 567, 1963.
[1-12]) H. B. Weiser and W. O. Milligan, Chem. Rev. **25**, 1, 1939.
[1-13]) H. B. Weiser and W. O. Milligan, J. phys. Chem. **44**, 1081, 1940.
[1-14]) H. B. Weiser and W. O. Milligan, Advances Coll. Sci. **1**, 227, 1941.
[1-15]) G. Y. Onoda and P. L. de Bruyn, Surface Sci. **4**, 48, 1966.
[1-16]) R. J. Atkinson, A. M. Posner and J. P. Quick, J. phys. Chem. **71**, 551, 1967.
[1-17]) L. T. Bult and N. Strafford, An. chim. Acta **12**, 124, 1955.
[1-18]) A. Ringbom, Complexation in analytical chemistry, Interscience Publ., 1963.
[1-19]) H. Lengweiler, W. Buser and W. Feitknecht, Helv. chim. Acta **91**, 796, 1961.
[1-20]) G. W. van Oosterhout and L. J. Noordermeer, Philips tech. Rev. **25**, 139, 1963.

2. THE HYDROLYSIS OF Fe^{3+} IONS IN VERY DILUTED SOLUTIONS

2.1. Introduction

As discussed in chapter 1 there are two possible mechanisms of the hydrolysis of Fe^{3+} ions; either a more or less continuous series of polynuclear species is generated (with a maximum in the size distribution depending on the degree of hydrolysis) or a precipitation process occurs differing only from the usually encountered precipitations in that extremely small crystallites are formed. So far our experimental results are in favour of the latter mechanism.

If there would be a series of polynuclear species in the partially hydrolyzed solution, a Smoluchowski type of flocculation will occur on complete hydrolysis giving rise to a precipitate consisting of particles with a continuous size distribution. If, on the other hand, small crystallites with defined size were present, on flocculation, the precipitate will consist of these crystallites or conglomerates of a number of them and hence will show a discontinuous size distribution; moreover, besides the Fe^{3+} ions, particles smaller than these crystallites could not be observed. A determination of the size distribution of the particles formed in very dilute solutions therefore seems interesting. This has been done making use of a sedimentation analysis with an ultracentrifuge. Such a method has also been used by Spiro et al. [2-1]). In our case the sedimentation velocity of the different particles was determined using a radioactive tracer. These experiments not only lead to knowledge of the size distribution of the particles but at the same time allow the determination of the concentration of Fe^{3+} ions in the solution. A knowledge of the latter is useful for a study of the recrystallization processes occurring on the ageing of the initial precipitate (chapter 5). The solubility product K_s, as determined by Biedermann and Schindler [2-2]) in acid medium is very small: $K_s = 10^{-38.7}$. Other authors found higher K_s values: $10^{-35.5}$ [2-3]), $10^{-36.5}$ [2-4]) or $10^{-37.7}$ [2-5]), no doubt due to differences in the experimental conditions. If these solubility data may be extrapolated to neutral solutions, the concentration of Fe^{3+} ions at pH = 7 would be $\approx 10^{-15}$ gion/l. Ultracentrifuge experiments using radioactive tracers by Feitknecht et al. [2-6]), however, show that in neutral or alkaline medium the solubility has a higher value, possibly as a result of the reaction

$$Fe^{3+} + 4\,OH^- \rightleftarrows FeO_2^- + 2\,H_2O.$$

The concentration of Fe^{3+} at pH = 7 estimated by these authors was 2.10^{-9} gion/l or lower, their results being limited by the specific activity of their ^{59}Fe tracer. Recently a ^{59}Fe tracer has become available with a specific activity higher than used by Feitknecht et al. This tracer has been used for the sedimentation analysis to be discussed in the next sections.

2.2. Experimental

Preparation of an NH_4NO_3 solution is carried out via precipitating a 1-molar $Fe(NO_3)_3$ solution (Merck, p.a.) with concentrated ammonia (prepared by leading NH_3 gas into distilled water) until pH = 7·5. The precipitate is filtered and the resulting filtrate is centrifuged for 18 hours in a Homef L.C. 30 centrifuge at 3000 r.p.m. The top of the 50-ml centrifuge vessel was at a distance to the axis of rotation of 6·5 cm, the bottom 14·5 cm. The pH is adjusted to 7·5. In this way a 3-molar NH_4NO_3 solution is obtained which certainly does not contain nuclei capable of initiating the formation of a precipitate other than those of the compound under study. Only some $Fe_2O_3.nH_2O$ is present: [Fe(III)] equals $1{\cdot}4.10^{-7}$ mole/l (as determined by gravimetric analysis).

Preparation of a radioactive $Fe(NO_3)_3$ solution is carried out as follows. Add 3 drops of HNO_3 (conc.) to 0·050 ml $^{59}FeCl_3$ (Philips Duphar) and expel the HNO_3 by heating; this is repeated again. Extract the residue (a bright white powder) with 5 drops of H_2O. The extract contains 4.10^{-5} gion $^{59}Fe^{3+}$/l and has a pH of 2·5-3 (solution 1). For a number of experiments a solution of $^{59}Fe(NO_3)_3$ obtained from R.C.C. Amersham Ltd was used (solution 2). The solutions contain some Co as a result of

$$^{59}Fe \xrightarrow{\beta^-} {}^{59}Co.$$

The Co content of the $^{59}Fe(NO_3)_3$ never exceeded 5% at the end of an experiment.

Two series of experiments are carried out:

(A) 50 ml of the NH_4NO_3 solution is brought into a polyethylene flask of 250 ml; to this solution $^{59}Fe^{3+}$ is added (using solution 1) and mixed thoroughly (final concentration $^{59}Fe^{3+} \approx 3.10^{-7}$ gion/l); 5 ml aliquots of this solution are pipetted into nitrocellulose centrifuge tubes (fig. 2.1); the time of centrifuging varies;

(B) 5 ml NH_4NO_3 solution are pipetted into the centrifuge tube; to this is added 0·030 ml $^{59}Fe^{3+}$ (solution 2) and mixed by stirring with a glass rod; the centrifuge tubes are placed in a desiccator over a 3-molar solution of NH_4NO_3 during 3 days; the stirring rate is varied.

Centrifuging is carried out with a Beckman-Spinco centrifuge, at 36 000 r.p.m. for the desired length of time. The geometry is as depicted in fig. 2.1. After the centrifuging process, an injection needle is punched through the bottom of a centrifuging tube and the centrifugate is collected in three portions taken from the lower, middle and upper part of the tube.

The radioactivity is counted with a Ø 3″×3″ NaI(Tl) well-type detector and a Philips single-channel pulse-height analyser. In the discrimination channel the two ^{59}Fe γ peaks are counted. The count efficiency is 29%.

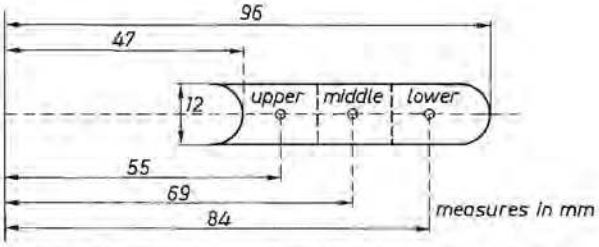

Fig. 2.1. Size and shape of the vessel used for the ultracentrifuge experiments.

Electron micrographs are made from samples prepared as follows. The dried centrifuging vessel is partly filled with a polymer ("Technovite") which is hardened. The hardened resin is expelled from the vessel and on the lower side of it carbon is evaporated. The polymer is dissolved in acetone and the carbon film is photographed, using a Philips EM 200 electron microscope.

2.3. Results

2.3.1. *Determination of the size distribution*

Both the addition of OH^- ions to a solution of Fe^{3+} ions and the reverse in such a way that $OH^-/Fe^{3+} \approx 2{\cdot}5$ gives rise to the formation of a number of very small particles. The concentration of these particles can be determined by their rate of sedimentation. This is done by placing the hydrolyzed solution in a gravitational field of an ultracentrifuge. Due to the large forces involved any large polymeric particles take part in the sedimentation process; only for extremely small particles (e.g. ions) does the effect of the Brownian motion counteract the sedimentation velocity [2–7]). Assuming that the sedimentation velocity of the particles — thought to be spheres — obeys Stokes' law, the size of the particles present in each part of the centrifugation tube can be calculated with the relationship

$$6\,\pi\eta r\,\frac{\mathrm{d}R}{\mathrm{d}t} = \frac{4}{3}\,\pi r^3\,(\varrho_1 - \varrho_2)\omega^2 R,$$

which can be rearranged to

$$\ln\frac{R_2}{R_1} = \frac{2r^2}{9\eta}\,(\varrho_1 - \varrho_2)\omega^2(t_2 - t_1), \qquad (1)$$

where

η = viscosity $\approx 1{\cdot}25.10^{-3}$ N s/m^2,
r = radius of the particle (m),
$v = \mathrm{d}R/\mathrm{d}t$ = velocity (m/s),
$\varrho_1 - \varrho_2$ = apparent density $\approx 3.10^{-3}$ kg/m^3,
R = distance from axis of rotation (m).

After a certain centrifuging time, there are at different levels in the centrifuging vessel particles of a size which can be calculated with the aid of this relationship. In our experiments the concentration of Fe(III) is determined in three compartments of the centrifuging vessel. Use has been made of a radioactive tracer, ^{59}Fe, of high activity and consequently a quantitative determination of [Fe(III)] could be carried out rapidly even at the very low concentration involved. Table 2-I lists a number of results obtained on centrifuging a hydrolyzed Fe(III) solution for different periods of time. The residual Fe(III) concentration after 64 hours of centrifuging (viz. $6{\cdot}9.10^{-9}$ mole/l) is not due to Fe^{3+} ions but is probably due to the back diffussion of the bottom product (particles of 6·3 Å). This can be shown as follows. The change in the number of particles, dN, is given by

$$dN = -N\frac{mg}{kT}\,dR,$$

where R is the height above zero level. Assuming spherical particles leads to

$$\ln\frac{N_2}{N_1} = -\frac{2\pi r^3}{3kT}(\varrho_1 - \varrho_2)\omega^2(R_2^2 - R_1^2).$$

TABLE 2-I

Concentration of Fe(III) $\times 10^9$ mole/l after different periods of centrifuging

centrifuging time (h)		$2\frac{1}{4}$	$7\frac{1}{2}$	24	64
$^{59}Fe^{3+}$ added ($\times 10^9$ gion/l)		254	444	225	307
^{59}Fe concentration ($\times 10^9$ mole/l) in different segments after centrifuging	upper	91	53	40·3	6·9
	middle	91	56	42·8	8·1
	lower	92	74	46·3	19·5
maximum hydrodynamic radius of particles in different segments (Å)	upper	20·1	12·8	6·2	—
	middle	30·1	18·6	8·3	—
	lower	33·3	20·8	10·2	6·3

For particles with $r = 6{\cdot}3$ Å, this expression gives $N_2/N_1 = 1{\cdot}8$. Hence, since the concentration of Fe(III) due to these particles in the lower compartment is $19{\cdot}5.10^{-9}$ mole/l, the concentration in the upper compartment, C, will be $(19{\cdot}5/1{\cdot}8).10^{-9} = 11{\cdot}8.10^{-9}$ mole/l. This more than accounts for the concentra-

tion actually found ($6{\cdot}9.10^{-9}$ mole/l). Probably only particles of 6·3 Å are present. It can be remarked that the concentration of Fe^{3+} ions is considerably lower, probably less than 10^{-9} gion/l. The data of table 2-I give the size distribution of the particles formed on hydrolysis. The results are presented graphically in fig. 2.2. This figure shows that there are mainly four types of particles:
particles with a diameter of 12, 24 or 37 Å and
particles with a diameter larger than 70 Å.
From the results it thus appears that a continuous size distribution does not exist; instead only a few types of particles are present with discrete radii.

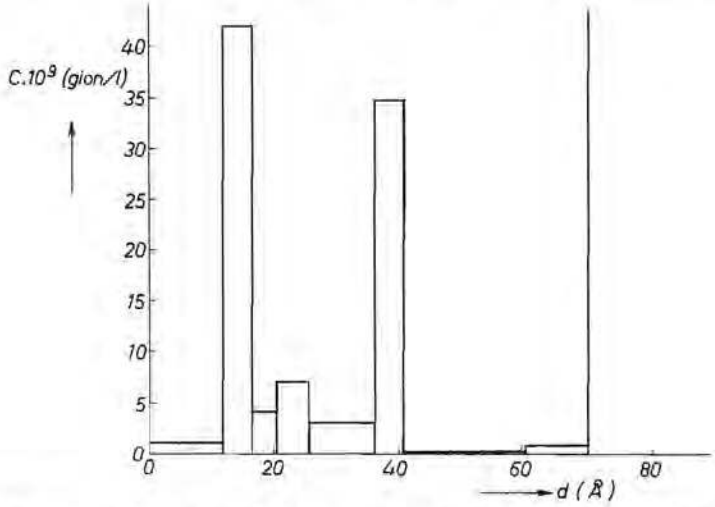

Fig. 2.2. The distribution of Fe(III) found with the sedimentation analysis.

2.3.2. *Electron micrographs of the sediment*

Electron micrographs were taken of the sediment present in the centrifuging tube. They do not reveal the presence of well-defined particles. Due to the technique used (isolation from the bottom of the vessel) it is not certain that particles with a size much below 70 Å could be observed. Crystallites with a size of 70 Å or more would not have escaped observation if present. It can be concluded therefore that the particles with a size larger than 70 Å as found in the ultracentrifuging experiment must be agglomerates of the smaller ones.

The spherical particles of 70 Å observed by Spiro et al. [2-1]), when using more concentrated solutions, are not observed with the present experiments. They therefore were presumably formed during the processes used by the investigators mentioned to make the particles formed during hydrolysis visible.

2.3.3. *Influence of the precipitation conditions on the size distribution*

It can be shown that the way in which the hydrolysis is carried out greatly influences the size distribution of the Fe(III) particles formed. In the experiments described in sec. 2.3.2 centrifuging was carried out for different lengths of time with samples taken from the same stock solution. To demonstrate the influence of the hydrolysis conditions, three different hydrolysates are made by adding the same amount of Fe^{3+} in each case directly in the centrifuging vessel, but while stirring at different rates (sec. 2.2, method (B)). Data are collected in table 2-II. The results presented in table 2-II demonstrate that the size distribution strongly depends upon the precipitation conditions which suggests that the particles found were not present already in the initial Fe^{3+} solution. They are formed indeed during the addition of Fe^{3+} to the NH_4NO_3 solution.

One might argue that the lower concentration of Fe(III) found in the different compartments of the centrifuging vessel on prolonged centrifuging (3 days, c.f. table 2-I) is at least partly due to sedimentation of larger crystals formed during this period. The decrease in the concentration is more than a factor 10; this cannot be attributed to ageing phenomena as such a rapid ageing may be excluded from experimental evidence, to be discussed in chapter 5. Also the differences initially present do not disappear after three days of ageing prior to centrifuging (table 2-II). This in turn means that ageing occurs very slowly.

TABLE 2-II

Concentration of Fe(III) after 3½ h of centrifuging. Centrifuging solutions prepared by method (B) (sec. 2.2)

Fe^{3+} added ($\times 10^9$ gion/l)		340	340	340
Fe(III) concentration ($\times 10^9$ mole/l) in different segments after centrifuging	upper	18	53	100
	middle	20	58	110
	lower	21	61	130

2.4. Summary

(1) Addition of Fe^{3+} ions to a solution of NH_4NO_3 with pH = 7, even in small concentrations ($[Fe^{3+}] = 10^{-7}$ gion/l) causes the formation of colloidal particles.

(2) The equilibrium concentration of Fe^{3+} ions under these conditions is $< 10^{-9}$ gion/l.

(3) The size distribution of the particles is discontinuous; four different sizes can be distinguished: 12, 24, 40 and > 70 Å.

(4) The amount of the different particles is dependent upon the way in which the Fe^{3+} ions are added to the NH_4NO_3 solution.

(5) The particles constituting the precipitate do not contain crystallites larger than 70 Å, as these are not visible on the electron micrographs. The particles with a diameter larger than 70 Å found with the ultracentrifuging experiments must therefore be considered as agglomerates of smaller particles.

REFERENCES

2-1) G. Spiro, S. E. Allerton, J. Renner, A. Terzis, R. Bils and P. Saltman, J. Am. chem. Soc. **88**, 2721, 1966.

2-2) G. Biedermann and P. Schindler, Acta chem. Scand. **11**, 731, 1957.

2-3) M. R. Evans and M. J. Pryor, J. chem. Soc. **5S**, 157, 1949.

2-4) P. A. Kriukov and G. P. Awsejewitsch, Z. elektr. Chem. **39**, 884, 1933.

2-5) H. S. Britton, J. chem. Soc. **127**, 2148, 1925.

2-6) H. Lengweiler, W. Buser and W. Feitknecht, Helv. chim. Acta **91**, 796, 1961; **91**, 805, 1961.

2-7) T. Svedberg and K. O. Pedersen, Die Ultrazentrifuge, Steinkopf Verlag, Leipzig, 1940.

3. THE DEHYDRATION OF IRON(III)-OXIDE–HYDRATE GELS

3.1. Non-destructive removal of the capillary water

3.1.1. *The low-temperature dehydration process*

It was briefly stated in chapter 1 that the ultimate hydrolysis product of Fe^{3+} solutions is a gelatinous precipitate which contains a large amount of water, about 90%. In general, gels consist of a network of macromolecules or are built up of chains of loosely aggregated sol particles held together by Van der Waals forces [3-1,2]. Iron-oxide–hydrate gel probably belongs to the second class.

De hydration of the gel at low temperature may be expected to offer the most reliable method for the isolation of its building units from it without any structural change. This dehydration can be carried out via a freezing process using liquid nitrogen [3-3]. When the gel is frozen, it does not retain its initial appearance after thawing. Instead it is separated into a brown powder and a water phase. Even when the gel has been washed thoroughly before freezing this water phase still contains some NO_3^-.

The powder after filtration and drying on P_2O_5 until constant weight, still contains considerable amounts of water. This water content greatly depends upon the preparation conditions. When the gel is prepared at 90 °C the powder isolated from it usually contains 11-15% H_2O, when the gel is prepared at 20 °C the powder contains 14-18% H_2O. When the dried powder is exposed to the air it rapidly takes up water again. In a typical example the H_2O content of a powder dried by exposure to the air was 25·5%; after drying on P_2O_5 the H_2O content decreased to 11% and after reexposure it took up its initial H_2O content within one hour. On prolonged air exposure (200 h) there was a further increase of the H_2O content of 10 wt%. The powder, which will be used for a number of studies to be described in the next chapters, will be designated further on as iron(III)-oxide hydrate.

The freezing process is most unlikely to change the particle properties as follows from a detailed discussion of the processes occurring during freezing and the subsequent thawing of the frozen gel.

3.1.2. *Experimental*

Preparation of gels has been carried out by dissolving 200 g $Fe(NO_3)_3.9\,H_2O$, Noury and Baker, in 500 ml deionized water, in a beaker of 1 l. This beaker is placed in a thermostat which is kept at 25 °C. Immediately after the preparation of the solution concentrated ammonia is added from a burette at a rate of two drops per second, under vigorous agitation (the ammonia has been prepared by leading NH_3 gas into distilled water until saturation). The ammonia addition

is stopped at pH = 7·5. Stirring is continued for five minutes after which the pH, which has dropped slightly, is readjusted.

Where the resulting gel is dehydrated for the preparation of iron(III)-oxide hydrate it is brought into a porcelain dish and frozen by pouring liquid nitrogen over it. The dish is covered with a watch glass and left standing overnight. The gel is then separated into a brown precipitate and an aqueous layer which is filtered off. The oxide hydrate, a compact powder, is washed with water containing a very small amount of ammonia (pH = 7·5) until the filtrate is nitrate-free (reaction with sulphanilic acid and α-naphtylamine) and dried in vacuum at room temperature over P_2O_5. The water content is determined by heating at 1000 °C for four hours in air; nitrogen is determined by gravimetric analysis.

Where the gel is used for a Mössbauer spectroscopy study as described in sec. 3.2, it is washed seven times with ammoniacal water of pH = 7·5 by decantation. The gel is then filtered by suction. Its nitrogen content is less than 0·0001 % by wt.

3.2. A study of the constitution and freezing behaviour of iron(III)-oxide–hydrate gels by means of the Mössbauer effect *)

3.2.1. *Introduction*

It will be shown that Mössbauer spectroscopy provides a means of studying the gel structure and its freezing behaviour.

Only a short discussion of some Mössbauer phenomena will be given here; for a more detailed introduction into the Mössbauer spectroscopy the reader is referred to ref. 3–5.

The basis of Mössbauer spectroscopy is the existence of different energy levels in the nucleus of an atom, that can be excited by a γ quantum of the appropriate energy. Such a γ quantum is emitted by a source when one of its nuclei undergoes a transition from an excited state to a lower energy level with an energy difference equal to the transition energy of the receiving atom. Due to the very small natural line width the difference in transition energy of the source and the receiving atom must be very small in order that resonance absorption can occur. The resonance couple ^{57}Co-^{57}Fe is very well suited for Mössbauer-resonance study of iron compounds (natural iron containing about 2% ^{57}Fe). Although, in the case of coarse crystals the positions of the emitting and receiving atoms are fixed by the rigid bounding to the crystal lattice, some recoil energy is lost. To correct for this and for the kinetic energy of the photon, the photon energy is shifted by the imparting to the source of a Doppler velocity (for the experiments under consideration varying between —5 and 5 mm/s). The intensity of the absorption as a function of the Doppler velocity gives the Mössbauer-resonance-absorption spectrum.

*) This section has already been published elsewhere [3–4].

The conditions mentioned for obtaining resonance are necessary but not sufficient. In order to obtain resonance absorption the recoil of the γ quantum must be absorbed by a large enough mass. Very small particles with a size below 200 Å, at least when not rigidly bound to a substrate, are no longer able to take part in the Mössbauer resonance due to their small mass. This can be understood as follows. When a γ quantum is absorbed by an iron atom, besides the rest energy, it also receives the kinetic energy of the quantum. When this energy is shared by all the atoms composing the particle the latter acquires a translation energy equal to $\frac{1}{2}mv^2$ in which m is the mass of the particle and v its velocity. The same energy is imparted to the source and thus the energy $h\nu$ of the quantum received by the nucleus is smaller than the transition energy E by the amount mv^2. Hence

$$h\nu = E - mv^2;$$

as

$$\frac{h\nu}{c} = mv,$$

it follows that

$$h\nu = E\left(1 - \frac{E}{mc^2}\right).$$

The quantity E^2/mc^2 gives rise to line displacement. The natural line width of the ^{57}Fe transition is $4{\cdot}6.10^{-9}$ eV and the transition energy E equals $14{\cdot}4.10^3$ eV. When assuming that the line displacement due to the loss in kinetic energy may not exceed the natural line broadening in order that resonance absorption occurs,

$$\frac{E^2}{mc^2} \leqslant 4{\cdot}6.10^{-9},$$

from which follows that $m \geqslant 10^{-16}$ g. This implicates that for FeOOH the absorbing particle must be built up of at least 5.10^5 FeOOH groups. Now, if resonance occurs it follows that the gamma-absorbing particles either have a mass exceeding this critical value or are bound to their surroundings *). It will be argued that the resonance observed in iron-oxide–hydrate gels is due to the second possibility. Hence the intensity of the absorption, i.e. the peak height, can be used to study changes in the particle surroundings occurring upon freezing in the gel.

For the gel under study the Mössbauer spectrum is not influenced by Brownian motion of the particles, contrary to what has been found for dispersions in liquids [3-6-9].

3.2.2. *Experimental*

Gels of iron(III)-oxide hydrate are prepared by the addition of ammonia to

*) Even when these binding forces are weak, e.g. in the case of a gas, some resonance absorption should occur [3-10].

a solution of $Fe(NO_3)_3$ at 20 °C as described in sec. 3.1.2. Samples suitable for investigation in the Mössbauer apparatus are prepared by putting the gel in a flat polystyrene vessel, so that uniform layers are formed; their thickness is varied between 0·5 and 2·5 mm.

Mössbauer spectra have been determined at temperatures between —100 °C and 40° C. The low temperatures can be maintained by cooling the sample holder, isolated with polyfoam, with cold nitrogen gas. Above room temperature the same arrangement is used with heated nitrogen gas. The measurements have been carried out with a constant-velocity Mössbauer spectrometer as described in ref. 3–11, using ^{57}Co in Pd as a source.

3.2.3. *Results*

The gel as prepared, the frozen gel and the dry iron-oxide–hydrate powder isolated from the gel via freezing, all show the same spectrum with two peaks; an example is given in fig. 3.1. The position of the centre of gravity of the spectrum varies only slightly with temperature: at 22 °C it is at 0·20, at —100 °C at 0·26 mm/s.

The peak heights and their temperature dependence in the three cases are different. Starting with a gel at room temperature the peak height increases slightly with decreasing temperature. This behaviour is reversible as long as the temperature does not attain values below —7 °C (curve a, fig. 3.2). Below this temperature the gel at least partially freezes, as verified by the increase of its stiffness and by D.T.A. measurements which at —7 °C show a temporary temperature rise to —0·1 °C. At the same time there is a sudden and strong increase of the Mössbauer peak height. Between —7 and —30 °C an irreversible behaviour is

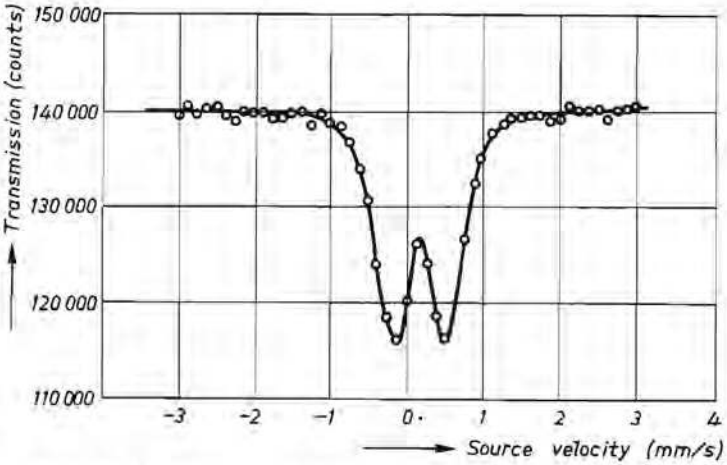

Fig. 3.1. Spectrum of dried powder at room temperature. Sample thickness 26 mg/cm².

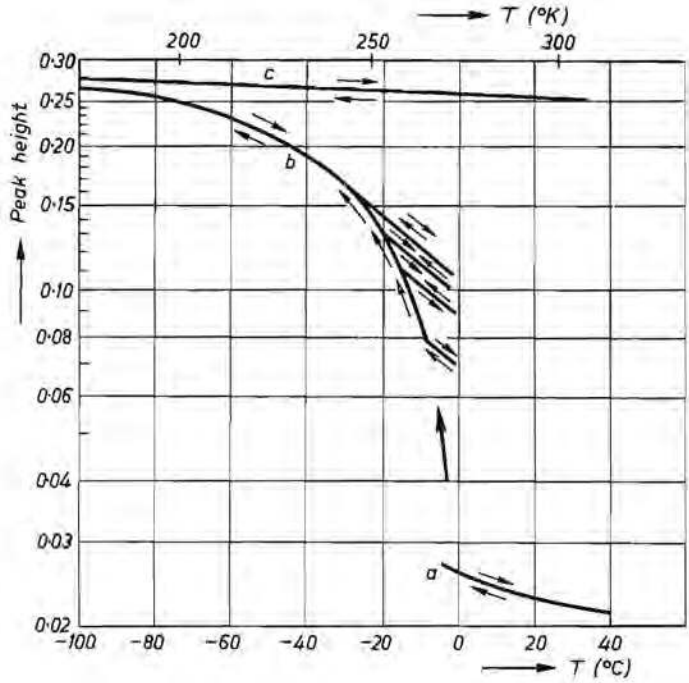

Fig. 3.2. Typical example of peak height (relative to total number of pulses in the 14-keV channel outside resonance) as a function of temperature. In the gel state the sample thickness was 320 mg/cm^2.
Curve a: gel as prepared.
Curve b: frozen gel. The irreversible behaviour above —30 °C during the first cooling is indicated for a specific temperature cycle: —8 → —2 → —15 → —2 → —20 → —2 → —30 → —2 → —60 → —2 → 100 → —2 °C.
Curve c: dried powder isolated from the gel.

found: the behaviour of the sample then depends on the lowest temperature it has reached previously. If for example the gel has been cooled down to —15 °C the peaks do not return to their former heights upon reheating to —7 °C, but stay higher, following a curve that can be traced up to the thawing point at 0·0 °C (fig. 3.2). As long as the gel temperature remains between —15 and 0·0 °C the peak-height vs temperature curve is reversible. Once the sample has been below —30 °C the peak height of the frozen gel behaves reversibly up to 0 °C. A gel that has been cooled to —7 °C or lower, upon thawing does not return to the original gel structure but decomposes into a slurry of iron-oxide powder and water. The powder isolated from this slurry has higher Mössbauer peaks than either the original or frozen gel. This is shown in curve c of fig. 3.2. The changes in the peak height with temperature are reversible for this powder.

3.2.4. *Discussion*

3.2.4.1. Constitution of the gels

The fact that in all cases, gel, frozen gel and oxide-hydrate powder, similar two-line spectra are found, indicates that we are dealing with the same iron compound. The height of the peaks provides information about the way in which iron nuclei are incorporated in the gel structure. The peak height depends on the probability of resonance absorption — or Mössbauer fraction — f, and this in turn depends on the elastic properties of the environment of the iron nuclei. If the environment is not the same for all iron nuclei the probability of resonance absorption becomes an average of the f's of iron nuclei in the different environments. This is e.g. the case with a colloidal solution of coarse and subcritical crystallites.

For our experiments the f value of the absorber was determined in the usual way [3-12]). The Mössbauer fraction of the source was taken to be 0·65 [3-13]). The relation between peak height and sample thickness was found to be in good agreement with theory. In fig. 3.3, f is shown as a function of temperature for the reversible states

(a) gel as prepared,
(b) frozen below —30 °C,
(c) dried powder.

As shown in fig. 3.3 (curve c), for this powder f is about equal to that of powder consisting of coarse, 1-μm, particles of the iron(III) compound γ-FeOOH, which has a similar two-line spectrum (curve d). Apparently, as the iron (III)-oxide–hydrate particles are below the critical size, the recoil is taken up by the whole assembly of particles in the powder.

The low f value of the unfrozen gel may be due to either of two causes:

(1) insufficient stiffness of a structure composed of small particles of about equal, subcritical, size surrounded by water;
(2) the presence of only a small number of large crystals or clusters of subcritical particles in a non-rigid assembly. In this case the remaining iron nuclei are present in subcritical particles and hence give a negligible contribution to f.

The second possibility can be ruled out however, because this would give the same temperature dependence of f for both the gel and the powder, contrary to what has been found (figs 3.2 and 3.3). Thus we are left with the first model.

In order to get some idea about the relation between Mössbauer fraction and elastic properties, in fig. 3.3 are also shown calculated f vs T curves for two hypothetical Debye lattices. The latter is a simple cubic lattice of identical atoms with harmonic force constants; its elastic properties are characterized by a Debye temperature T_D. In our calculations the mass number of the atoms was taken either 56 (iron) or 16 (oxygen). As depicted in fig. 3.3, in spite of the big differ-

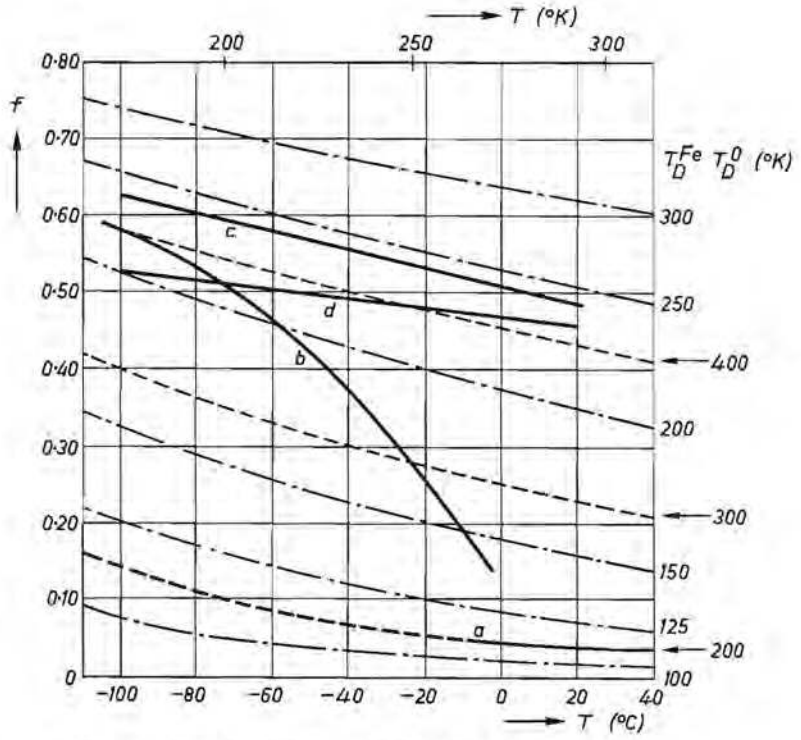

Fig. 3.3. Mössbauer fraction f as a function of temperature.
Curve a: original gel.
Curve b: frozen gel after having been at −100 °C.
Curve c: dried powder isolated from the gel.
Curve d: γ-FeOOH powder composed of particles of about 1 μm.
Also shown are the calculated values for Debye lattices with iron (dashed-dotted curves) and oxygen mass (dashed curves) for various Debye temperatures T_D^{Fe} and T_D^O, respectively.

ence in mass number the curves are qualitatively the same. Comparison of the experimental f vs T relationship with the calculated curves shows that

(1) down to −7 °C the gel as prepared behaves like a lattice with a very low T_D, i.e. it has a very small rigidity;
(2) the frozen gel behaves like a lattice which is fairly rigid at low temperatures but becomes looser above 200 °K (fig. 3.3, curve b).

This behaviour of the frozen gel is similar to that of pure ice, where, below 200 °K, only the translational lattice vibrations are excited, but above this temperature the librations become more and more excited as well [3–14]). This similarity can be explained by assuming that in the frozen gel the particles are present in an ice matrix, which absorbs the gamma recoil. Agglomeration apparently occurs to a minor extent, the agglomerates then being smaller than the critical size of 200 Å. Hence the separation of the particles is essentially

preserved after freezing; the collapse of the network, leading to the formation of the powder, does not occur during freezing but upon thawing.

3.2.4.2. The freezing process

In four respects the freezing behaviour of the iron(III)-oxide–hydrate gel is peculiar:

(1) the initial freezing temperature is —7 °C, although the electrolyte content is less than 10^{-5} mole%;
(2) freezing is not completed until the gel has been cooled below —30 °C;
(3) the freezing process is not reversible;
(4) melting occurs at 0·0 °C; after thawing the gel is separated into a powder and a water phase.

The low initial freezing temperature can be ascribed to undercooling; this is also observed in organic gel systems [3–15]). We found that after solidification has started, although the sample is cooled steadily, the temperature remains at the constant level of —0·1 °C during a certain length of time. This points to a depression of the freezing point [3–15]), but could also be an erroneous result due to the experimental technique [3–16]).

On further cooling the freezing continues until at —30 °C all particles are frozen in. The range of freezing points observed in our gels cannot be explained by kinetic effects (nucleation rate): no change in peak height and its temperature dependence is observed within 20 hours. A range of freezing points down to —40 °C is also observed in porous glass [3–17]). The phenomenon can be ascribed to the differences in surface energy within a porous system containing water in pores with various diameters. As the surface energy of water in a pore differs from that of ice, the freezing point is depressed. According to Kuhn et al. [3–15]) the relation between freezing-point depression ΔT and pore diameter d is: $\Delta T\, d = 3{\cdot}7.10^{-6}$. Thus freezing points of —0·1 and —30 °C observed in our gels correspond to pore diameters of 3700 Å and 12 Å, respectively, indicating that there is a large variation in pore sizes.

A difference between freezing temperature and melting temperature — here 0·1 °C — is also observed in organic gels [3–15]). Kuhn tried to explain this with a model in which the ice crystals in adjacent capillaries have the same orientation while the intermediate network remains undamaged during freezing. Kanig, however, observed with electron micrographs that after freezing the pore system in the gel was damaged [3–16]). For inorganic systems, the same was concluded by Weiss from the increase of the freezing point upon repeated freezing and thawing [3–18]). Our experimental results demonstrate that for the gel under study the latter explanation is the most probable. Upon ice formation the chains of the particles forming the gel network break in several places. When freezing proceeds more contacts between the particles are broken. Hence larger capillaries are formed and remelting does not occur until close to 0 °C. The fact that

only chains break and no agglomeration takes place is concluded from the observed rigidity of the surroundings of the particles in the frozen gel which shows that the particles remain separate in the ice matrix. The final collapse of the network occurs upon thawing, when the contacts are not restored and agglomeration starts. The powder isolated from the gel in this way, thus consists of agglomerates of primary gel particles.

The fact that the agglomerates are composed of the original crystallites, forming the gel, follows from the further evidence that the magnetic susceptibilities of powders either isolated from the gel via freezing or by drying the gel on P_2O_5 without freezing are the same within the experimental error. Also the X-ray spectrum of the gel and the powder isolated from it upon freezing are identical (chapter 5).

3.3. Summary

Iron-oxide-hydrate gels contain a large amount of capillary water. This water can be removed by a special dehydration procedure. This involves freezing of the gel, for instance with liquid nitrogen, followed by thawing at room temperature. The gel then separates into a water phase and a brown powder, which after drying on P_2O_5 contains about 15% H_2O by weight. This powder, designated as iron(III)-oxide hydrate, most probably is composed of the crystallites originally constituting the gel. This is suggested by a study of the dehydration processes using Mössbauer spectroscopy and is further supported by the fact that its magnetic and crystallographic properties are unchanged.

The Mössbauer spectrum of iron-oxide-hydrate gels both as prepared and after subsequent freezing consists of two peaks of equal height. The temperature dependence of the peak height can be related to the elastic properties of the gel structure and its freezing behaviour. The results agree with the picture that the gel consists of a network of small particles (< 200 Å). The recoil of the absorbed gamma radiation is taken up by the surroundings of the particles. The network contains capillaries which freeze at a lower temperature, the smaller their diameter. At —30 °C all particles are rigidly frozen in. During freezing the coherence of the network is diminished but the particles still remain separate in the ice and during the subsequent thawing the network collapses and the particles agglomerate. Hence after thawing the gel is separated into a powder and a liquid phase.

REFERENCES

3-1) E. J. W. Verwey and J. Th. G. Overbeek, Theory of the stability of lyophobic colloids, Elsevier, Amsterdam, 1948.
3-2) H. R. Kruyt, Colloid science, Elsevier, Amsterdam, 1949, vol. 2, p. 483.
3-3) A. A. van der Giessen, J. inorg. nucl. Chem. **28**, 2155, 1966.
3-4) A. A. van der Giessen, J. G. Rensen and J. S. van Wieringen, J. inorg. nucl. Chem., in print.
3-5) R. H. Herber, J. Chem. Education **42**, 180, 1965.

3-6) K. S. Singwi and A. Sjölander, Phys. Rev. **120**, 1093, 1960.
3-7) P. P. Craig and N. Sutin, Phys. Rev. Letters **10**, 460, 1963.
3-8) D. St. P. Bunbury, J. A. Elliott, H. E. Hall and J. M. Williams, Phys. Letters **6**, 34, 1963.
3-9) T. Bonchev, P. Aidemirski, I. Mandzhudov, N. Nedyalkova, B. Skorchev and A. Strigachev, J. exptl theor. Phys. (U.S.S.R.) **50**, 62, 1966; Sov. Phys. JETP **23**, 42, 1966.
3-10) L. Eyges, Am. J. Phys. **33**, 790, 1965.
3-11) J. S. van Wieringen, Philips tech. Rev. **28**, 33, 1967.
3-12) R. S. Preston, S. S. Hanna and J. Heberle, Phys. Rev. **128**, 2207, 1962.
3-13) W. A. Steyert and R. W. Taylor, Phys. Rev. **134A**, 716, 1964.
3-14) N. Ockman, Adv. Phys. **7**, 199, 1958.
3-15) W. Kuhn, R. Bloch and P. Läuger, Kolloidz. **193**, 1, 1963.
3-16) G. Kanig, Koll. Z. **173**, 97, 1960.
3-17) A. A. Antoniou, J. phys. Chem. **68**, 2755, 1964.
3-18) A. Weiss, Rheologica Acta **2**, 292, 1962.

4. THE STRUCTURE OF IRON(III)-OXIDE HYDRATE

4.1. Crystallographic properties

4.1.1. *Introduction*

The existence of a crystallographic ordering in iron-oxide–hydrate gel has been extensively examined with the aid of X-ray-diffraction techniques. Nearly all authors arrive at the same conclusion, i.e. that the material is amorphous, see for instance refs 4–1, 2. Frei and co-workers are of the same opinion, although in their products, dried at 60 °C, some faint reflections were observed at $d = 2{\cdot}54$, 2·23, 1·97, 1·71 and 1·49 Å [4–3]).

Weiser and Milligan however are not convinced of the amorphous character of the gel and more generally speaking of oxide gels: "the gels are believed to consist of agglomerates of extremely minute crystals of oxide or simple hydrate (or hydroxide) which hold large amounts of water by adsorption and capillary forces" [4–4,11]). This conclusion was supported by results obtained with electron diffraction. This technique has, however, the disadvantage that the hydrate has to be studied in the vacuum of the microscope and, due to heating with the electron beam can easily decompose or recrystallize. This most probably explains the observation of diffraction patterns which could be attributed to α-Fe_2O_3 [4–4]). Their evidence for crystallinity in iron-oxide–hydrate gels is therefore believed not to be conclusive.

From the investigations described in the preceding chapters it was concluded that the gel or the oxide hydrate isolated from it is composed of particles with a size considerably below 200 Å. Investigation of such small crystallites with radiation of a rather long wavelength with respect to the particle size, for instance the commonly used CoKα radiation, should lead to an X-ray diagram with such a considerable line broadening that one erroneously could conclude to the absence of any ordering. It seemed worth while trying to take X-ray-diffraction patterns using radiation of a short wavelength (MoKα radiation with $\lambda = 0{\cdot}71$ Å); in that case the diffraction bands become much more distinguishable from the background. Experiments are described below.

4.1.2. *Experimental*

The preparation of the oxide hydrate has been described on page 21. X-ray-diffraction patterns are made with the aid of a Philips diffractometer using CoKα and MoKα radiation and with a Debye-Scherrer camera taking a twelve-hours exposure to MoKα radiation. In the latter case a Zr filter is laid on the film.

Electron micrographs and electron-diffraction patterns are made with a Philips E.M. 200 electron microscope with a resolution of 7 Å, 80 keV.

The specific surface area, S, is determined by argon adsorption; the results are

interpreted with the B.E.T. method assuming that the argon molecule occupies a surface of 18·2 Å². A number of samples are also measured using nitrogen: the same S values were found as with argon.

4.1.3. *Results and discussion*

4.1.3.1. Crystallographic properties

Debye-Scherrer diagrams, together with diagrams made on a diffractometer, using MoKα radiation, show a number of broad reflections. Both the original gel and the oxide hydrate obtained from it after freezing with liquid nitrogen, show the same diagram. The reflections observed on samples prepared at 20 °C are somewhat broader than those observed on samples prepared at 90 °C. Table 4-I gives a number of reflections which are observed in a sample prepared at 70 °C.

TABLE 4-I

Reflections of the D.S. diagram of the iron(III)-oxide hydrate using MoKα radiation ($\lambda = 0{\cdot}71$ Å). Sample prepared at 70 °C. Intensities are determined from the corresponding bands observed in the diffractogram

no.	θ ($\pm$ 0·1°)	$10^3 \sin^2 \theta$	d (Å)	I/I_0
1	6·0	10·9	3·39	—
2	8·2	19·4	2·52	100
3	9·1	25·1	2·24	20
4	10·35	32·3	1·97	10
5	11·85	42·2	1·73	15
6	13·8	56·9	1·49	60
7	16·4	79·7	1·26	7
8	17·7	92·4	1·17	—
9	18·5	100·8	1·12	$\Sigma I = 10$
10	19·85	115·3	1·04	
11	21·6	135·5	0·96	2
12	22·7	148·9	0·92	—
13	23·8	162·9	0·88	1
14	24·7	174·6	0·85	3
15	26·4	197·7	0·80	—
16	27·9	219·0	0·76	—
17	28·8	232·0	0·74	—
18	30·1	251·5	0·71	—
19	32·4	287·1	0·66	—
20	39·65	407·2	0·56	—

The existence of an X-ray diagram with about twenty lines indicates that the material under investigation is at least partially crystalline. The resolution of the diffraction peaks in the diffractograms appeared to be less than in the D.S. diagram. The shape of the peaks in the diffraction diagram suggests that some reflections are composed of several bands, especially the strongest reflections at $d \approx 2{\cdot}50$ Å and $d \approx 1{\cdot}50$ Å. The diffraction pattern is shown in fig. 4.1. A comparison is made with the X-ray diagrams of the well-known oxides and oxide hydroxides of Fe(III). A identification of the main reflections of these oxides together with their relative intensity are depicted schematically in fig. 4.2. The figure clearly demonstrates that the iron(III)-oxide hydrate is different from the hitherto known oxide hydroxides and oxides. The oxide hydrate shows the greatest resemblance to δ-FeOOH. There is also some resemblance to the Van Bemmelen hydrate [4–5], a crystallographic study of which has been published by Collongues and Thery [4–6].

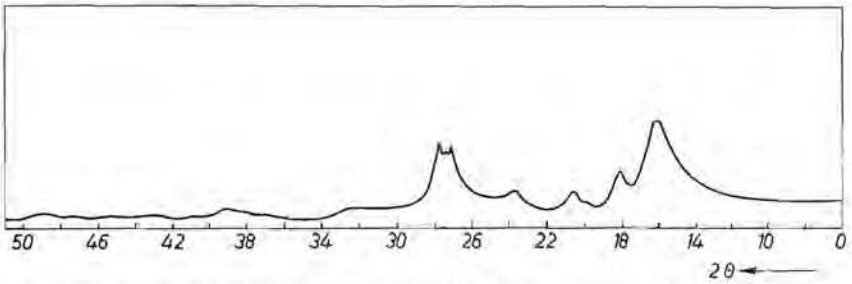

Fig. 4.1. Diffraction pattern of the iron(III)-oxide hydrate; MoKα radiation.

An elucidation of the structure is hampered not only by the fact that the reflections are broad and in some cases possibly consist of several overlapping ones but also by a lack of knowledge of the composition. It will be argued in the next chapter that this is either FeOOH or $Fe_2O_3.H_2O$; in the latter case probably the water is adsorbed on the surface of the particles. It was stated in a publication by the present author that the D.S. diagram could be indexed by taking a cubic unit cell with $a_0 = 8{\cdot}37$ Å [4–7]. Accounting for the results to be discussed in the next sections, which indicate that the iron ions are placed in two groups of identical positions, it is questionable however whether the compound really has such a cubic unit cell: it proved to be impossible to place the iron ions in a cubic arrangement which leads to calculated intensities of the reflections that are in reasonable accord with the observed ones. Another possibility could be that we are dealing with a hexagonal compound, for instance with $a_0 = 3{\cdot}0$ Å and $c_0 = 9{\cdot}3$ Å. But also in that case the iron ions could not be placed in the oxygen lattice in such a way that reasonable intensities can be calculated.

It is difficult to judge from these X-ray mearsurements which fraction of the gel

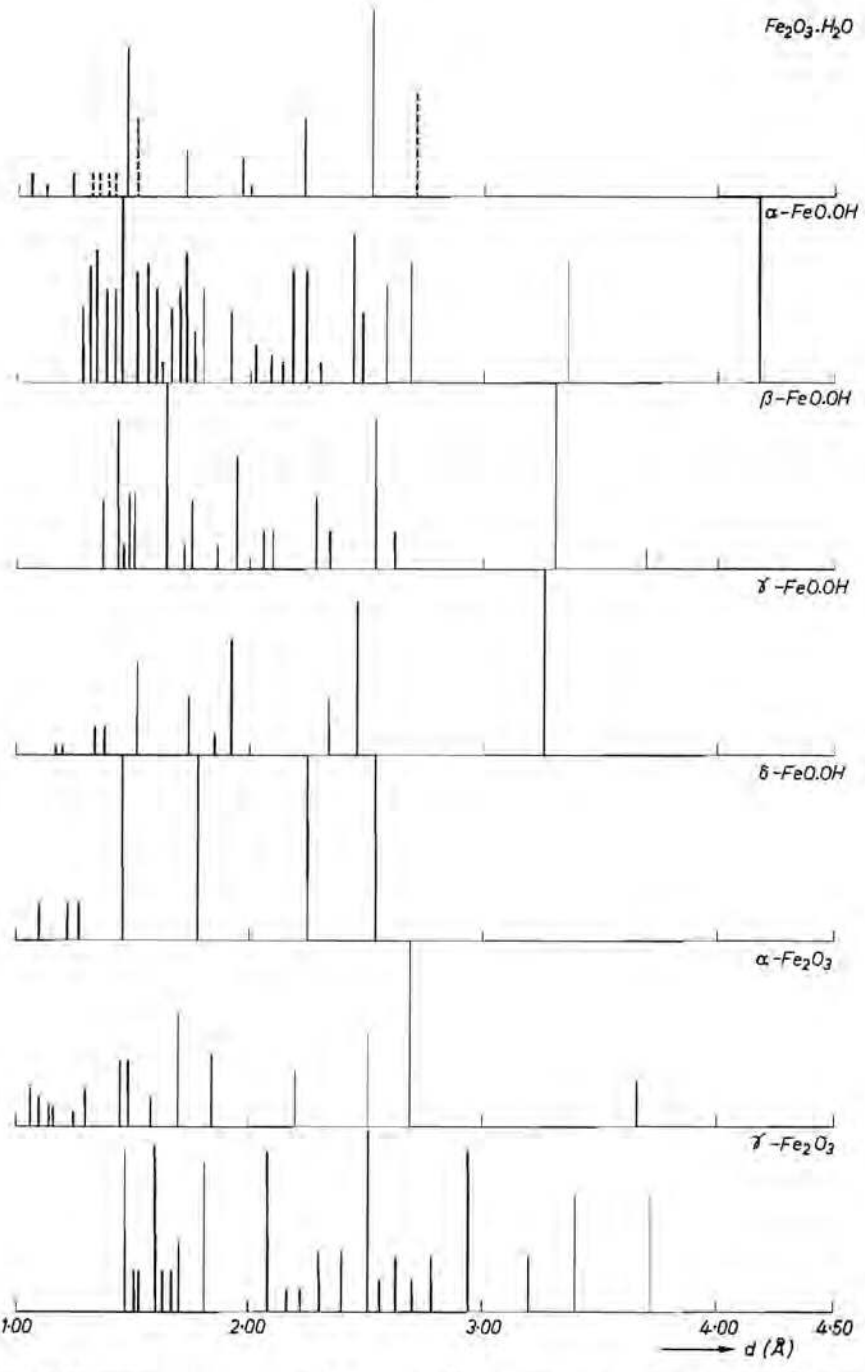

Fig. 4.2. Schematic representation of the main diffraction peaks of α-, β- and γ-FeOOH, α- and γ-Fe_2O_3 together with those of the iron(III)-oxide hydrate.

material has an ordered structure. Magnetic measurements, to be described further on, will give additional information to this point. The observation that the wet gel and the oxide-hydrate powder isolated from the gel after freezing have the same X-ray diagram is in favour of the idea that the isolation technique used does not affect the particle properties.

The fact that the material is crystalline strongly supports the proposed ideas about the hydrolysis as outlined in chapter 1.

4.1.3.2. Morphology

The powder obtained by dehydrating the gel with liquid nitrogen has a light brown colour. As indicated already by the considerable line broadening of the X-ray diagrams the particles constituting it must be small. Electron micrographs confirm that it does indeed consist of extremely small particles, the largest observable being 20 to 30 Å. These particles of irregular size and shape, some being more or less threadlike, are agglomerated to a spongy mass. They are considered to be present in the gel already before dehydration. A typical photograph is given in fig. 4.3.

Particles with the observed size should have a surface area S of about 600 m^2/g, when assuming a cubic particle with an edge of 25 Å and density 4 g/cm^3. This value may be compared with the values actually found. It is noted that the sample preparation before measuring can have a considerable influence on the value of S observed. For instance, the specific surface area depends upon the temperature used for — vacuum — degassing during the measurement. This is illustrated for sample C 131, an oxide hydrate isolated from a solution aged at pH = 2 during 24 h before precipitation. The particles constituting it are somewhat larger than those of the gel obtained by direct precipitation and hence the specific surface area is smaller. From table 4-II it is clear that degassing for 30 minutes at 80 °C is the proper procedure; at higher temperatures sintering takes place.

The surface areas of the various oxide hydrates are not exactly the same but vary between 280 and 350 m^2/g. When prepared at higher temperature the oxide hydrate has a somewhat smaller area. In a typical example the surface area of the particles of the oxide hydrate was 305 m^2/g when prepared at 20 °C and 280 m^2/g when prepared at 90 °C. When assuming cubic or spherical particles, the size calculated from S would be 50 Å which is larger than that observed with the electron micrographs. In case of a cylindrical particle with a length of three times the diameter, the calculated diameter would be about 30 Å, in conformity with the electron-microscope observation. The comparatively small specific surface area can thus be attributed to the non-cubic shape of the particles but it could also be explained as due to sintering of the particles during degassing in the B.E.T. apparatus.

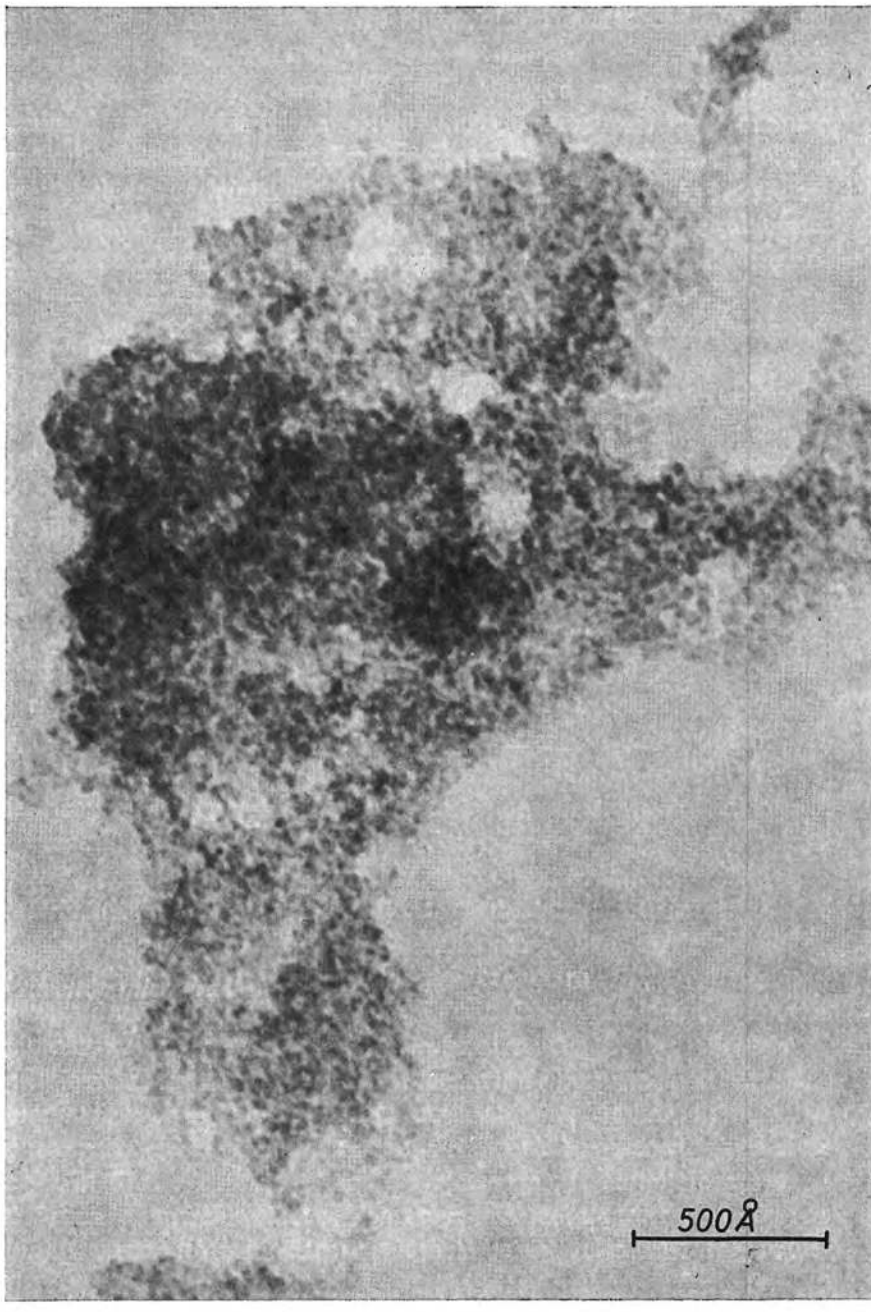

Fig. 4.3. Electron micrograph of the dehydrated gel.

TABLE 4-II

The dependence of the specific surface area, S, upon the time and temperature of degassing

temperature (°C)	S (m^2/g) after degassing during	
	30 minutes	8 hours
20	195	—
80	235	225
200	200	—
350	72	—

4.2. Mössbauer spectroscopy

4.2.1. *Introduction*

Whereas X-ray diffraction gives information about the ordering prevailing at distances that are long compared to the size of the ions (atoms) composing the compound, Mössbauer spectroscopy enables to study the coordination sphere of the iron nucleus. In the absence of an electric-field gradient or a magnetic field on the iron nucleus, the Mössbauer spectrum shows only one peak, due to the transition from the ground state to the excited level. When the iron nucleus is present in an electric-field gradient, the excited level is split into two new levels giving rise to quadrupole splitting which leads to a Mössbauer spectrum of two lines. When a magnetic field is present the ground level is split into two levels and the excited level is split into four, thus making possible six energy transitions resulting in a six-line spectrum (magnetic and electric hyperfine splitting). So if the iron is in an antiferro-, ferro- or ferrimagnetic lattice, a six-line spectrum is observed. When the compound is paramagnetic and hence on the average no magnetic field exists, one single resonance line is observed, but when at the same time an electric-field gradient exists quadrupole splitting occurs. The latter gradient can be caused by the surrounding oxygen ions. For instance when in a paramagnetic compound an iron ion is situated in the symmetry centre of a perfectly tetrahedral, or octahedral, oxygen hole no splitting occurs, but when the hole is distorted quadrupole splitting is observed. If the peaks are sharp the coordination sphere must be identical for all iron ions, but if the lines are broad the gradient differs from iron to iron ion and hence the coordination sphere is different for the various iron ions.

The extent of the quadrupole splitting depends upon the strength of the field gradient. The symmetry line of the spectrum generally does not coincide with

a zero Doppler velocity. Instead the spectrum is shifted to Doppler velocities the values of which depend on the chemical bonding of the iron nucleus. This is called isomer shift.

From the foregoing it appears that the Mössbauer spectrum makes a valuable contribution to the knowledge of the direct surroundings of the iron ion. It also reveals the magnetic ordering. A comparison of the Mössbauer spectrum of the compound under investigation with the spectra of the other iron-oxygen compounds could be a direct method for its identification. However, such an identification is complicated by the fact that the size of the particles may strongly influence the spectrum. If the particles of a magnetic material are below a certain size the original six-line spectrum changes into a two-line spectrum. This has been studied particularly with antiferromagnetics like α-Fe_2O_3 [4–8·10]) and α-FeOOH [4–11]) but also for ferrimagnetic materials such as $NiFe_2O_4$ and $CoFe_2O_4$ [4–12]). The shape of the peaks may change too.

This change in the Mössbauer spectrum coincides with a change in the magnetic behaviour: the ferri- or ferromagnetic material behaves superparamagnetically when composed of particles with a size below 100 Å.

4.2.2. *Experimental*

The samples are prepared at 20 °C according to the procedure described on page 21.

No iron with a valency lower than Fe(III) could be found by chemical analysis [4–13]). The Mössbauer spectra of ^{57}Fe are made with a source of ^{57}Co in palladium. For the measurements at liquid-nitrogen and at liquid-helium temperature a cryostat is used in which the sample is in a vacuum and in thermal contact with the inner container. Consequently the sample temperature might have been slightly higher than indicated.

4.2.3. *Results and discussion*

Mössbauer spectra of the oxide hydrate, at room temperature show quadruple splitting with $2\varepsilon = 0{\cdot}62 \pm 0{\cdot}05$ mm/s. At 290 °K the isomer shift $\delta = 0{\cdot}20$ mm/s, at 130 °K $\delta = 0{\cdot}23$ mm/s and at 77 °K $\delta = 0{\cdot}27$ mm/s. The spectrum does not change its character down to the temperature of liquid nitrogen; at that of liquid helium, however, the spectrum shows magnetic hyperfine splitting, fig. 4.4. The quadrupole lines are sharp. An estimate of the number of iron ions contributing to these spectral lines reveals that probably all iron ions contribute to them. This means that all the iron ions have the same coordination sphere. This suggests that the crystallographic ordering as revealed by the X-ray diagram is not due to a small fraction of a crystalline compound present in an otherwise amorphous substance but may be attributed to the whole material.

For the interpretation of the Mössbauer spectrum of the iron(III)-oxide hydrate a comparison with the spectra of the other iron(III)-oxygen compounds

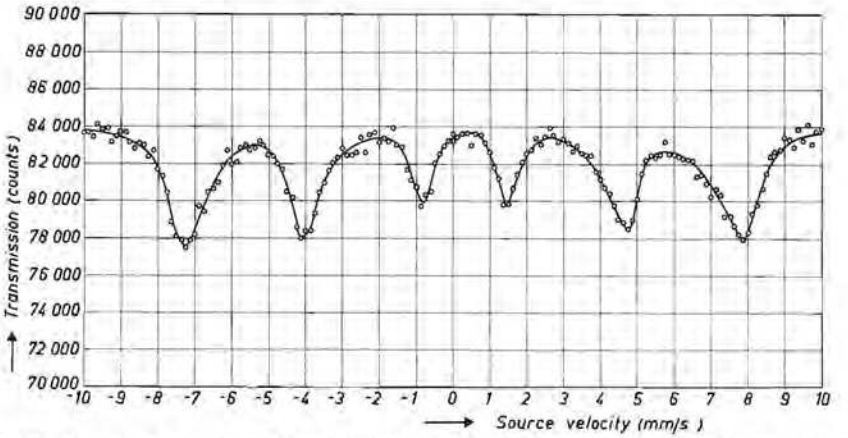

Fig. 4.4. Mössbauer spectrum of iron (III)-oxide hydrate at the temperature of liquid helium.

may give valuable information. α-Fe_2O_3 in the coarse crystalline form has a six-line spectrum in accordance with its antiferromagnetic structure. Below 300 °K α- and β-FeOOH also show hyperfine splitting indicating that they are antiferromagnetic. At room temperature however the latter compound is paramagnetic. γ-FeOOH is paramagnetic down to 110 °K: the spectrum shows quadrupole splitting. A detailed description of the α-FeOOH spectra is given in ref. 4–14; magnetic hyperfine splitting occurs at room temperature. In table 4-III the Mössbauer spectra of the oxides mentioned above are compared with that of the iron(III)-oxide hydrate of the present investigation.

TABLE 4-III

Mössbauer spectra of various Fe(III)-oxygen compounds at room temperature *)

	spectrum	quadrupole splitting Q (mm/s)	isomer shift I.S. (mm/s)	ref.
α-FeOOH	H.F.S.	0·38	0·27	4–14
β-FeOOH	Q	0·62	0·17	4–14, 18
γ-FeOOH	Q	0·54	0·22	4–14
δ-FeOOH	—	0	0·19	4–14, 18
α-Fe_2O_3	H.F.S.	0·40	0·20	4–16
γ-Fe_2O_3	H.F.S.	0·03	0·16	4–16
ferritine	Q	0·60	0·24	4–17
$Fe_2O_3.nH_2O$	Q	0·62	0·20	4–15

*) The results are all compared to a source of ^{57}Co in Pd.

The table shows that γ-Fe_2O_3 has a slight isomer shift compared to the other compounds, included the oxide hydrate under study. This compound has about a third of its iron ions in tetrahedral positions; this could be the reason for the low I.S. The quadrupole splitting of the oxide hydrate is large compared to that of nearly all compounds except β- and γ-FeOOH. The large Q value, according to Kundig and Ando, is probably due to the small size of the particles [4-10]. They assumed that the quadrupole spectrum is the sum of two quadrupole spectra: a spectrum caused by the ions lying in the surface of the particles and another caused by the ions lying in the particles. The smaller the particle the larger the contribution of the surface ions; for α-Fe_2O_3 the quadrupole splitting increases whereas the isomer shift decreases with decreasing particle size. Based on these results the quadrupole splitting measured for the iron(III)-oxide hydrate—then considered as a hydrated α-Fe_2O_3—should correspond to a particle size of about 125 Å. Hence it seems probable that the hydrate has a structure different from α-Fe_2O_3, as the actual observed diameter of the particles lies between 20 and 30 Å. Although a correct interpretation of the Mössbauer spectrum is hampered by the effects due to the small particle size, the tentative conclusion can be drawn that all iron ions occupy a similar octahedral position. The conclusion that all iron ions occupy the same position could be drawn from the high absorption efficiency (peak height). The conclusion that the iron ions occupy an octahedral position is based on the values of the isomer shift and the quadrupole splitting which most probably are large compared to those of γ-Fe_2O_3 and δ-FeOOH where iron also occupies tetrahedral lattice sites.

4.3. Magnetic measurements

4.3.1. *Superparamagnetic behaviour*

The superparamagnetic behaviour initially observed on ultrafine Ni powders was explained by Néel by assuming that each powder particle has a constant but freely rotating magnetic moment [4-20]. A powder composed of such particles when placed in a magnetic field attains a magnetization which is described by the Langevin function

$$\sigma = \sigma_s \left(\coth a - \frac{1}{a} \right), \quad \text{where} \quad a = \frac{mH}{kT},$$

m is the magnetic moment of a single particle and σ_s stands for the saturation magnetization. When $a < 1$ the function may be simplified by: $\sigma = \sigma_s a/3$. In the case of ferro- and ferrimagnetic materials the origin of the particle moment is clear. The fact that also small particles of an antiferromagnetic compound can have a magnetic moment, according to Néel, is a result of statistical deviations in the number of sites of the sublattices which are occupied by cations [4-21]. According to Néel, when the particles are formed very quickly the difference in the number of ions occupying one sublattice compared to the other equals

$\sqrt{N}$, when N is the number of metal ions in the particle. Assuming that all ions interact with each other, the magnetic moment of each particle then equals $\mu\sqrt{N}$, when μ is the magnetic moment per cation. The saturation (per gramme material) of a powder composed of these particles is given by

$$\sigma_s = \frac{N_A \mu \sqrt{N}}{MN},$$

where N_A is Avogadro's number and M is the mole weight. Hence ($a < 1$)

$$\sigma = \frac{N_A \mu \sqrt{N}}{MN} \frac{\mu H \sqrt{N}}{3kT} = \frac{N_A \mu^2 H}{3MkT} = \chi H.$$

The magnetic susceptibility χ is thus independent of the number of cations per particle, and is not much different from the value found for the same number of paramagnetic ions in the free state.

In this description it is assumed that the number of iron ions occupying the sites of the two magnetic sublattices is determined by a random process. It could well be, however, that the introduction of one stacking fault in the growing particle activates the formation of another one and hence the difference in the number of iron ions occupying the sublattices could well exceed $\sqrt{N}$. There is also a second possible explanation for a difference of more than $\sqrt{N}$ ions in the sublattices which especially holds for a somewhat large particle, $d \approx 100$ Å. As discussed by Néel [4-21]), when the particle is perfectly crystalline there still remains a number of unpaired cations when the particle contains an odd number of lattice planes; the difference between the number of occupied sites in both sublattices is then no longer $N^{1/2}$ but instead $N^{2/3}$. In the latter case

$$\sigma = \frac{1}{2} \frac{N_A \mu N^{2/3}}{MN} \frac{\mu N^{2/3} H}{3kT} = \frac{N_A N^{1/3} \mu^2 H}{6MkT},$$

the factor $\frac{1}{2}$ accounting for the fact that only half of the particles contains an unequal number of lattice planes. Accordingly the susceptibility might be exceedingly high for powders composed of small single crystals. Yet there are several reasons why this will not be the case. In the first place, when $\mu N^{2/3} H/kT > 1$ saturation occurs; for FeOOH this would be the case at room temperature and in a field of 10^4 Oe for $N \approx 1000$ Fe(III) ions. Second, there is a certain temperature below which the magnetic vector is no longer free to move. This blocking temperature is determined by $KV = kT_B$, where K is the magnetic-anisotropy energy per unit volume (V). For α-Fe_2O_3 the value of T_B will be above room temperature for particles with a size larger than 100 Å.

Superparamagnetic behaviour has been found for ultrafine powders of various oxides such as NiO, Fe_2O_3, $NiFe_2O_4$ and $CoFe_2O_4$ by measuring the relation between magnetization and field strength at various temperatures [4-22-24]).

These investigations are all performed with oxide particles prepared via de-

composition of starting compounds (e.g. α-FeOOH). Due to the pseudomorphic character of these reactions the newly formed crystallites are still coherent; the crystallite size as determined from X-ray line broadening gives only an average value of N. Yet the results are in rather good accord with theory.

Magnetic measurements on ultrafine non-coherent particles have hitherto only been carried out on the material ferritine [4–17]. This is a biological material consisting of iron(III)-oxide–hydrate particles of 50 Å surrounded by a mantle of protein. For this material also a superparamagnetic behaviour has been found; the results show that a strong antiferromagnetic magnetic coupling in such small particles is well possible.

The material under investigation also consists of very small discrete particles which are bound together by only weak forces. The theoretical considerations of Néel may be expected to apply to these particles and a further quantitative treatment based on Néel's theory seems allowed.

On the basis of the theory outlined above it might well be that the superparamagnetic particles, upon recrystallization, show an increase of the susceptibility due to the fact that they slightly grow and become bounded by perfect lattice planes. Upon further growth, when a certain critical size is reached (50-100 Å) the susceptibility decreases again (blocking). As will be shown in chapters 5 and 7 a study of the magnetic properties can give useful information for an elucidation of the mechanism of the recrystallization of iron-oxide hydrate taking place in aqueous solutions or upon heating in air.

4.3.2. *Result and discussion*

Magnetic measurements are done on iron (III)-oxidehydrate according to a method described in the literature [4–25].

The experimental data of the magnetic measurements are given in fig. 4.5. Above 30 °K the curves are reversible. The magnetic moment per gramme, σ, is plotted as a function of the field strength H for different temperatures, T. It appears that the data for temperatures above 30 °K can be brought onto one curve by plotting σ as a function of H/T. This curve (fig. 4.6) can be described by the Langevin function. The values of σ_s and m can be found by the following method: $\log \sigma$ is plotted as a function of $\log (H/T)$ and $\log (\coth a - 1/a)$ as a function of $\log a$, on separated sheets, where a varies from 0·01 to 10. One sheet is moved over the other until the curves coincide. In this way all experimental data are used for the determination of the parameters. This leads to a value of $\sigma_s = 11$ gauss cm^3/g and $m = 1{\cdot}49.10^{-18}$ erg/Oe, which is large compared to the moment of an iron(III) ion. The corresponding Langevin curve has been drawn in fig. 4.6. From this figure it is clear the material is superparamagnetic.

From the saturation magnetization and the magnetic moment per particle, the number of particles present in one gramme of material can be calculated as

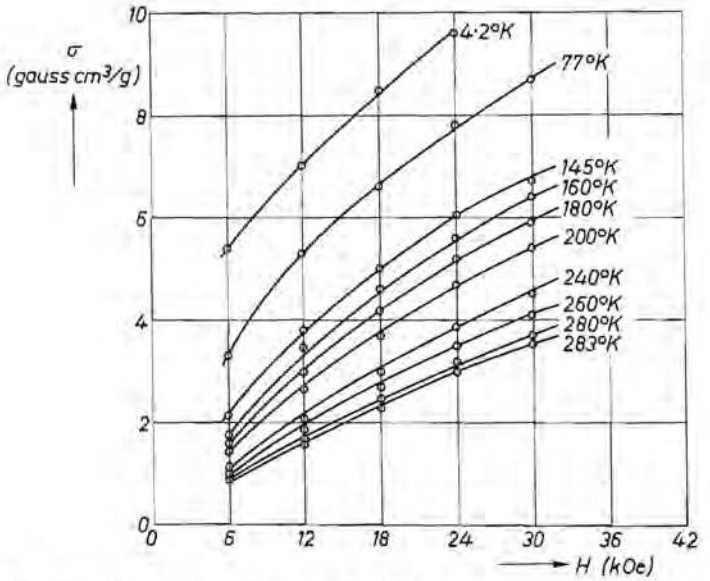

Fig. 4.5. The magnetization σ as a function of the field strength H at various temperatures.

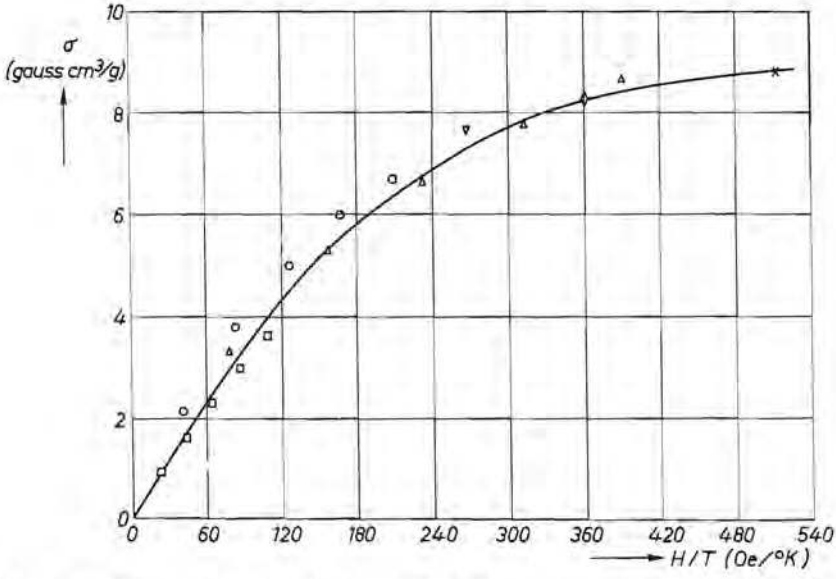

Fig. 4.6. The magnetization σ as a function of H/T. Measurements are carried out at various field strengths at: □ 293 °K; ○ 146 °K; △ 77 °K; and at a fixed field strength of 18 000 Oe but at various temperatures: ▽ 68 °K; ◇ 50 °K; × 30 °K. The drawn curve represents a Langevin function with $m = 1{\cdot}49.10^{-18}$ erg/Oe and $\sigma = 11$ G cm^3/g.

$$\frac{\sigma_s}{m} = \frac{11}{1{\cdot}49.10^{-18}} = 7{\cdot}4.10^{18} \text{ particles/gramme.}$$

The specific density of the material as measured is about 4 g/cm^3. From the number of particles per gramme the average particle size, d, can be calculated:

$$d = \left(\frac{10^{24}}{4 \times 7{\cdot}4.10^{18}}\right)^{1/3} = 30 \text{ Å}$$

for particles with a cubic shape (when taking into consideration that the material contains about 15% H_2O, probably adsorbed on the particle surface, the calculated particle diameter would be somewhat smaller). This average particle size estimated from the magnetic measurement is in good agreement with that obtained from measurements with the electron microscope, viz. 20-30 Å (fig. 4.3).

The average number of iron ions present per particle (as derived from the magnetic measurements) is equal to

$$\frac{N_A}{(\sigma_s/m)\,(M/2)} = \frac{6.10^{23}}{7{\cdot}4.10^{18} \times 80} \approx 1000 \text{ iron ions/particle,}$$

where N_A = Avogadro's number and M = mole weight Fe_2O_3. The average contribution of an iron ion to the particle moment then amounts to

$$\frac{1{\cdot}49.10^{-18}}{1000} = 1{\cdot}49.10^{-21} \text{ erg/Oe} = 0{\cdot}16 \text{ Bohr magnetons.}$$

This value, low compared to the value of 5 μ_B for the iron ion in the paramagnetic state, can be explained by assuming that there is an antiferromagnetic coupling between the magnetic moments of the iron ions. The existence of a magnetic ordering in the compound under study at the temperature of liquid helium has been demonstrated with the aid of Mössbauer spectroscopy. At these low temperatures the spectra show magnetic hyperfine splitting. The absence of hyperfine splitting at room temperature must then be considered as due to the high frequency of the rotation of the magnetic vector, compared to the lifetime of the excited level, 10^{-8} s. The existence of a magnetic moment in an antiferromagnetic compound can be explained, according to Néel, as a result of unequal numbers of iron ions in the sublattices due to the small particle size. Assuming this difference equal to $\sqrt{N}$, N being the number of iron ions per particle, then the calculated number of iron ions present per particle should be

$$N = \left(\frac{\text{moment per particle}}{\text{moment per } Fe^{3+} \text{ ion}}\right)^2 = \left\{\frac{1{\cdot}49.10^{-18}}{5 \times 9{\cdot}3.10^{-21}}\right\}^2 = 1050 \text{ iron ions/particle.}$$

This is in agreement with the results given above and hence the assumption

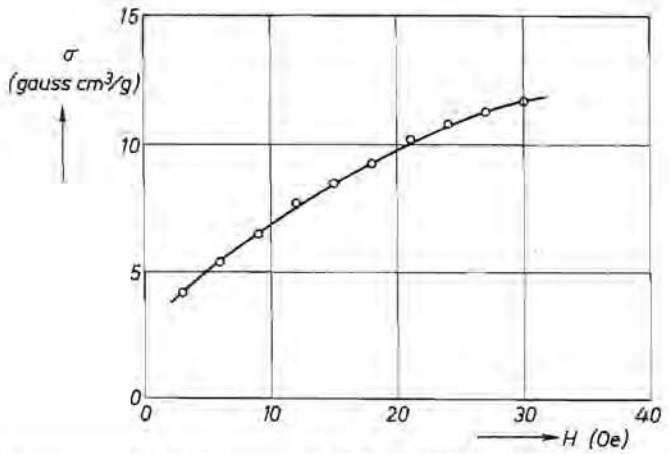

Fig. 4.7. The magnetization σ as a function of the field strength at the temperature of liquid helium. The material is cooled down in a field of 30 000 Oe.

seems justified. The experimental results indicate that above 30 °K the material is superparamagnetic; evidently the magnetic-anisotropy energy is small compared to kT. On cooling such a paramagnetic material in a strong field to temperatures below the blocking temperature, it acquires a remanent magnetization. This is verified for the material under study by cooling it down to 4·2 °K in a field of 30 000 Oe, and subsequently reducing the applied field: the magnetization of the sample then diminishes but a remanent magnetization remains, fig. 4.7. This remanence is much smaller than half of the saturation magnetization which is a surprising result as it might be expected from the occurrence of a six-line Mössbauer spectrum at 4·2 °K that the blocking temperature of the particles lies above 4·2 °K. This low remanence is probably due to an interaction between the particle moments. This is frequently found for ferromagnetic powders, c.f. ref. 4–26.

4.4. Summary

Iron(III)-oxide hydrate has been investigated using radiation of a comparatively short wavelength, MoKα radiation ($\lambda = 0{\cdot}71$ Å), an X-ray diagram is obtained consisting of at least twenty, broadened, reflections. This indicates that the material is at least partially crystalline. The diagram differs from the diagrams of the hitherto known iron(III)-oxygen compounds. Due to the many uncertainties regarding the exact spacings of the reflections and the composition of the compound, either FeOOH or hydrated Fe_2O_3, an elucidation of the structure is not possible.

Mössbauer spectroscopy reveals that all iron ions have the same coordination sphere, probably being octahedral: the spectrum shows a quadrupole splitting with rather sharp lines to which approximately all iron ions contribute. This

suggests that all particles may be considered as being crystallites. The quadrupole spectrum is a result of the superparamagnetic character of the material. The superparamagnetic character can be verified by measuring the magnetization as a function of H/T. Assuming a random occupation of both lattice sites, it could be estimated from the magnetic results that about 1000 iron ions are present in one crystallite.

REFERENCES

4–1) A. Simon and Th. Schmidt, Kolloidz. **36**, 65, 1925.
4–2) O. Glemser and G. Rieck, Z. anorg. allg. Chem. **297**, 175, 1958.
4–3) V. Cáslavská, V. Frei and A. Blazek, Coll. Czech. chem. Comm. **27**, 2168, 1962.
4–4) H. B. Weiser and W. O. Milligan, J. phys. Chem. **44**, 1081, 1940.
4–5) J. M. van Bemmelen and E. A. Klobbie, J. prakt. Chem. **46**, 497, 1892.
4–6) R. Collongues and J. Thery, Bull. Soc. chim. France, 1141, 1949.
4–7) A. A. van der Giessen, J. inorg. nucl. Chem. **28**, 2155, 1966.
4–8) A. Z. Hrynkiewicz, D. S. Kulgawczuk and K. Tomala, Phys. Letters **17**, 93, 1965.
4–9) T. Nakamura et al., Phys. Letters **12**, 178, 1964.
4–10) T. Nakamura and S. Shimizu, Bull. Inst. chem. Res. Kyoto Univ. **42**, 299, 1962.
4–11) A. M. van der Kraan and J. J. van Loef, Phys. Letters **20**, 614, 1966.
4–12) W. J. Schuele, S. Shtrikman and D. Treves, J. appl. Phys. **36**, 1010, 1965.
4–13) G. W. van Oosterhout and J. Visser, Anal. chim. Acta **33**, 330, 1965.
4–14) M. J. Rossiter and A. S. M. Hodgson, J. inorg. nucl. Chem. **27**, 63, 1965.
4–15) A. A. van der Giessen, J. G. Rensen and J. S. van Wieringen, J. inorg. nucl. Chem., in print.
4–16) J. S. van Wieringen, private communication.
4–17) A. Blaise, J. Chappert and J. L. Girardot, C.R. Acad. Sci. Paris **261**, 2310, 1965.
4–18) I. Dészi, L. Kezthelyi, D. Kulgawczuk, B. Mcinaí and N. A. Eissa, Phys. Stat. sol. **22**, 617, 1967.
4–19) W. Kündig and K. J. Ando, Czech. J. Phys. **B17**, 467, 1967.
4–20) L. Néel, C.R. Acad. Sci. Paris **228**, 664, 1949.
4–21) L. Néel, J. phys. Soc. Japan Suppl. B-1, **17**, 676, 1962.
4–22) K. M. Creer, J. phys. Soc. Japan Suppl. B-1, **17**, 690, 1962.
4–23) J. Cohen, K. M. Creer, R. Pauthenet and K. Srivastava, J. phys. Soc. Japan Suppl. B-1, **17**, 685, 1962.
4–24) J. T. Richardson and W. O. Milligan, Phys. Rev. **102**, 1289, 1956.
4–25) G. W. Rathenau and J. L. Snoek, Philips Res. Repts **1**, 239, 1946.
4–26) C. P. Bean and J. W. Livingstone, J. appl. Phys. Suppl. **30** (4), 120S, 1959.

5. RECRYSTALLIZATION OF THE IRON(III)-OXIDE–HYDRATE GEL IN AQUEOUS SOLUTIONS

5.1. Discussion of the literature

The crystallographic study of the iron-oxide–hydrate gel, prepared as described in chapter 3, is hampered by the fact that the particles are so small that in the X-ray diagram considerable line broadening occurs. It would therefore be of interest to have this compound in the form of larger crystals. Crystal growth in contact with an aqueous solution might be a possible method for the preparation of larger crystals, provided that nuclei of another phase, a more stable one with respect to the first compound, are absent. In the presence of such nuclei, instead of crystal growth, recrystallization towards this more stable phase might well occur. A search of the literature shows that the latter crystallization mechanism is dominant in many cases; ageing of partially hydrolyzed Fe(III) solutions or of gels may finally lead to α-Fe_2O_3, α-FeOOH or β-FeOOH, depending on the experimental conditions. Anions greatly determine which compound will be formed. Whereas in the presence of ClO_4^- and NO_3^- ions — which are considered to be unable of complex formation with Fe^{3+} ions — α-Fe_2O_3 and α-FeOOH are formed [5-1,2]), the presence of Cl^- ions may lead to β-FeOOH [5-3,4]). These compounds are formed with particles that are of submicroscopic dimensions even after prolonged ageing in acid solutions. Heller et al. showed with the aid of light scattering that in $FeCl_3$ solutions colloidal particles are formed with an elongated shape[5-5,6,7]). Similar results have been found by Lamb and Jaques [5-8]). In partially hydrolyzed solutions of $Fe(ClO_4)_3$, as found by Feitknecht and Michaelis, needle- and platelet-shaped particles of α-FeOOH or γ-FeOOH are formed on ageing, together with more or less spherical α-Fe_2O_3 and spherules with a size of 50 Å which are supposed to be amorphous [5-9]).

Gels, when left in contact with the mother liquor, recrystallize on prolonged standing with the formation of α-Fe_2O_3, α-FeOOH or a mixture of both, also with particles of submicroscopic dimensions, independent of the experimental conditions.

Before the introduction of electron microscopes of sufficient resolution, Krause and co-workers developed a number of chemical methods to obtain some knowledge of the morphology and the structure of the particles present in the gel and its ageing products. According to Krause those OH groups of the oxide hydrate which are in contact with the solution react with Ag^+ ions in boiling alkaline solutions to give a ferrite, e.g. $Ag_2Fe_2O_4$ [5-10]), whereas the OH groups built in the lattice, such as in α-FeOOH, do not react with Ag^+ ions. From this kind of experimental evidence the conclusion was drawn that the gel consists of small colloidal particles, being linear polymers of the type

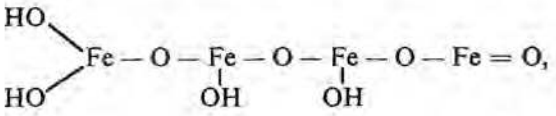

see for instance refs 5–11, 12. These chain polymers, at pH = 11, polymerize to larger units, which on further ageing form associates, still being amorphous. These finally crystallize under the formation of α-Fe_2O_3. The amount of goethite (α-FeOOH) — if present in the reaction mixture — can be detected by treating the samples with HNO_3 (32·5%) in which the goethite does not dissolve, unlike the polymers. The work of Krause has been disputed by Feitknecht and Glemser, who stated that physical methods instead of chemical methods should be used for the elucidation of the structure and morphology of the gel and its recrystallization products [5-13,14]).

The pH affects which compound will be formed, and also has considerable influence on the rate of the crystallization process. The formation of α-Fe_2O_3 occurs most rapidly at pH = 11; at still higher pH α-FeOOH is formed. In solutions containing NaOH in concentrations greater than 4-molar the recrystallization is very slow; even after some 50 days no crystallization occurs [5-15]). This has also been found by Weiser and Milligan [5-16]). The latter authors, regarding the colour change which occurs upon ageing (from brown to red), also found a slowing down of the crystallization rate in the presence of NH_4Cl when working with gels prepared from $FeCl_3$. Using the same criterion Krause found that also cations can influence the ageing process; when the solution of the iron salt is made alkaline with NH_4OH the yellow intermediate product, observed when using NaOH, could not be observed.

As can be expected, the temperature is of considerable significance. Below 100 °C the recrystallization takes place very slowly; in many cases even after one year no equilibrium has been reached. At temperatures above 100 °C, however, the reaction rate is much higher. Krause succeeded in the rapid conversion of the "amorphous" gel into α-FeOOH at 150 °C [5-17]).

Regarding the morphology of the intermediate and the end products of the recrystallization process, the work of Steele and Wefers may be mentioned here. Steele observed the formation of particles of cubic shape (of about 1 μ) composed of much smaller primary particles, when a gel prepared from $FeCl_3$ was hydrothermally recrystallized[5-18]). Wefers describes the morphology of the crystals obtained upon ageing a gel in slightly alkaline solutions [5-2]). He found that, at 20 °C, mainly needle-shaped α-FeOOH is formed and, above 70 °C, hexagonal α-Fe_2O_3. Some part of the crystals often consist of α-FeOOH platelets grown topotactically on the α-Fe_2O_3 crystals.

A very sensitive measure for the study of changes that the material undergoes during recrystallization is the magnetic susceptibility. Aumeras and Mounique studied the change of the susceptibility upon ageing of a partially hydrolyzed

$FeCl_3$ solution [5-19]). Chevallier and Mathieu showed that the magnetic properties of a gel largely depend upon the way the hydrolysis has been carried out [5-20]): when precipitating a gel with more concentrated NaOH, preparations are obtained with a higher χ value. Upon ageing, the gel's susceptibility increases but after ten days of ageing at room temperature the susceptibility decreases again. The same phenomena have been found by Albrecht and Wedekind for gels prepared with NH_4OH [5-21]). These authors attributed the maximum in the susceptibility to an intermediate product formed during ageing. They did not succeed in obtaining more details of this alleged compound.

Summarizing it can be said that the ageing of the gel proceeds via a series of intermediate products towards α-FeOOH and α-Fe_2O_3.

In the next sections investigations are described, which were carried out to get a better understanding of the mechanism underlying the ageing phenomena occurring in partially hydrolyzed colloidal iron(III) solutions or in iron-oxide–hydrate gels.

5.2. Experimental

Ageing experiments

200 g Fe $(NO_3)_3$.9aq. (Merck, p.a.) are dissolved in 500 ml of deionized water in a beaker of 1 l, which is placed in a thermostat kept at 20 °C. After one hour the alkali is added to the solution from a burette at a rate of two drops per second, while vigorously stirring and bubbling N_2 gas through it. Three preparations are made with resp. conc. ammonia (prepared as mentioned in chapter 1), 4-molar ammonia (prepared by dilution of the concentrated ammonia) and 3·5-molar NH_4HCO_3 prepared by leading CO_2 gas into the ammonia. The alkali is added until the solution has reached a pH = 2·2. The pH meter is equipped with electrodes as mentioned in chapter 1. The solutions are kept in the thermostat; at time intervals of 0, 48 and 340 hours portions are taken from it which are further treated with concentrated ammonia. The gel thus obtained is filtered off by suction and dehydrated as described in chapter 3.

In another series of experiments the pH is brought directly to pH = 7·5; the sample is then placed in a conical flask with a ground stopper fitted with a water lock in order to prevent the entrance of CO_2.

Physical measurements

Viscosity is measured using an Ubbelohde viscosimeter. Electron micrographs, X-ray diffractions and magnetic measurements are all done as described in chapter 4.

5.3. Ageing phenomena occurring in partially hydrolyzed solutions

5.3.1. *Crystallographic properties of the ageing products*

A series of hydrolysis experiments has been carried out by adding, at room temperature, concentrated NH_4OH, 4-molar NH_4OH and 3·5-molar NH_4HCO_3 to a 1-molar solution of $Fe(NO_3)_3$ until pH = 2·2, which corresponds to about 2 OH^- ions per Fe^{3+} ion. At this pH no precipitate is formed. The solution is kept for 48-340 hours at room temperature. The products which are formed upon ageing are isolated from the solution by bringing the pH to 7·5, which leads to the formation of a gel in which the particles, formed during ageing, are dispersed.

When the hydrolysis is carried out incompletely ($OH^-/Fe^{3+} < 3$) the solution remains acid. In such an acid solution changes take place on prolonged standing at room temperature and from the decrease of the pH it appeared that even after 340 hours no equilibrium was established. These changes are due to a recrystallization which the primarily formed particles undergo. Already after 48 hours the X-ray diagram is different from that of the gel. After a period of 340 hours the X-ray diagram shows a number of broadened lines which are typical for α-FeOOH; the observed reflections all could be indexed by taking an orthorhombic unit cell with $a_0 = 4{\cdot}64$, $b_0 = 10{\cdot}0$ and $c_0 = 3{\cdot}03$ Å. The X-ray data are presented in table 5-I.

Besides the reflections 1-11 also a number of very weak and very broadened reflections are observed, a-b ,which can be indexed with less certainty due to the large error of θ involved. It is clear that in the presence of NH_4^+ and NO_3^- ions together with or without CO_3^{2-}/CO_2, upon ageing at room temperature only α-FeOOH is formed; no reflections can be observed which could not be indexed with the unit cell of this compound. Hence the formation of γ-FeOOH which was observed by Feitknecht et al. in their experiments [5-9], using $Fe(ClO_4)_3$ solutions, may be excluded in the hydrolyzed $Fe(NO_3)_3$ solutions. In case the hydrolysis is carried out with NaOH instead of NH_4OH similar results are obtained.

Particles having the same structure as observed in a non-aged gel (chapter 4) are not found in the form of larger crystals in the gels obtained from aged partially hydrolyzed solutions. It is conceivable that these primary particles do not grow at all. The formation of larger particles upon ageing is accompanied by a structural transformation, mainly into α-FeOOH.

5.3.2. *Morphology*

5.3.2.1. Tyndall effect

Valuable additional information about the size and shape of the primary particles present in partially hydrolyzed solutions can be obtained from a

TABLE 5-I

Reflections observed in a sample which is aged at room temperature for 340 hours. Hydrolysis has been carried out with NH_4OH, pH = 2·2, $OH^-/Fe^{3+} \approx 2$ (CoKα radiation), $a_0 = 4{\cdot}64$ Å, $b_0 = 10{\cdot}0$ Å, $c_0 = 3{\cdot}03$ Å

no.	d	I	$10^3 \sin^2\theta$ observed	$10^3 \sin^2\theta$ calculated	hkl
1	5·02	25	31·7	32·0	020
2	4·22	100	44·8	45·1	110
3	2·70	50	109·2	109·1	130
4	2·59	30	119·2	119·1	021
5	2·46	90	131·9	132·2	111
6	2·26	20	156·9	156·4	210
7	2·20	25	165·3	165·1	140
8	1·72	30	269·0	267·6	221
9	1·57	20	326·0	324·3	151
10	1·51	20	349·5	348·8	002-250
11	1·45	10	378·4	380·8	022
a	3·40		69	69	120
b	1·80		247	244	211
c	1·69		279	276	240
d	1·66		289	287	051

combined Tyndall-viscosity investigation. Solutions of 0·1-molar $Fe(NO_3)_3$ containing 3 mole/l $NaNO_3$ are hydrolyzed by the addition of 1-molar NaOH such that OH^-/Fe^{3+} equals 1·0 resp. 2·5. These partially hydrolyzed solutions are studied with the Tyndall microscope, the results of these observations are collected in table 5-II.

The Tyndall effect after 90 hours has been compared with that of a sol of the same concentration consisting of α-Fe_2O_3 particles of 1000 Å. Then a very bright beam is visible caused by countless moving particles, whereas in the hydrolyzed Fe^{3+} solution a much smaller number of particles is visible. These particles are less bright and move much more slowly indicating that they are either much larger than they appear to be or that they have a rough surface. From the Tyndall data it can be concluded that the initially formed particles have at least two dimensions smaller than 50 Å. As evidenced by the results of table 5-II these primary particles crystallize very slowly to larger ones.

TABLE 5-II

Tyndall effect in partially hydrolyzed Fe^{3+} solutions. The solution contains 0·1 mole/l $Fe(NO_3)_3$ and 3 mole/l $NaNO_3$

time elapsed after hydrolyzing (h)	Tyndall picture	
	$OH^-/Fe^{3+} = 1{\cdot}0$	$OH^-/Fe^{3+} = 2{\cdot}5$
0	very feeble, hardly visible beam	very feeble, hardly visible beam; also some aggregates which have disappeared after three hours
3	—	weak, bright blue beam, no particles are visible
90	—	bright yellow beam in which are visible separate particles; upon tenfold dilution with HNO_3 (2-molar), the Tyndall effect disappears entirely within 30 minutes

5.3.2.2. Electron microscopy

As mentioned in the preceding sections, on prolonged standing in hydrolyzed Fe^{3+} solutions α-FeOOH is formed. The habitus of the α-FeOOH crystals is mostly acicular; this shape is found for samples prepared by hydrothermal recrystallization of an iron(III)-oxide–hydrate gel (results not described in this thesis) and is also reported in the literature for samples prepared by hydrolysis of solutions of $Fe(ClO_4)_3$ with NH_4HCO_3. Yet electron micrographs reveal that the α-FeOOH crystals — developed in acid $Fe(NO_3)_3$ solutions in the presence of NH_4^+ or Na^+ ions — are not needle-shaped but instead they are platelets; in some cases these exhibit a hexagonal form but in the majority of cases the boundaries of the crystals are not sharp. An example has been given in fig. 5.1; the particles have a size mainly between 100 and 150 Å after 48 hours of ageing. From the line broadening in the X-ray diagram also a size of the particles can be estimated; correcting for the line broadening due to the apparatus from the relation $d = 0{\cdot}9\lambda/\beta_{1/2} \cos\theta$ a particle size of 100 Å is calculated for the same preparation as shown in fig. 5.1. After 340 hours of

Fig. 5.1. Electron micrograph of particles which are formed in a partially hydrolyzed 1-molar $Fe(NO_3)_3$ solution ($OH^-/Fe^{3+} \approx 2$) after ageing at room temperature for 48 hours. Hydrolysis has been carried out with 4-molar NH_4OH.

ageing the crystallite size is 130 Å. After 116 hours of ageing in a partially hydrolyzed solution containing Na^+ ions ($NaOH/Fe^{3+} \approx 1$) the crystals are smaller: $\approx$ 100 Å, see fig. 5.2.

5.3.2.3. Viscosity

It could well be that the primary particles are very thin acicular α-FeOOH crystals which, slowly, recrystallize under the formation of larger ones. If the initial particles were of acicular shape then the presence of these particles may give rise to a viscosity which is large compared to the viscosity of the solution containing the same amount of iron in the form of free ions. A number of viscosity data is graphically represented in fig. 5.3; the curves show that up to the point when on the average the ratio OH^-/Fe^{3+} is adjusted at about 2·5, the viscosity hardly changes. This indicates that the primary particles are more or less spherical, anyhow not acicular. This result agrees with the electron micrographs of the gel. Only on prolonged standing does the viscosity increase. It is remarkable that when the ratio OH^-/Fe^{3+} is smaller than 2·5 the crystallization takes place very slowly, whereas when $OH^-/Fe^{3+} > 2{\cdot}65$ a relatively rapid crystallization takes place, as indicated by the viscosity change. This evidently must be correlated with the fact that the colloid in the latter case is

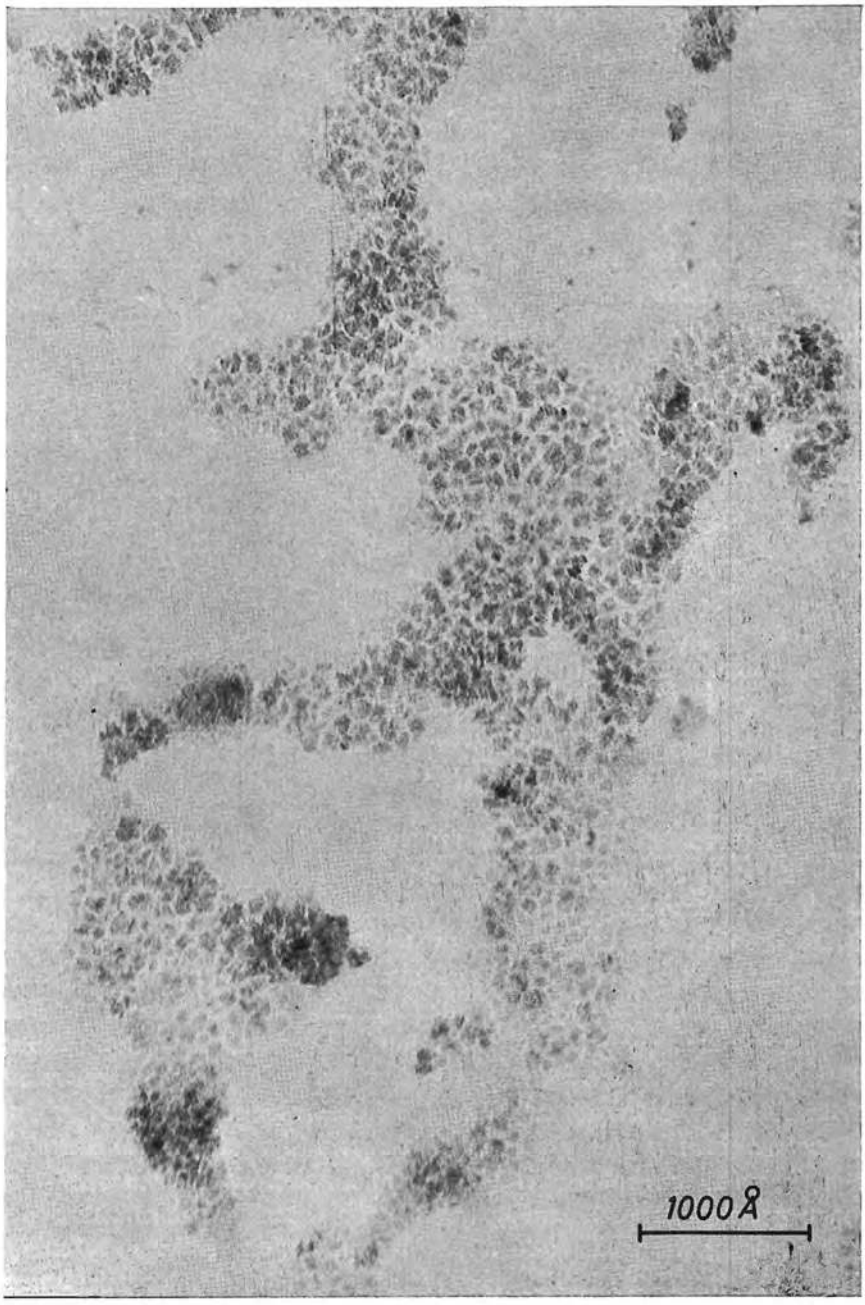

Fig. 5.2. Electron micrograph of the particles present, after ageing at room temperature for 120 hours, in a 0·1-molar $Fe(NO_3)_3$ solution partially hydrolyzed with 1-molar NaOH until $OH^-/Fe^{3+} \approx 1$.

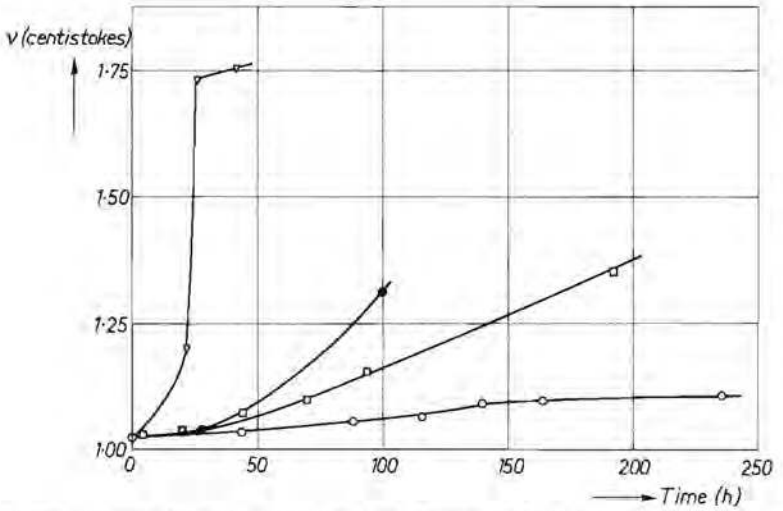

Fig. 5.3. The change of the viscosity at various degrees of hydrolysis upon ageing at room temperature:

OH^-/Fe^{3+}
○ 2·42
□ 2·48
• 2·54
▽ 2·65

more close to its point of electroneutrality. The increase of the viscosity points to the fact that recrystallization leads to particles with at least one dimension smaller than the other two, i.e. platelets or needles.

5.3.3. *Magnetic measurements*

In chapter 4 it has been discussed that for small particles the magnetic susceptibility is a valuable measure for their characterization. In antiferromagnetic ultrafine particles with random occupation of the sublattices the susceptibility is independent of the size of the particles. When, however, the particles grow and become bounded by lattice planes, the susceptibility increases until the particle has attained such a size that its blocking temperature lies above room temperature. As discussed in chapter 4, the critical size is probably 50-100 Å. Hence, after a certain ageing period, depending on the rate of crystal growth, one may find a higher as well as a lower value of the susceptibility compared to the starting value. The occurrence of either one of these possibilities can be demonstrated with the aid of two series of experiments.

One series of hydrolysis experiments is done by using alkaline solutions of various strengths in such a way that in all cases the ratio OH^-/Fe^{3+} equals about 2. The still acid solutions are aged at room temperature. The magnetic susceptibility is measured after various ageing times. The results of these experiments are collected in table 5-III. The table shows that upon precipitation

TABLE 5-III

Magnetic susceptibility per gramme, χ (c.g.s. units), for samples prepared by precipitation with conc. NH_4OH (A), 4-molar NH_4OH (B) and 3·5-molar NH_4HCO_3 (C) after varying ageing times; pH = 2·2

ageing time (h)	$\chi.10^6$ (c.g.s.)		
	A	B	C
0	115	100	60
48	80	55	50
340	70	50	50

without ageing the lower the OH^--ion concentration of the alkaline solution added, the lower will be the χ. This points to the formation of crystallites with less defects and is in accord with the results reported in chapter 1. Chevallier and Matthieu also found a lower χ when using more diluted solutions. As to ageing, one can see that the susceptibilities become smaller in all cases. The low χ value obtained after prolonged ageing for this series of experiments indeed can be attributed to the formation of particles with a size larger than the critical one. Electron micrographs and X-ray line broadening reveal that, as mentioned already, after 48 hours particles with a size of 100 Å are formed (series B).

In a second series hydrolysis is carried out with NaOH; the Fe^{3+} solutions are hydrolyzed to various degrees and kept at room temperature for 116 h. The results are collected in table 5-IV.

TABLE 5-IV

Magnetic susceptibility per gramme, χ (c.g.s. units) of samples prepared from solutions with various degrees of hydrolysis before further precipitation. The samples are aged for 116 hours at room temperature

$NaOH/Fe^{3+}$	$\chi.10^6$
0·0	70
1·0	80
2·0	95
2·5	100

All oxide-hydrate powders isolated from gels prepared with an intermediate ageing step have a higher susceptibility. The susceptibility is larger the higher the degree of hydrolysis before ageing. This can be understood by assuming that after partial hydrolysis and ageing, products are formed with a higher χ than when obtained by direct precipitation. The value of χ thus can be considered as due to the contribution of two compounds: the first compound, A, is formed during the ageing period and the second compound, B, is formed during the final precipitation. The latter compound is that which constitutes the gel and evidently has a $\chi = 70.10^{-6}$ c.g.s. units. Assuming the amount of the first compound to be proportional to the number of OH^- ions added, the χ value of the compound formed upon ageing — which will be designated "α-FeOOH" — can be calculated (table 5-V). The value of the magnetic

TABLE 5-V

Calculated χ values of "α-FeOOH" formed upon ageing in partially hydrolyzed solutions

no.	$NaOH/Fe^{3+}$	$\chi.10^6$
A	1	103
B	2	103
C	2·5	105

susceptibility of compound B calculated in this way is indeed constant. Evidently ageing in the partially hydrolyzed solutions proceeds in all cases along the same course: after 116 hours of ageing "α-FeOOH" has been formed with a susceptibility of 104.10^{-6}. The crystallites are about 100 Å and have a striated appearance, fig. 5.2.

5.4. Recrystallization of the iron(III)-oxide–hydrate gel in alkaline solution

5.4.1. *The rate of crystallization of the gel*

5.4.1.1. Chemical characterization

Gels of iron-oxide hydrate are prepared by adding ammonia to a solution of $Fe(NO_3)_3$, until pH = 7·5. Two gels are prepared: one at 20 °C, the other at 90 °C. Ageing is performed at 70 °C in the mother liquor.

In order to follow the ageing process quantitatively we characterize the extent of the ageing by the amount of material insoluble in nitric acid, as originally proposed by Krause[5–22,23]). The results of the solubility tests are collected in

TABLE 5-VI

The solubility in HNO_3 (1 : 1) of an iron(III)-oxide–hydrate gel after ageing in the mother liquor at 70 °C and pH = 7·5

ageing time (h)	% insoluble of a gel prepared at 20 °C	90 °C
0	1	16
4	2	38
24	9	56
48	—	64
72	—	71
96	61	73
150	—	—
170	—	77

table 5-VI. The solubility test gives different results for gels prepared at 20 °C and 90 °C. This indicates that gels prepared at 90 °C contain a substantial quantity of less soluble i.e. larger or better-ordered crystals than gels prepared at 20 °C.

It must be remarked that for these gels neither X-ray diffractions nor electron micrographs show significant difference. In this respect the solubility test is more sensitive.

5.4.1.2. Structural and morphological transformations

Recrystallization in general proceeds faster at higher temperature, as might be expected. If a gel, prepared at 90 °C, is aged for 24 h at 20 °C and pH = 7·5 no change can be perceived neither with X-ray diffraction nor with the electron microscope. Ageing at 70 °C, after 24 h results in the same unchanged X-ray diagram but electron micrographs reveal the presence of platelet-shaped structures with a diameter of 500 Å amidst a mass of the primary particles indicating that crystallization has started locally, see fig. 5.4. When the ageing is carried out at 90 °C, after 24 hours the X-ray diagram indicates the presence of substantial amounts of α-Fe_2O_3 together with some α-FeOOH. The material then is for the greater part converted into platelet-shaped crystals with a diameter of 500 Å, surrounded by the primary particles, fig. 5.5. Upon boiling, the gel is still more rapidly converted into α-Fe_2O_3 and α-FeOOH. These transformations are accompanied by a colour change from brown to red.

The influence of the pH is shown by ageing the same gel at a pH = 7·5 resp. 10·5. As mentioned after 24 hours of ageing at 70 °C and at pH = 7·5

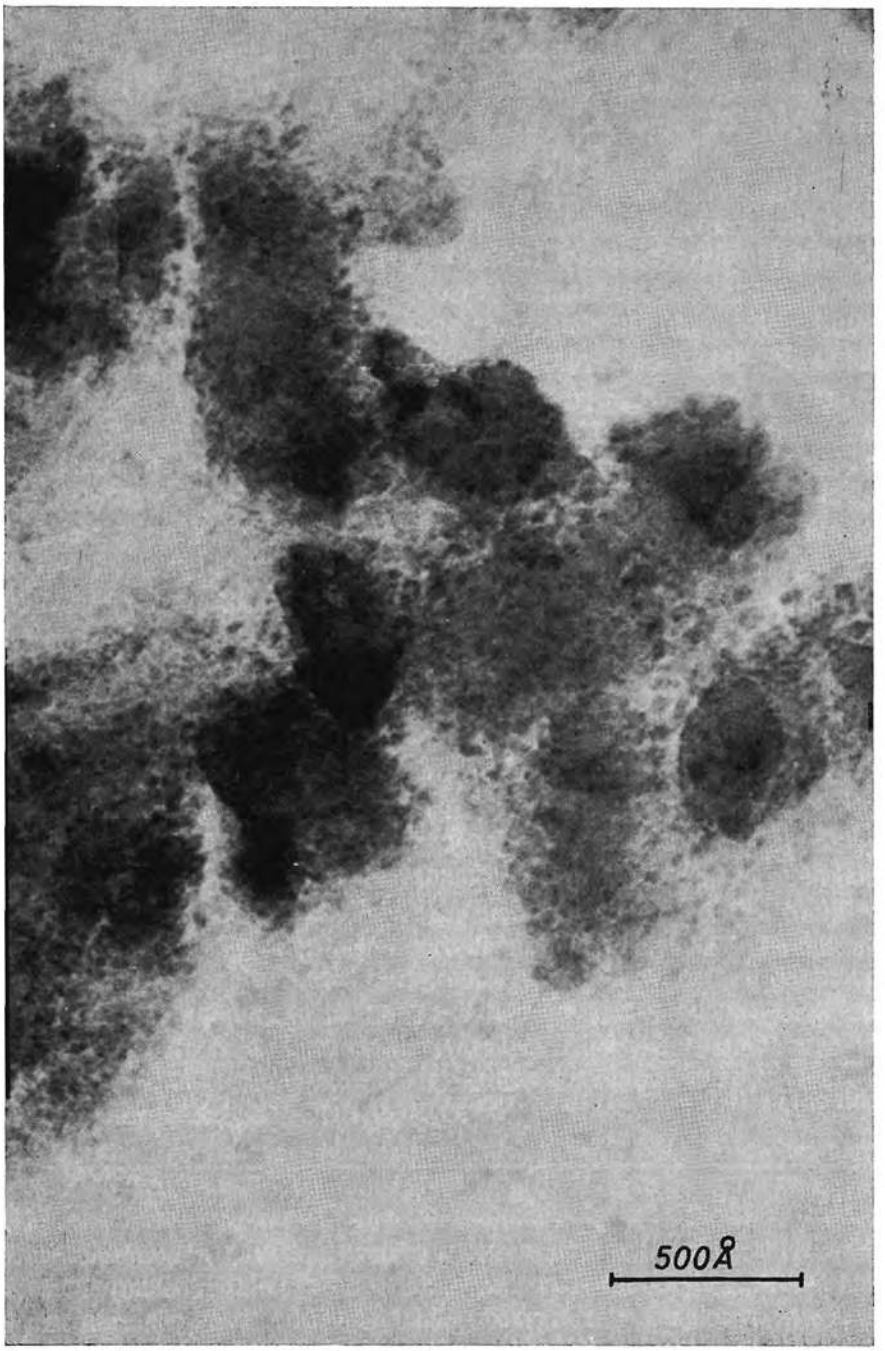

Fig. 5.4. Electron micrograph of a powder obtained after the ageing of a gel for 48 hours at 70 °C and pH = 7·5, in the mother liquor. The gel has been precipitated at 20 °C.

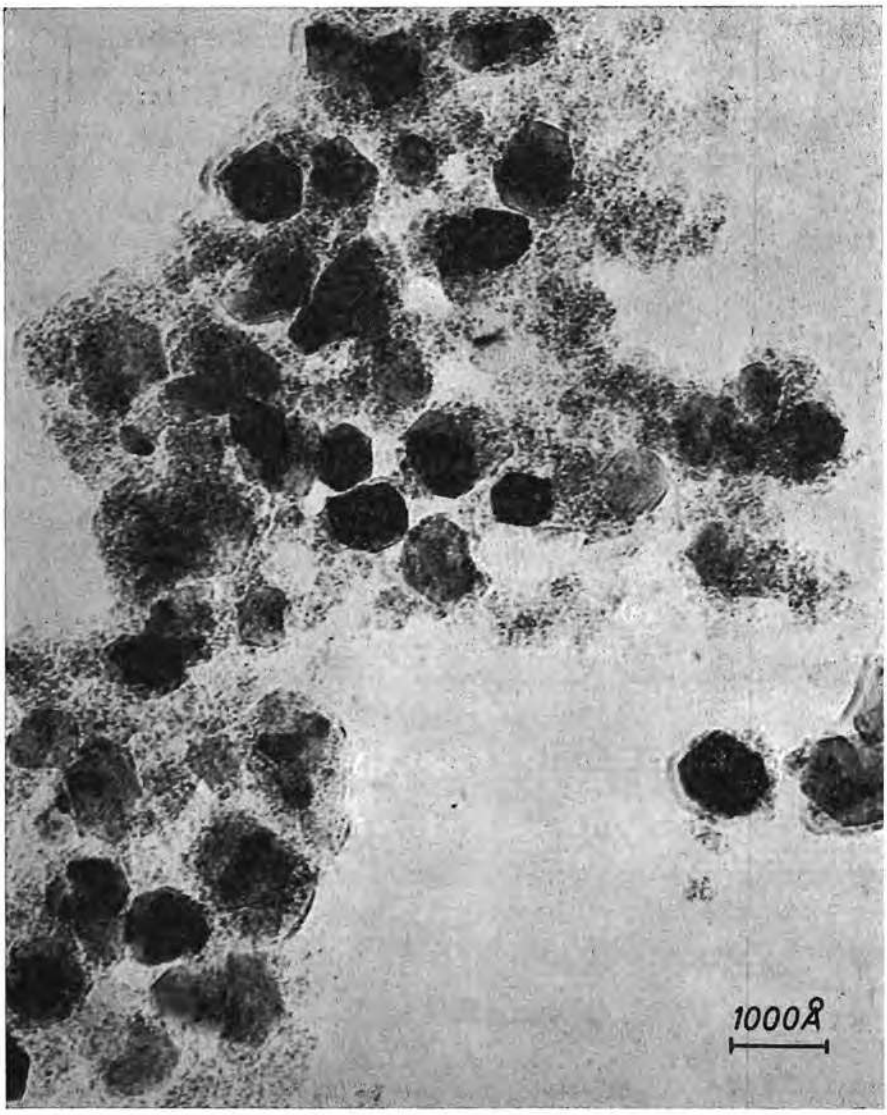

Fig. 5.5. Electron micrograph of a sample obtained by the ageing of a gel (precipitated at 20 °C) at 90 °C for 24 hours at pH = 7·5.

no change is observed in the X-ray diagram but after ageing during the same length of time at pH = 10·5 a well-developed X-ray diagram is observed which can be attributed to a mixture of α-FeOOH and α-Fe_2O_3.

When the ageing is carried out at high pH (> 10), the morphology of the crystals is different from those obtained at pH = 7. The α-Fe_2O_3 crystals then mostly have the shape of diamonds; part of them exhibit bars intergrown with

the basal plane of the Fe_2O_3 crystals. These bars, after Wefers [5-2]), can be attributed to α-FeOOH grown topotactically on the α-Fe_2O_3 crystal.

Remark. The diamond-shaped structures have been examined in more detail making use of stereo techniques. This revealed that the crystals have the shape of hexagonal bipyramids, see fig. 5.6. This is a remarkable result as this indicates that the iron oxide is crystallized in the hexagonal bipyramidal crystal class, whereas it is known from the literature that this compound usually crystallizes in the skalenohedral class [5-24]).

The residues insoluble in HNO_3 have been examined with the electron microscope. The photographs show the presence of three types of particles, see fig. 5.7:

(1) chains with a diameter of several hundred Å which seem to be composed of smaller particles having a more or less hexagonal shape;
(2) thin rods with a length of about 1000 Å, together with threadlike particles which are much smaller;
(3) particles with approximately the same size as the primary particles constituting the non-aged gel.

X-ray diagrams show the presence of α-Fe_2O_3 together with some α-FeOOH. It is assumed that the rods observed in the electron micrographs are α-FeOOH crystals and the chains are composed of α-Fe_2O_3; probably the very small particles are also α-Fe_2O_3.

5.4.2. *Mechanism of the ageing*

Generally a precipitate will recrystallize via the solution. In many cases the recrystallization rate is determined by the equilibrium concentration of the composing ions. The recrystallization processes occurring in partially hydrolyzed solutions of Fe^{3+} ions (pH < 3) may proceed via the solution. In these solutions a rather large concentration of Fe^{3+} ions exists. In case of complete hydrolysis, i.e. when gels are formed, the equilibrium concentration of Fe^{3+} ions is much lower: at pH = 7·5 the concentration of Fe^{3+} ions is smaller than 10^{-9} gion/l (see chapter 2). At such a low Fe^{3+} concentration a recrystallization via the solution seems hardly possible. In strongly alkaline solutions (pH > 10), however, such a mechanism seems again to be valid as pointed out by Wefers. This author succeeded in performing the conversion of α-Fe_2O_3 into α-FeOOH and vice versa, depending on the temperature. Equilibrium between the two phases exists at about 70 °C. The existence of this equilibrium clearly points to a recrystallization via the liquid phase in alkaline solutions with a pH above 10. This can be understood from the results of Feitknecht et al., who showed that in solutions with such a high pH the solubility of the iron compounds is considerably higher than at pH = 7 [5-1]). On condition of low solubility, i.e. for neutral solutions and at temperatures below 70 °C, it is

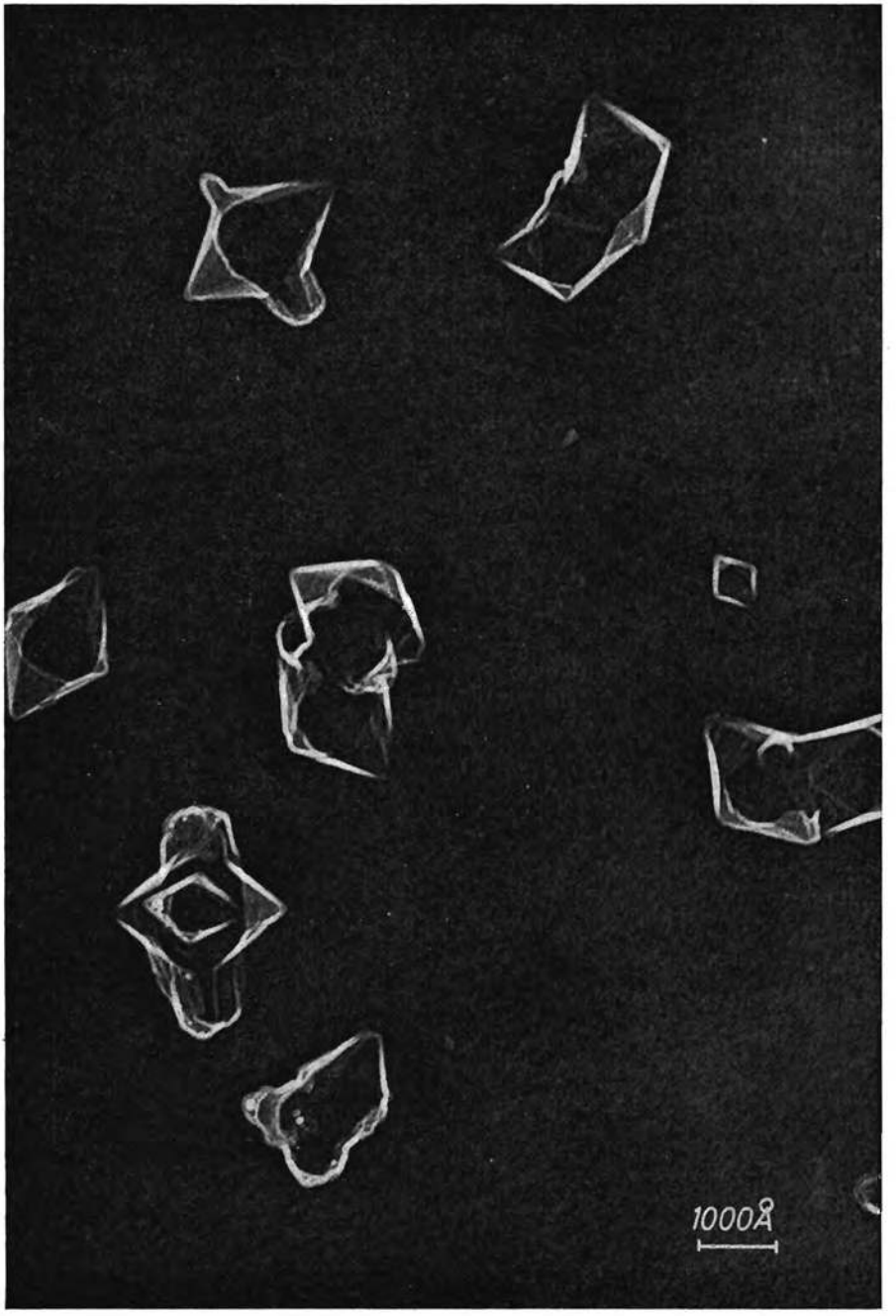

Fig. 5.6. Electron micrograph of a sample prepared by the ageing of a gel at 70 °C and pH = 11, showing α-FeOOH grown topotactically on α-Fe_2O_3.

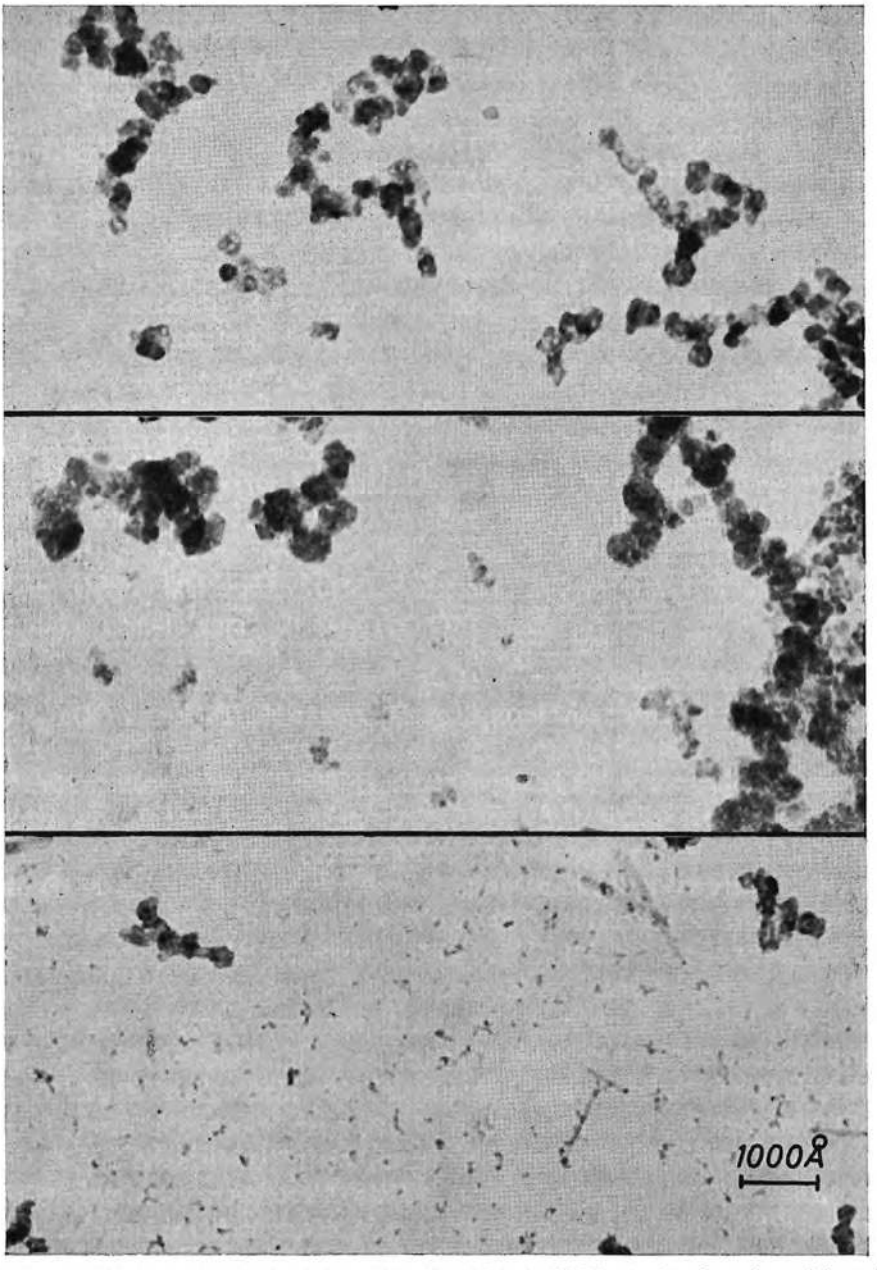

Fig. 5.7. Electron micrograph of the residue insoluble in HNO_3 1 : 1, of a gel precipitated at 90 °C and aged at 70 °C for 170 h at pH = 7·5.

assumed that a different mechanism governs the crystallization behaviour; the recrystallization takes place by a growing together of the primary particles. This mechanism is proposed on account of the following arguments.

(1) The equilibrium concentration of Fe^{3+} ions is extremely small ($< 10^{-9}$ gion/l) and hence material transport via the solution is not well possible.
(2) The recrystallization starts with the formation of small nuclei; after a few hours of ageing these often show sharp edges and well-defined (multiples of 60 °C) angles, but still are of irregular shape (fig. 5.4).
(3) After prolonged ageing particles are formed of irregular size that seem to consist of chains of intergrown smaller crystals with diameters varying between 100 and 500 Å. Contrarily, in partially hydrolyzed solutions where the recrystallization certainly occurs via the solution, after prolonged ageing the material is converted into single crystals of equal size.
(4) Under conditions of relatively high solubility i.e. at low as well as at high pH, α-FeOOH is obtained with platelet- or needle-shaped single crystals, whereas at pH $\approx$ 7 nearly exclusively α-Fe_2O_3 is obtained, consisting of the particles mentioned above. This also points to a different recrystallization mechanism.

5.4.3. *Magnetic properties*

The ageing mechanism has also been studied by measuring the change of the magnetic susceptibility. In fig. 5.8 a number of measurements are presented graphically, carried out on samples prepared at 20 °C and aged at pH = 7 and at 70 °C for different lengths of time. The figure clearly shows that there is a pronounced maximum in the χ-t curve. In the literature the occurrence of this maximum has been ascribed to an intermediate compound which should be formed during recrystallization; despite all effort this intermediate compound could not be isolated or detected with X-ray diffraction. It is not necessary

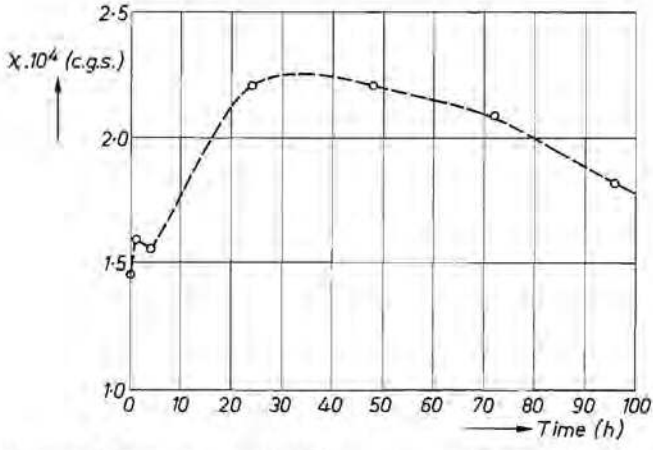

Fig. 5.8. The change of the magnetic susceptibility — measured at room temperature — with ageing time.

however to assume the formation of a new magnetic compound to account for the increase of the susceptibility χ. As discussed in chapter 4 the latter can be explained as a consequence of the growth of superparamagnetic particles.

The fact that only particle growth causes the increase of χ and not the formation of a new compound is further confirmed by X-ray diagrams which reveal that also in preparations having the maximum χ value only α-Fe_2O_3 and α-FeOOH are present.

5.5. Summary

In solutions of ferric nitrate which are partially hydrolyzed by the addition of NH_4OH, NH_4HCO_3, or NaOH, at room temperature slow transformations occur due to recrystallization of the initially formed products. At pH = 2 the final product is mainly α-FeOOH consisting of particles that are platelet-shaped with a diameter of about 100 Å as shown by electron micrographs. Viscosity measurements agree with this picture. The particles show a superparamagnetic behaviour which can be expected for α-FeOOH crystals of that size. The recrystallization of gels, which are formed upon complete hydrolysis of the Fe(III) solution, elapses very slowly. On standing for several days at pH = 7·5, α-Fe_2O_3 and some α-FeOOH are formed in the mother liquor.

In strongly alkaline solutions (pH > 9) the ageing is faster than at pH = 7; the final product is α-FeOOH. At high temperature (70 °C) and pH = 11, α-FeOOH and α-Fe_2O_3 are formed, which are intergrown topotactically.

Recrystallization in acid and strongly alkaline solutions is assumed to proceed via transport of ions through the solution. It is questionable whether recrystallization in neutral solutions follows the same path, the concentration of Fe^{3+} ions being extremely low, viz. $< 10^{-9}$ gion/l in this case. An alternative mechanism might be, in neutral solutions, that the formation of the comparatively large α-Fe_2O_3 crystals occurs mainly through agglomeration of the primary particles. This mechanism is suggested by the morphology of the growing particles. The fact that the final product is α-Fe_2O_3 may be also an indication for a mechanism different from that prevailing at pH < 3 and pH > 8, where α-FeOOH is formed.

When following the ageing at pH $\approx$ 7 with measurements of the magnetic susceptibility a strong increase in the latter is observed followed by a decrease upon prolonged ageing. The maximum χ value found is very high, viz. about 250.10^{-6} c.g.s. units, which may be compared with the value 16.10^{-6} of coarse crystalline α-Fe_2O_3. The magnetic results may be understood by assuming that the growing particles in the gel are superantiferromagnetic α-Fe_2O_3 crystals.

Growth of the primary particles, constituting the gels formed by direct precipitation without ageing, towards larger crystals has not been observed.

REFERENCES

5-1) H. Lengweiler, W. Buser and W. Feitknecht, Helv. chim. Acta **44**, 766, 1961.
5-2) K. Wefers, Ber. dt. ker. Ges. **43**, 703, 1966.
5-3) H. B. Weiser and W. O. Milligan, J. phys. Chem. **40**, 1, 1936; **40**, 1195, 1936.
5-4) J. H. L. Watson and W. Heller, J. phys. Chem. **66**, 1757, 1962.
5-5) W. Heller, C.R. Acad. Sci. Paris **201**, 831, 1935.
5-6) W. Heller and H. Zocher, Z. phys. Chem. **A166**, 365, 1933.
5-7) J. H. L. Watson, W. Heller and L. E. Poplawski, Proc. 3rd Eur. regional Conf. Electr. Micr., Czech. Acad. Sci., Prague, 1964, p. 315.
5-8) A. B. Lamb and A. G. Jaques, J. Am. chem. Soc. **50**, 967, 1938; **50**, 1215, 1938.
5-9) W. Feitknecht and W. Michaelis, Helv. chim. Acta **45**, 213, 1962.
5-10) A. Krause, Z. anorg. allg. Chem. **306**, 216, 1960; **306**, 223, 1960.
5-11) A. Krause and M. Ciokowna, Z. anorg. allg. Chem. **204**, 20, 1932.
5-12) A. Krause and H. Torno, Z. anorg. allg. Chem. **211**, 98, 1933.
5-13) W. Feitknecht and K. Moser, Z. anorg. allg. Chem. **304**, 181, 1960.
5-14) O. Glemser, Z. anorg. allg. Chem. **306**, 228, 1960.
5-15) A. Krause and A. Lewandowski, Z. anorg. allg. Chem. **206**, 328, 1932.
5-16) H. B. Weiser and W. O. Milligan, J. phys. Chem. **39**, 30, 1935.
5-17) A. Krause, Z. anorg. allg. Chem. **149**, 212, 1925.
5-18) F. A. Steele, J. Coll. Sci. **9**, 167, 1954.
5-19) M. Aumeras and M. Mounic, Bull. Soc. chim. franç. **3**, 1823, 1936.
5-20) R. Chevallier and S. Mathieu, C.R. Acad. Sci. Paris **206**, 1469, 1938; **206**, 1955, 1938.
5-21) W. H. Albrecht and E. Wedekind, Ber. dt. chem. Ges. **60**, 2239, 1927.
5-22) A. Krause and I. Garboczówna, Z. anorg. allg. Chem. **211**, 297, 1933.
5-23) A. Krause, Z. anorg. allg. Chem. **219**, 217, 1934.
5-24) E. S. Dana, A textbook of mineralogy, John Wiley and Sons, 4th ed., p. 483.

6. THE LOCALIZATION OF THE PROTONS IN THE IRON(III)-OXIDE HYDRATE

6.1. Introduction; discussion of the literature

The main constituent of the iron(III)-oxide–hydrate gel resulting from the treatment of a solution of a ferric salt with alkali, is water. As discussed in chapter 3 the greater part of this water is capillary water. The idea that not all the water is present as capillary water but that part of it is bonded with the iron oxide in such a way that hydrates or hydroxides of definite composition exist has been postulated by several authors already in the beginning of this century. Simon et al. tried to establish the presence of such compounds in a wet gel with the aid of measurements of the dependence of the vapour pressure on the temperature [6-1]) (see also sec. 7.1). Foote and Saxton measured the dilation of the gel upon freezing [6-2]); the idea underlying these experiments is that only the water which is not chemically bonded will contribute to the dilation. Indications of the occurrence of definite compounds were not found in this way. The work of Krause who tried to establish the presence of OH groups with chemical methods, has been mentioned already in chapter 5. Willstätter et al. tried to replace the capillary water by organic liquids [6-3]). This method has been used more recently by Frei who treated the gel with formamide [6-4]). In this way compounds of the composition $FeOOH.nHCONH_2$ were obtained indicating that the original gel probably may be represented by the general formula $FeOOH.nH_2O$. Similar experiments where carried out by the same author with aqueous solutions containing F^- ions, which gave rise to compounds of the composition $FeOF.nH_2O$ [6-4]).

The capillary water of the gel can be removed, for instance by drying at elevated temperatures or by freezing with liquid nitrogen (see chapter 3). In the latter case a powder results which after prolonged drying on P_2O_5 still contains a considerable amount of water, the average composition being $Fe_2O_3.1{\cdot}6\,H_2O$. There are three possible bonding states for this water:

(1) Adsorption water, present on the surface of the particles. A monomolecular layer of water on the surface of particles with a size of 25 Å corresponds already to about 7% by weight.

(2) Hydrate water built in the crystal lattice. The material then would have the composition $Fe_2O_3.m\,H_2O$ or more probably $Fe_2O_3.H_2O$ with some adsorption water. To the author's knowledge such hydrates of Fe(III) oxide or of the closely allied Al(III) oxide are not known *).

*) Thiessen reported the existence of a large number of hydrates in gels prepared by slow hydrolysis of Fe(III) ethylate [6-10,11]); these are the disputed Thiessen compounds [6-12]). However his results could not be reproduced by Weiser et al. [6-13,14]).

(3) The material is an oxy-hydroxide which can be written formally $FeOOH.nH_2O$, with the water being adsorbed on the particle surface or perhaps built in the lattice. There are examples of such iron compounds: α-FeOOH (formally $Fe_2O_3.H_2O$) mostly contains more OH or H_2O than corresponds to the theoretical composition [6-5,6]). Van Oosterhout considers this water as built in the crystal lattice [6-5]).

Kohlschütter et al. tried to elucidate the structure of a dried material by studying its electric behaviour [6-7]). According to these authors a negative temperature coefficient of the dielectric constant is characteristic for rigidly bonded water; an iron(III)-oxide hydrate with overall composition $Fe_2O_3 . 1{\cdot}3H_2O$ appeared to have a positive coefficient, which is an indication that at least part of the water is mobile, such as could be expected for adsorbed water.

Especially suitable for a study of the localization of the protons (besides the dielectric method mentioned) are non-destructive methods such as infrared spectroscopy and nuclear magnetic resonance, further indicated as I.R. and N.M.R. Glemser, on investigating the iron-oxide hydrate with both methods, concluded the presence of both OH and H_2O and, on this basis, he considers the material as an incompletely condensed hydroxide [6-8,9]). His conclusions are doubtful however. The reason why will be discussed in the next sections.

In conclusion it may be said that the evidence presented so far leaves it still questionable whether the dried powder obtained from iron(III)-oxide gels must be described as $Fe_2O_3.mH_2O$ or as $FeOOH.nH_2O$.

6.2. Infrared spectroscopy

6.2.1. *Introduction*

In the infrared spectra of hydrated oxy-hydroxides the following vibrations, with corresponding (approximate) wavenumber are possible; for a detailed discussion see ref. 6-15.

(1) O ⟷ H 3400 cm^{-1},

(2) H—O—H 1600 cm^{-1},

(3) O—H·····O 1000 cm^{-1}.

The OH stretching vibration (1), causes a strong absorption band at about 3400 cm^{-1}. The bending vibration (2) at about 1600 cm^{-1}, typical of the H_2O molecule, has a much smaller absorbance. The third absorption band is due to an OH deformation vibration. For strong hydrogen bridges its maximum lies at about 1000 cm^{-1} and it is usually very pronounced (see fig. 6.1). Thus

an absorption band at about 1600 cm^{-1} idicates the presence of H_2O and a band at 1000 cm^{-1} points to the presence of OH.

Both OH and H_2O give a strong absorption band at about 3400 cm^{-1}. The wavelength at maximum absorbance as well as the band width are dependent upon the bonding state of the protons. For instance the maximum occurs at 3657 cm^{-1} for H_2O in the vapour state; in the liquid state two maxima can be distinguished at 3450 resp. 3580 cm^{-1} and ice has a maximum at 3256 cm^{-1}. The H_2O in $NaBr.2H_2O$ gives a number of maxima between 3200 and 4000 cm^{-1}. In $MnSO_4.7\ H_2O$ three maxima can be distinguished at 3236, 3400 and 3477 cm^{-1}. Moreover the positions of these maxima (those given before are all measured at room temperature) are temperature-dependent.

A compilation of the literature dealing with the dependence of the wave-number of OH stretching vibrations on interatomic distances has been given by Nakamato et al. for many organic and inorganic compounds [6-16]). Glemser and Hatert have presented a similar study for a large number of hydroxides [6-17]). These authors could establish a definite relationship between the frequency of the OH stretching vibration and the O-O distance: for $d = 2{\cdot}66$ Å, $\varkappa = 2900\ cm^{-1}$ (α-AlOOH); for $d = 2{\cdot}90$ Å, $\varkappa = 3500\ cm^{-1}$, see also ref. 6–18.

In view of these results it is questionable whether to the presence of OH groups in the iron-oxide hydrate may be concluded from the position of "the centre of gravity and the extension to smaller wavenumbers" of the absorbtion band at about 3400 cm^{-1}, as Glemser did [6-8,9]). On the contrary, the spectrum published by Glemser even suggests that the material under study does not contain OH groups: the strong band or couple of bands typical for oxide hydroxides around 1000 cm^{-1} is not present in the spectrum of the iron-oxide hydrate. It is stated in the literature, however, that the crystal habit influences the extinction of these deformation bands considerably [6-6]).

6.2.2. *Experimental*

Infrared spectra are recorded of the oxide hydrate, dispersed in paraffin oil or in KBr, using a Hitachi infrared spectrometer (double-beam apparatus, E.P.I.G.). The spectra appeared to be similar in the two media. Since paraffin oil has a number of absorptions in the wavelength region of interest, all spectra referred to are made using KBr as a dispergent. Samples consisting of 0·5 mg Fe_2O_3-aq. and 300 mg KBr were dried above P_2O_5 and milled in an agate ball mill of 3 cm^3, provided with two balls of 3 mm diameter, during ten minutes. The powder is transferred into a steel mould placed in a glove box through which dried nitrogen is blown and is subsequently compacted at a pressure of 15 to 20.10^3 kg; the resulting tablet has a diameter of 15 mm and a thickness of about 1 mm.

In order to carry out D_2O-exchange experiments the tablet is mounted in a measuring cell provided with two CaF_2 windows and gas-inlet and -outlet tube.

D_2O exchange has been carried out by bringing inside this cell (placed in an exsiccator) a droplet (0·2 ml) of D_2O. After being left for half an hour the cell is mounted in the photometer and nitrogen (containing less than 10 ppm H_2O), is passed through the cell during ten minutes after which the absorption spectrum is determined.

6.2.3. *Results and discussion*

The infrared-absorption spectrum of the oxide hydrate is depicted in fig. 6.1. It exhibits a band at 3400 cm^{-1} which is extended to long wavelengths (2000 cm^{-1}) together with a rather strong band at 1630 cm^{-1}; in the region of 1000 cm^{-1} only very weak bands are observed. There are also bands at 1490 and 1360 cm^{-1}. The spectrum at large wavelengths shows the presence of strong broad bands at 460 and 580 cm^{-1} with a shoulder at 690 cm^{-1}. On D_2O exchange, besides the bands at 3400 and 1600 cm^{-1}, also the band at 1490 cm^{-1} diminishes in intensity which indicates that the latter also must be attributed to H_2O but then bonded in a somewhat different manner. The band at 1360 cm^{-1} is not subject to change on D_2O treatment. It might be an overtone of the lattice vibrations absorbing at long wavelengths (such overtones have been found frequently in oxide systems [6–19]), but it could also be due to OH groups that do not exchange protons with deuterons. These protons then must be bonded in a manner different from the other protons. This could be a distinction between protons present in the lattice and adsorbed as water on the surface.

The spectrum may be compared with the spectra of some well-known iron-oxide hydroxides, notably α-, β- and γ-FeOOH (fig. 6.1). These have strong bands at 905 and 800 cm^{-1}, a doublet at about 830 cm^{-1} and a strong doublet at 670 cm^{-1} and weak bands at 1020 and 745 cm^{-1} resp., which can be attributed to OH bending vibrations.

The infrared spectrum clearly indicates the presence of H_2O in our iron-oxide hydrate. Although the I.R. spectrum suggests that OH groups are absent, it is not certain that this conclusion holds. In fact the question may be asked whether it is possible that OH bending vibrations are shifted towards longer wavelengths and hence are overlapping the bands due to the lattice vibrations. Unfortunately these bands could not be investigated with D_2O exchange as the CaF_2 windows used in our experiments have strong absorption in this region.

A second attempt has been made by trying to perform a quantitative analysis. This has been carried out by a comparison of the ratio of the integrated intensities of the bands at 3400 and 1600 cm^{-1} for a number of hydrates such as KBr.aq., $CuSO_4.5H_2O$ and $MgSO_4$.aq. on the one hand and those of the iron(III)-oxide hydrate on the other hand. Due to the uncertainty of the base line, particularly for the latter material, this method did not allow of a definite conclusion.

Another trial has been made by comparing the integrated intensities of the band at 3400 cm^{-1} for the hydrates mentioned with those of α-, β- and γ-FeOOH in

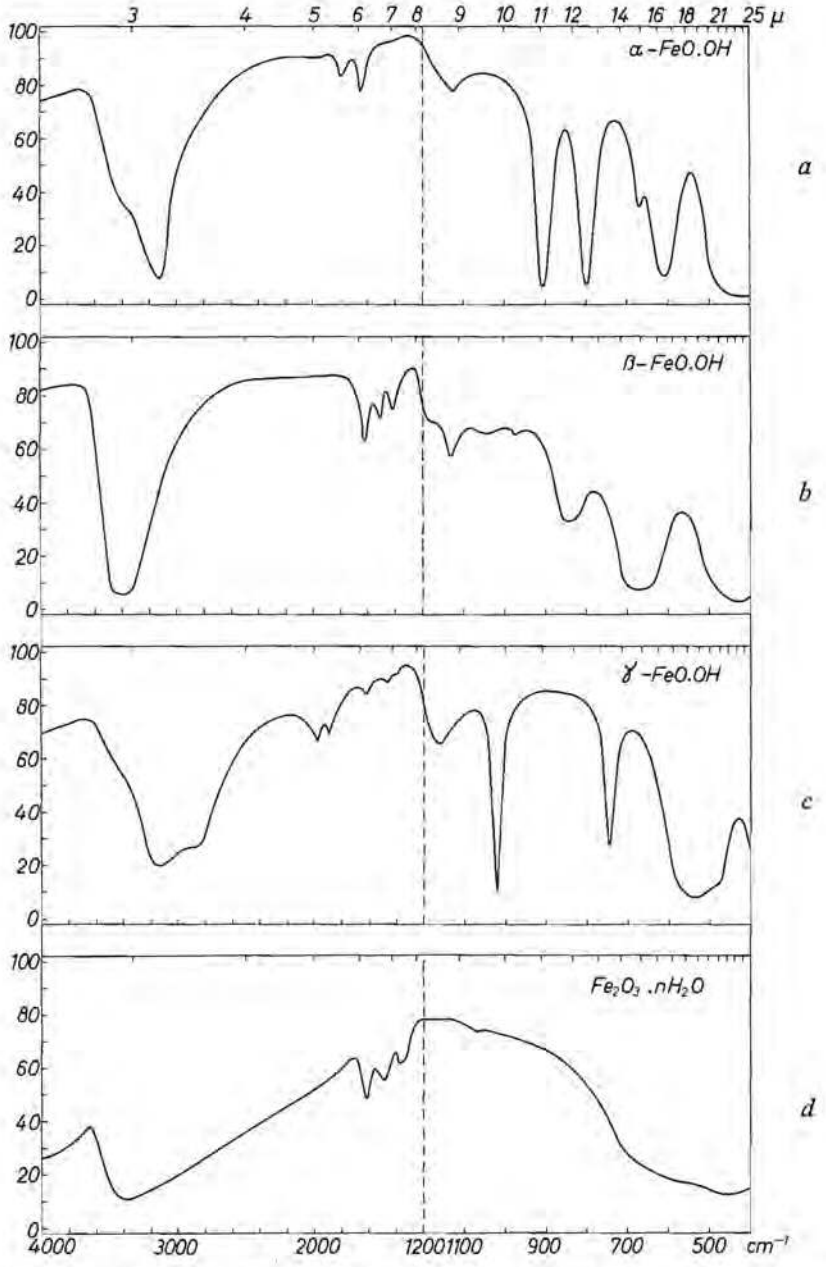

Fig. 6.1. The infrared spectra of α-FeOOH, β-FeOOH, γ-FeOOH and of the iron(III)-oxide hydrate under study.

order to investigate whether the extinction of the OH band is the same for all oxy-hydroxides and differs by a constant factor from that of the hydrates. In this way a distinction between hydrates and hydroxides could not be made, however, and hence the problem remains unsolved.

Glemser tried to distinguish between adsorbed water and OH groups by heating the sample at 120 °C [6-8]). After five hours the H_2O band at 1630 cm^{-1} had disappeared, whereas at 3400 cm^{-1} a rather strong band still existed. The latter, according to Glemser, should be due to OH. It is not certain, however, whether the experiments allow this conclusion as upon heating the material might have changed. In chapter 7 it will be shown that upon heating at 100 °C within a few hours changes occur indeed; however, these may be only of minor importance. The suggestion that protons are present which are rigidly bonded to the iron-oxygen lattice seems justified by our measurements of dispersions of the iron-oxide hydrate in KBr tablets, after prolonged drying at room temperature *), show that the absorbance of the band at 1630 cm^{-1} decreases much sharper than that of the OH stretching band at 3400 cm^{-1}. A quantitative estimation of the number of protons contributing to the remaining band at 3400 cm^{-1}, by taking the average extinction of the OH bands of α-, β- and γ-FeOOH, teaches that about half of the protons take part in it. From the absence of the band at 1630 cm^{-1} it could be thought that these protons are not present as H_2O; more information is necessary to draw a definite conclusion about the bonding state of these protons. N.M.R. measurements, as discussed in the next section, could provide some more information on this point.

From the spectrum at long wavelengths (10-25 μ) valuable additional information can be obtained regarding the iron-oxygen lattice. Comparison with the spectra of α-Fe_2O_3, γ-Fe_2O_3 and α-, β- and γ-FeOOH shows that the compound under investigation is different from these, although there is some resemblance to β-FeOOH (see fig. 6.1).

6.3. Nuclear magnetic resonance

6.3.1. *Discussion of the literature*

Only a few data are available on N.M.R. spectra of the iron-oxide hydrate. From the observed line broadening, about 5 Oe, Glemser concluded to the presence of OH groups [6-9]). This conclusion is, however, open to criticism; H_2O, when rigidly bound, such as in well-crystallized hydrates, for instance $CaSO_4.2H_2O$, exhibits a line width of 10 Oe, but when adsorbed on a particle surface, the H_2O-line width can be considerably smaller, due to the mobility of the H_2O molecules, which is large especially on a surface with small radius[6-21,22]).

*) Carried out by passing a stream of nitrogen gas over it containing less than 1 ppm H_2O.

Even when the water molecules are localized and can only rotate, the corresponding line width should be 5 Oe [6-23]).

Moreover, Glemser did not take into account the superparamagnetic character of the material; the high magnetic moment present in the particles interferes with the applied field and hence influences the line width considerably, as will be discussed further on.

6.3.2. *Experimental*

The N.M.R. measurements were carried out on a sample consisting of a pressed pellet of 2 g powder of $Fe_2O_3.1{\cdot}5\,H_2O$, placed in a saeled glass tube 10 mm in diameter. A coil of insulation-free copper wire is wound around the tube. The number of turns of the coil was between 10 and 20, depending on the operation frequency range. The coil with sample could be shielded and covered by a brass vessel. It is mounted in a Dewar vessel. A coaxial lead consisting of a stainless-steel shield and an inner wire of copper provided for the connection of the top of the coil with the top of the cryostat. With a piece of flexible coaxial cable the system was connected to the electronic detection system. The coil formed part of the circuit of a marginal autodyne oscillator. The conventional methods of low-frequency magnetic-field modulation and phase-sensitive amplification of the N.M.R. signal were applied.

For the low-temperature measurements a mixture of ethanol and solid CO_2 was used for cooling the sample system.

6.3.3. *Results and discussion*

The proton nucleus has a spin $I = \frac{1}{2}$ which means that when placed in a — static — magnetic field two energy levels can be occupied, differing in energy by 2 $M_z H_z$ where $M_z = \frac{1}{2}\gamma\hbar$ (γ = constant) is the magnetic moment in the direction of the applied field H_z. Now when a second alternating magnetic field H_x perpendicular to the field H_z is applied, resonance absorption can occur when its frequency is equal to the Larmor precession frequency of the nuclear spins, given by $\omega = \gamma H_z$; for protons $\gamma = 2{\cdot}68.10^4$ rad/Oe s. In the material to be investigated other fields can act on the nucleus, in addition to the applied field, for instance fields due to neighbouring atoms.

Hence, when measuring the absorption as a function of the applied field H_z resonance occurs not at a definite frequency but in a certain frequency range giving rise to line broadening ΔH.

For the iron(III)-oxide hydrate the line broadening ΔH has been measured as a function of H_z at two different temperatures; the results of these measurements are presented graphically in fig. 6.2. The results show that at 20 °C the line broadening extrapolated to zero field strength equals about 0·5 Oe and, at —70 °C the line broadening is equal to about 1·5 Oe. It will be shown that

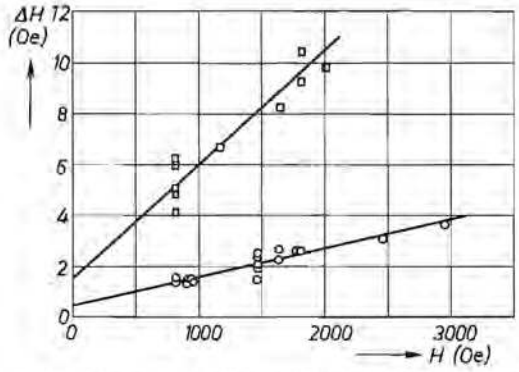

Fig. 6.2. Field-dependent line broadening observed in the N.M.R. spectrum of iron(III)-oxide hydrate at 20 °C (○) and at −70 °C (□).

from these values conclusions can be drawn regarding the bonding state of the protons.

Causes of line broadening

The material under study consists of superparamagnetic particles. Hence, line broadening can be caused in the first place by superparamagnetic fields. In this case two possibilities can be distinguished.

(A) One possibility is that the resulting moment of the whole particle is shared by all ions. In this case the internal fields are proportional to the measured magnetization. As mentioned in chapter 4 each crystallite contains about 1000 ions. The magnetic moment per particle equals 170 μ_B. The magnetic measurements discussed in chapter 4 indicate that at 200 °K and a field strength of 2000 Oe the magnetization in the direction of the field strength equals $0{\cdot}1\ \sigma_s = 0{\cdot}1 \times 170\ \mu_B$ which corresponds to a contribution $170 \times 10^{-1} \times 10^{-3} \times 9{\cdot}1 \times 10^{-21}$ erg/Oe for one Fe^{3+} ion. Assuming that the proton is at a distance of 2·5 Å from the Fe^{3+} nucleus the field due to one iron ion acting on the proton is

$$H_{eff} \approx \frac{1{\cdot}6.10^{-22}}{2{\cdot}5^3.10^{-24}} \approx 11 \text{ Oe.}$$

This source of line broadening may give rise to symmetric as well as asymmetric lines [6–24]). At 2000 Oe the measured line broadening amounts to 10 Oe. This equality may be accidental, however; apart from the fact that we did not account for all iron ions in the sample the measured line width of 10 Oe can partially be due to demagnetizing fields resulting from the porosity of the sample [6–24]).

(B) Another possibility is that the resulting moment is not shared by all the Fe^{3+} ions, but is caused by a minority of n unpaired Fe^{3+} ions per particle of N Fe^{3+} ions. The other Fe^{3+} ions obey an antiferromagnetic ordering and

do not contribute to the external magnetization. The average moment of the Fe^{3+} ion then equals under the same conditions as mentioned before: $0{\cdot}1 \times 5 \times 9{\cdot}1 \times 10^{-21} \approx 5.10^{-21}$ erg/Oe. The field on the proton then equals

$$H_{\text{eff}} \approx \frac{5.10^{-21}}{2{\cdot}5^3.10^{-24}} = 300 \text{ Oe.}$$

At first view this possibility should be excluded. However, the field at the proton is a summation of the fields due to all the iron ions in the sample; the resulting field thus depends on the crystallographic surroundings of the proton. In fact if the proton should be surrounded symmetrically by iron ions this field should be zero.

(C) Dipole fields between neighbouring protons can also be the cause of line broadening. It can be calculated that, at a distance of 1·6 Å between the protons, i.e. the distance in H_2O, the value for ΔH amounts to 10 Oe [6–23]). This line broadening is independent of the applied field. However, as mentioned before, if for instance the H_2O molecules are adsorbed on the surface of the particles in such a way that the H_2O molecule can rotate around its symmetry axis instead of a broadening of 10 Oe, a ΔH equal to 5 Oe should be observed, which again is independent of the field strength [6–23]).

(D) A fourth possible reason for the observed line width could be that the H_2O molecules, being adsorbed on the particle surface, are still moving very rapidly along the surface. The line broadening should then be caused by the spatial inhomogeneity in the magnetic field as arising from the magnetized crystallites. In this case it should be probable that the observed lines should be asymmetric, which has not been found.

Taking all arguments together it is tentatively concluded that the observed line widths must be attributed to OH groups. An estimation of the total amount of protons contributing to the supposed OH line gives a quantity of at least 50% or more. Therefore in connection with the I.R. results it is most probable that the iron-oxide hydrate under study — with the composition $Fe_2O_3.1{\cdot}6\ H_2O$ — can be described as $FeOOH.0{\cdot}3H_2O$.

6.4. Summary

(1) The infrared spectrum of the iron(III)-oxide hydrate shows a band at 1630 cm^{-1}, typical for H_2O. The spectrum does not exhibit bands which are typical for OH-O deformation vibrations, but on drying at room temperature the band at 1630 cm^{-1} disappears almost completely, whereas a strong band at 3400 cm^{-1} remains. This band is attributed to protons present in the iron-oxygen lattice. From the intensity of this band it is estimated that about half of the protons contribute to it.

(2) The line broadening in nuclear-magnetic-resonance spectra equals about 1 Oe. This points to the presence of OH. An estimation shows that at least 50% of the protons must be present as OH.

(3) Combining the infrared and N.M.R. data it is proposed to describe the hydrate $Fe_2O_3.1{\cdot}6\ H_2O$ as $FeOOH.0{\cdot}3H_2O$; in general $FeOOH.nH_2O$.

REFERENCES

6-1) A. Simon and Th. Schmidt, Kolloidz. **36**, 65, 1925.
6-2) H. W. Foote and B. Saxton, J. Am. chem. Soc. **38**, 588, 1916; **39**, 1103, 1917.
6-3) R. Willstätter, H. Kraut and W. Fremery, Ber. dt. chem. Ges. **57**, 1491, 1924.
6-4) V. Frei, Coll. Czech. chem. Comm. **27**, 775, 1962; **27**, 782, 1962.
6-5) G. W. van Oosterhout, Proc. int. Conf. Magn. (Nottingham 1964), The Inst. of Physics and The phys. Soc., London, 1965, p. 529.
6-6) V. M. Zolotarev, L. D. Kislovskii and L. V. Riskin, Optics and Spectroscopy (transl. from Russ.) Suppl. **2**, 142, 1962.
6-7) H. W. Kohlschütter, H. H. Stamm and G. Kämpf, Z. anorg. allg. Chem. **278**, 264, 1954; **278**, 270, 1954.
6-8) O. Glemser and G. Rieck, Z. anorg. allg. Chem. **297**, 175, 1958.
6-9) O. Glemser, Nature **4666**, 943, 1959.
6-10) P. A. Thiessen and R. Köppen, Z. anorg. allg. Chem. **200**, 18, 1931.
6-11) P. A. Thiessen and R. Köppen, Z. anorg. allg. Chem. **228**, 57, 1936.
6-12) R. Fricke and G. Hüttig, Hydroxide und Oxid-hydrate, Akad. Verlagsges., Leipzig, 1937, p. 523.
6-13) H. B. Weiser and W. O. Milligan, J. phys. Chem. **39**, 25, 1935.
6-14) H. B. Weiser, W. O. Milligan and W. J. Coppoc, J. phys. Chem. **43**, 1109, 1939.
6-15) J. Lecomte, Encyclopedia of physics, Springer Verlag, Berlin, 1958, Vol. 26, p. 244.
6-16) K. Nakamoto, M. Margoshes and R. E. Rundle, J. Am. chem. Soc. **77**, 6480, 1955.
6-17) O. Glemser and E. Hatert, Z. anorg. allg. Chem. **283**, 111, 1956.
6-18) E. Schwarzmann and H. Marsmann, Naturwiss. **53**, 349, 1966.
6-19) S. Hafner and F. Lages, Z. f. Krist. **115**, 321, 1961.
6-20) S. Hafner, Z. f. Krist. **115**, 331, 1961.
6-21) R. K. Webster and T. L. Jones, Proc. Brit. ceram. Soc. **153**, 1965
6-22) W. S. Brey and K. D. Lawson, J. phys. Chem. **68**, 1474, 1963.
6-23) G. Hardeman, private communication.
6-24) D. J. Kroon, Philips Res. Repts **15**, 501, 1960.

7. THE RECRYSTALLIZATION OF IRON(III)-OXIDE HYDRATE AT ELEVATED TEMPERATURES

7.1. Introduction

In the preceding chapter the results have been discussed of an investigation of the iron(III)-oxide hydrate with respect to the occurrence of stoichiometric hydrated compounds with infrared spectroscopy and nuclear magnetic resonance. Another approach to the examination of the existence of hydrates could be a study of its dehydration behaviour upon heating. In the literature there are quite a number of papers dealing with such experiments.

Heating of a wet gel under a vapour pressure of 10 mm Hg up to 400 °C leads to a continuous dehydration as shown by Simon [7-1]); this was taken as an indication that no definite hydrate exists. If the wet gel is dried in air at slightly elevated temperature (40-60 °C) the greater part of the capillary water evaporates resulting in products containing 25-35 % H_2O [7-2,3]). From the thermobalance experiments carried out by Frei et al. on dried gels it was suggested that the dehydration behaviour depends upon the anion present during the hydrolysis and upon the way in which the hydrolysis of the ferric salt has been carried out. When precipitated from SO_4^{2-}-containing solutions the resulting oxide hydrate shows a continuous dehydration diagram, the dehydration occurring at a maximum rate at about 150 °C [7-2]). On the other hand similar products prepared from NO_3^--containing solutions show a discontinuous curve. It must be emphasized however, that the oxide hydrates of Frei et al. were prepared in boiling solutions and dried at 60 °C in air; under these conditions the precipitate initially formed could easily recrystallize. The influence of the precipitation temperature on the dehydration behaviour of the gel has been demonstrated by Mackenzie [7-4]). This author found a relationship between the precipitation temperature and the temperature at which the highest dehydration rate occurs.

Another attempt to demonstrate the existence of a hydrate or hydroxide has been done by Albrecht and Wedekind by measuring the magnetic susceptibility χ. These authors found a continuous increase in the susceptibility (per gramme of oxide) on decreasing water content [7-6]) in the dried gel. At water contents between 11 and 15 %, χ is at maximum, viz. 300-400.10^{-6} cm^3/g [7-5,6]), which according to the opinion of the authors must be due to a definite hydrate or hydroxide different from the well-known α- and γ-oxy-hydroxides (water content $\approx$ 10 %) as these compounds have much lower χ values, $\approx$ 20.10^{-6} cm^3/g [7-7]). The authors did not succeed in identifying this alleged compound: they did not find a relation between X-ray-diffraction patterns of the dehydrated products and the value of the susceptibility. As will be discussed in sec. 7.4 it is not necessary to assume the formation of a new, hitherto unknown hydrate,

to explain the changes in the susceptibility.

A study of the dehydration behaviour of iron(III)-oxide hydrate has been performed by Fricke et al. [7-9,10]) with the aid of calorimetry together with X-ray diffractometry. They arrived at the following conclusions.

(1) Upon heating the energy content of the material increases and attains a maximum value between 150 and 200 °C.
(2) Above 250 °C a rapid decrease of the energy content occurs.
(3) Samples (prepared at 20 °C) after heating at 250 °C show the presence of α-Fe_2O_3 with a size of the crystallites of about 80 Å.
(4) Above 350 °C rapid crystal growth occurs; after one hour at 600 °C α-Fe_2O_3 crystals with a size of about 250 Å are present.

The formation of α-Fe_2O_3 at 300 °C has also been reported by Frei who found, however, in the X-ray diagram also the spacing $d \approx 2{\cdot}0$ Å which is not observed in α-Fe_2O_3 in the coarse crystalline form.

Summarizing it can be said that from studying the dehydration behaviour of gels prepared from aqueous solutions of a ferric salt (nitrate, sulphate, chloride and perchlorate) no indication has been found for the occurrence of stoichiometric compounds between Fe_2O_3 and H_2O. Yet the existence of such a compound is suggested by the results of the preceding chapter. For an elucidation of its composition — tentatively described by $FeOOH.nH_2O$ — a more precise knowledge of the quantities of hydrate or adsorption water and of hydroxyl is necessary. For that purpose a number of D.T.A. and T.G.A. experiments are done which are described in the following.

7.2. Thermogravimetric analysis and differential thermal analysis

7.2.1. *Experimental*

Differential thermogravimetry is carried out using a Cahn microbalance. The sample weight is continuously registered on a recorder. The sample, about 90 mg Fe_2O_3.aq., in an alumina crucible measuring 10×5 mm² (wall thickness 0·5 mm), is placed on an alumina support fastened to the arm of the balance with an alumina rod of 0·3 mm diameter. The temperature is measured with a Pt-Rh thermocouple, placed in the vicinity of the sample. The temperature is increased at a rate of 520 °C/h. The heating furnace has a zone of constant temperature with a length of 15 mm. The balance and its furnace system is vacuum-pumped. The H_2O pressure in the balance system is kept constant by connecting the latter with a reservoir containing melting ice. A blank gives no measurable weight changes in the temperature region of interest.

Differential thermal analysis. Samples of 50 mg, are placed in a cylindrical container of $10 \times 3{\cdot}5$ mm², wall thickness 0·1 mm. The Pt sample holder together with the reference — an identical crucible containing Al_2O_3 — are placed

on top of an alumina rod which is kept carefully centred in the furnace by means of alumina rings. Over the crucibles a Pt cylinder (height 5 cm) is placed which in turn is surrounded by a closed alumina tube provided with four holes (diameter 3 mm) for the passage of nitrogen gas. This tube just fits in the furnace tube. The temperature is measured with a Pt-Rh thermocouple and the temperature difference between the sample and the reference is measured by similar couples which are placed at the bottom of the crucibles. The heating rate is 500 °C/h. The water vapour formed during the reaction is removed by passing air through the furnace (inner tube width 28 mm) at a velocity of 0·5 l/min. Measurements are also done using an apparatus constructed by Bureau de Liaison, Paris. The detecting head of this apparatus has sample holders formed by the junction of the detecting thermocouple [7–11]). The results obtained with both apparatuses were essentially the same; fig. 7.2 is obtained with that of B.D.L.

7.2.2. *Results and discussion*

Thermogravimetric and differential thermal analysis

As mentioned already, the oxide hydrate prepared at 90 °C after drying on P_2O_5 contains about 13% H_2O and after re-exposure to the air at room temperature the water content easily rises to 25%. The dehydration-rehydration behaviour of a sample has been studied at higher temperatures by heating the oxide hydrate on a thermobalance in an H_2O atmosphere with a constant vapour pressure of 0·4 mm Hg. If the temperature is increased a gradual decrease in the weight of the sample results up to 70 °C. Already at 60 °C a rapid loss of H_2O occurs, at 200 °C 60% and at 300 °C 90% of the total quantity of water is given off. When the temperature is increased stepwise and kept at a constant value for a certain time an equilibrium etablishes. If the temperature is then lowered and kept constant again a new equilibrium results by adsorption of H_2O from the atmosphere. The results are summarized in table 7-I and shown graphically in fig. 7.1. The dehydration is nearly complete at 300 °C; it elapses gradually and thus the existence of a definite compound is not indicated. This, however, does not exclude the existence of such a compound. For, even when having OH groups on definite lattice sites, small crystallites, on decomposition, can loose their protons gradually due to the formation of H_2O, which must evaporate from the surface, this being the equilibrium-determining step [7–12]). When the temperature is lowered water is taken up again. This will be due to adsorption on the particle surface; a restoration of OH groups inside the particle is not probable. The initial water content is not reached even after 10 hours. This decrease in adsorption capacity is not evidence for an initial existence of OH groups as it could also be explained as being due to the fact that, at the

TABLE 7-I

Weight of an Fe_2O_3.aq. sample as a function of the temperature on stepwise heating in an H_2O atmosphere of 0·4 mm Hg. Each temperature level is maintained during at least one hour

temperature (°C)	weight (mg)
20	91·3
38	90·5
60	87·9
96	86·3
122	85·1
145	84·0
184	83·4
142	83·7
230	82·8
265	82·4
300	82·2
100	83·6
65	84·1
20	86·5

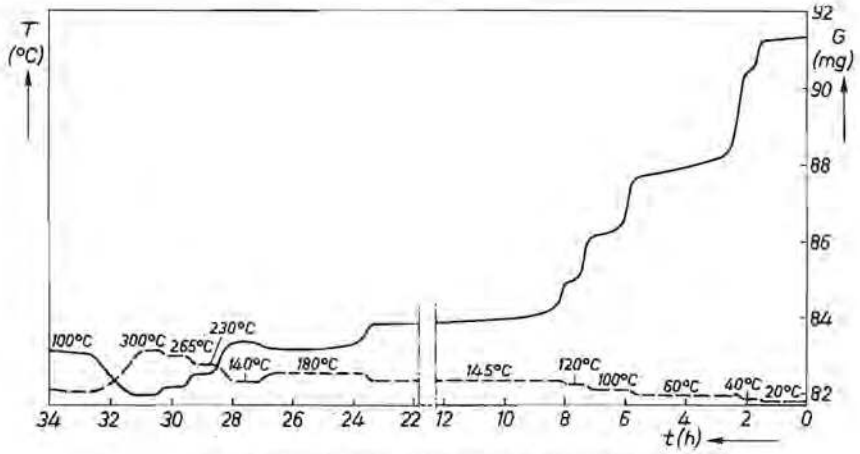

Fig. 7.1. Thermogravimetric curve of iron(III) oxide.

temperature of 300 °C, sintering has taken place (the specific surface area decreases 35 %).

T.G.A. only gives information regarding those processes which involve a weight loss. D.T.A. allows the detection of processes occurring during thermal dehydration which are accompanied by a change in the enthalpy, e.g. recrystallization processes. The same preparation as used for the T.G.A. has been studied by means of D.T.A. The results are presented graphically in fig. 7.2. A rather broad endothermic peak exists between 20 and 200 °C, with a maximum at 150 °C, no doubt due to the evaporation of water. Between 350 and 450 °C a sharp exothermic peak is observed which may be related to the recrystallization of the dehydrated iron oxide (see also sec. 7.3). Clearly, the dehydration (20-200 °C) and the recrystallization (350-450 °C) are separate processes. The anhydrous product formed upon dehydration is stable from 200 to 350 °C until recrystallization starts. This does not prove that the expelled water was adsorbed on the particle surface. Similar phenomena are observed on dehydration of well-crystallized oxide hydroxides [7-13]. The fact that the lattice does not necessarily collapse has been explained by Freund [7-12] as due to a stabilization of vacancies created by the disappearance of OH groups; the energy thus stored in the lattice is liberated suddenly in a narrow temperature range, in our case around 430 °C.

The combined D.T.A. and D.T.G. results show the following.

(1) It is not possible to get a definite answer with these techniques regarding the bonding state of the protons; OH groups as well as H_2O built in the lat-

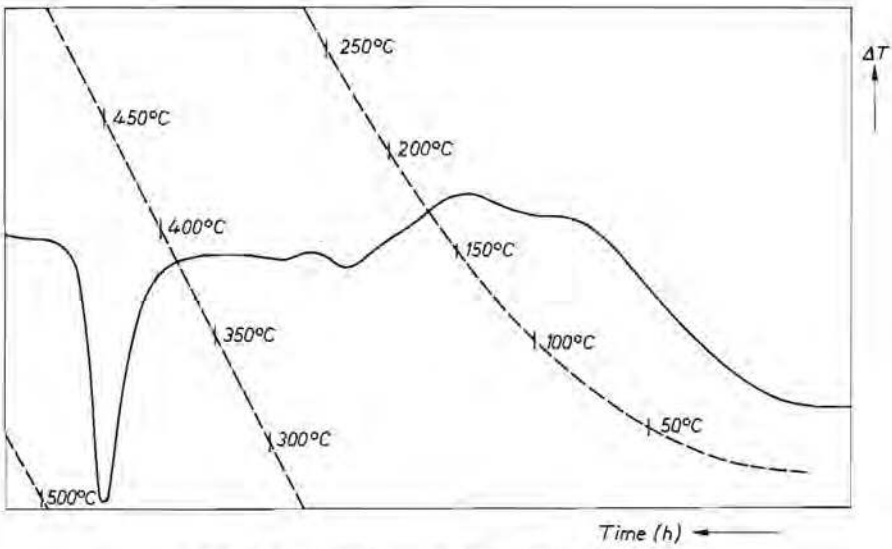

Fig. 7.2. Thermogram of iron(III)-oxide hydrate.

tice or adsorbed on the surface of the particles should be able to cause the phenomena observed.

(2) On heating already below 200 °C the gel dehydrates nearly completely. This dehydrated gel is stable in a rather large temperature traject, 200-350 °C.

(3) On rehydration this product takes up H_2O again, but less than 50% of the amount originally present. This does not prove that the expelled H_2O was originally present as OH groups; the phenomenon can also be explained as due to a decreased adsorbing capacity.

7.3. Crystallographic transformations; morphology

The results presented thus far clearly show that in the temperature region of 200-350 °C a dehydrated compound exists in a form which is stable under our experimental conditions. For a further elucidation of the dehydration mechanism a knowledge of the chemical and physical properties of the products existing in this intermediate state is of special interest.

For a crystallographic study two samples are chosen that are obtained from gels prepared at 20 or 90 °C. Each is heated at 201, 227 or 302 °C, respectively. The main reflections observed in the corresponding X-ray diffractions of these compounds are listed in table 7-II. All lines are broad and overlapping. The d values given in table 7-II are therefore approximations. A comparison of the d values of the various "intermediate products" with those of the well-known iron-oxide hydroxides shows that (2) contains α-Fe_2O_3 as indicated by the reflections $d = 3{\cdot}70$, $2{\cdot}69$, $2{\cdot}44$ and $1{\cdot}84$ Å. These reflections are not present in the samples (3) and (4) obtained from starting compounds prepared at 90 °C; when heated at 227 °C some change is observed; there is probably a band at $d = 2{\cdot}83$, whereas the value of $d = 1{\cdot}70$ could not be observed. When the material is heated at 302 °C, however, a strong band is observed at $d = 2{\cdot}71$ Å. This indicates again the presence of α-Fe_2O_3. In the latter case the other bands can be attributed to α-Fe_2O_3 as well as to the structure of the starting compound; the absence of the reflection belonging to $d = 1{\cdot}99$ Å makes it plausible that this material mainly exists of α-Fe_2O_3. When heated at 450 °C, all samples exhibit the diagram of rather well crystallized α-Fe_2O_3.

Clearly on dehydration some crystallographic transformations take place; there are indications of the formation of α-Fe_2O_3. Only slight crystal growth, if any at all, occurs up to 250 °C. At still higher temperatures and particularly at about 430 °C (the maximum of the exothermic peak in the D.T.A. diagram) a rapid crystallization towards α-Fe_3O_2 takes place under the formation of crystals with a comparatively large size, as derived from the observed line broadening. Electron microscopy confirms these conclusions. As pictured in fig. 7.3, when heated to 227°C the particles have a size below 50 Å, but when heated to about 450 °C they attain a size of about 300 Å.

TABLE 7-II

X-ray diffractions (d values) of samples as prepared and dehydrated by heating for two hours to 210, 227 and 302 °C, resp. (s = strong)

samples		prepared at 20 °C		prepared at 90 °C			
as prepared (1)		heated to 201 °C (2)		heated to 227 °C (3)		heated to 302 °C (4)	
		3·70	s	3·0	?	3·0	?
3·0	?	3·0	?				
2·85	?	2·85	?	2·83	ss	2·83	sss
		2·69	sss			2·71	sss
		2·61	?			2	
2·52	sss	2·52	sss	2·54	sss	2·52	sss
		2·44	ss				
2·23	ss	2·22	s	2·25	ss	2·23	ss
1·98	s			1·99	s		
		1·84	s				
1·72	ss	1·70	s			1·70	s
		1·52	s	1·51			
1·49	sss	1·48	sss				

7.4. Magnetic properties of the dehydrated products

The Mössbauer spectra of the products obtained after heating at 200 and 300 °C for two hours, are similar to that of the starting product. This suggests that the particles are superparamagnetic. As the values of the isomer shift and the quadrupole splitting are equal to that of the starting compound, it must be concluded that the surroundings of the Fe^{3+} ion have not changed. Superparamagnetism should be expected when the particles have a size smaller than 100 Å; this is in accordance with the electron micrographs, fig. 7.3. The superparamagnetic character of the material is also revealed by magnetic measurements; there is a linear relationship between the magnetization and field strength up to fields of 5000 Oe; the susceptibility largely depends on the dehydration temperature. At high field strengths (10 000 Oe) the χ-H curve shows a slight curvature due to the fact that saturation occurs as mH/kT no longer is smaller than unity (compare chapter 4); this is illustrated in table 7-III where a number of χ measurements is listed together with magnetization values at 10 000 Oe for samples prepared at 20 resp. 90 °C and heated at various temperatures.

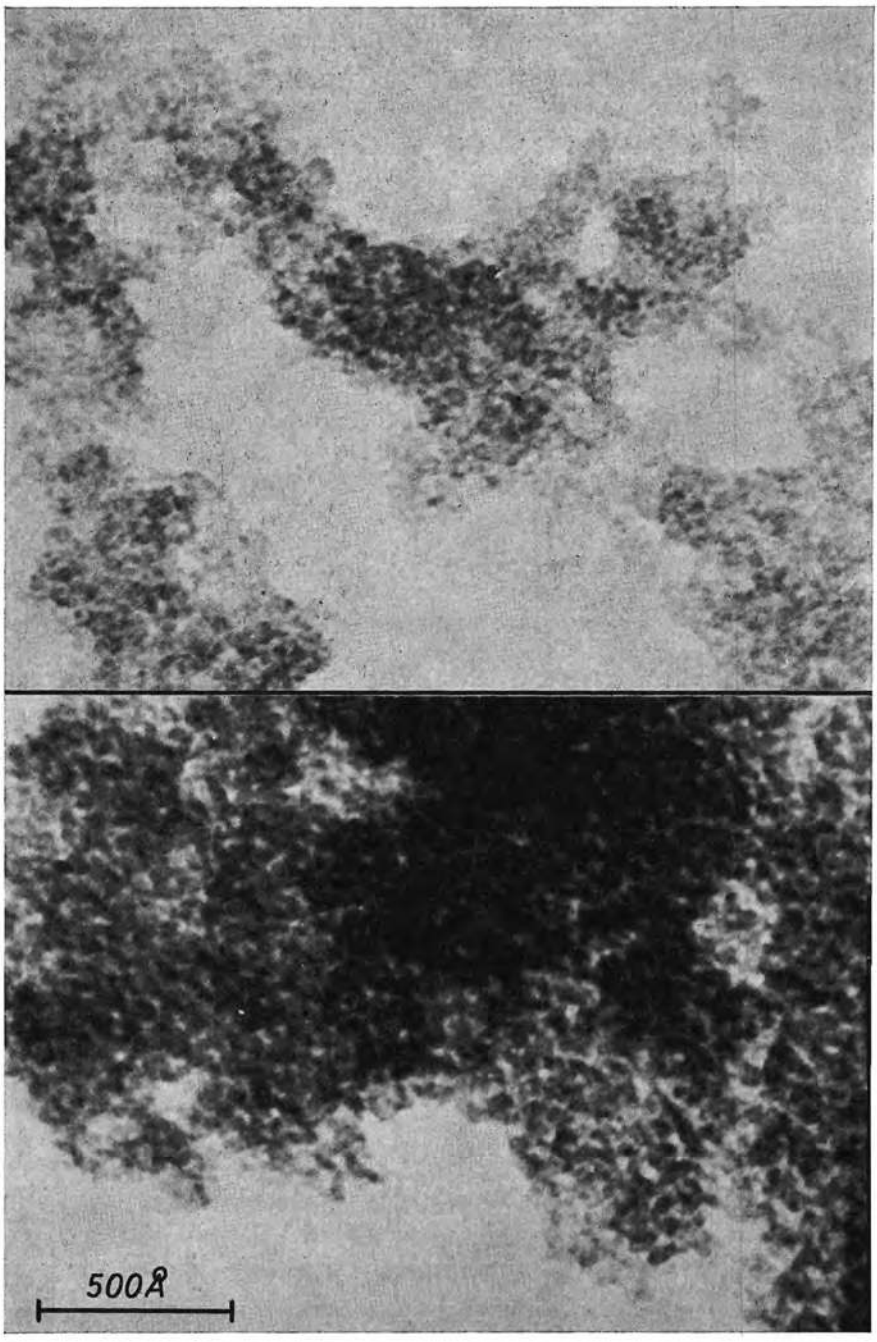

Fig. 7.3. Electron micrographs of iron(III)-oxide hydrate (*a*) as prepared, (*b*) 227 °C, (*c*) 302 °C and (*d*) 350 °C. The oxide hydrate has been prepared at 20 °C.

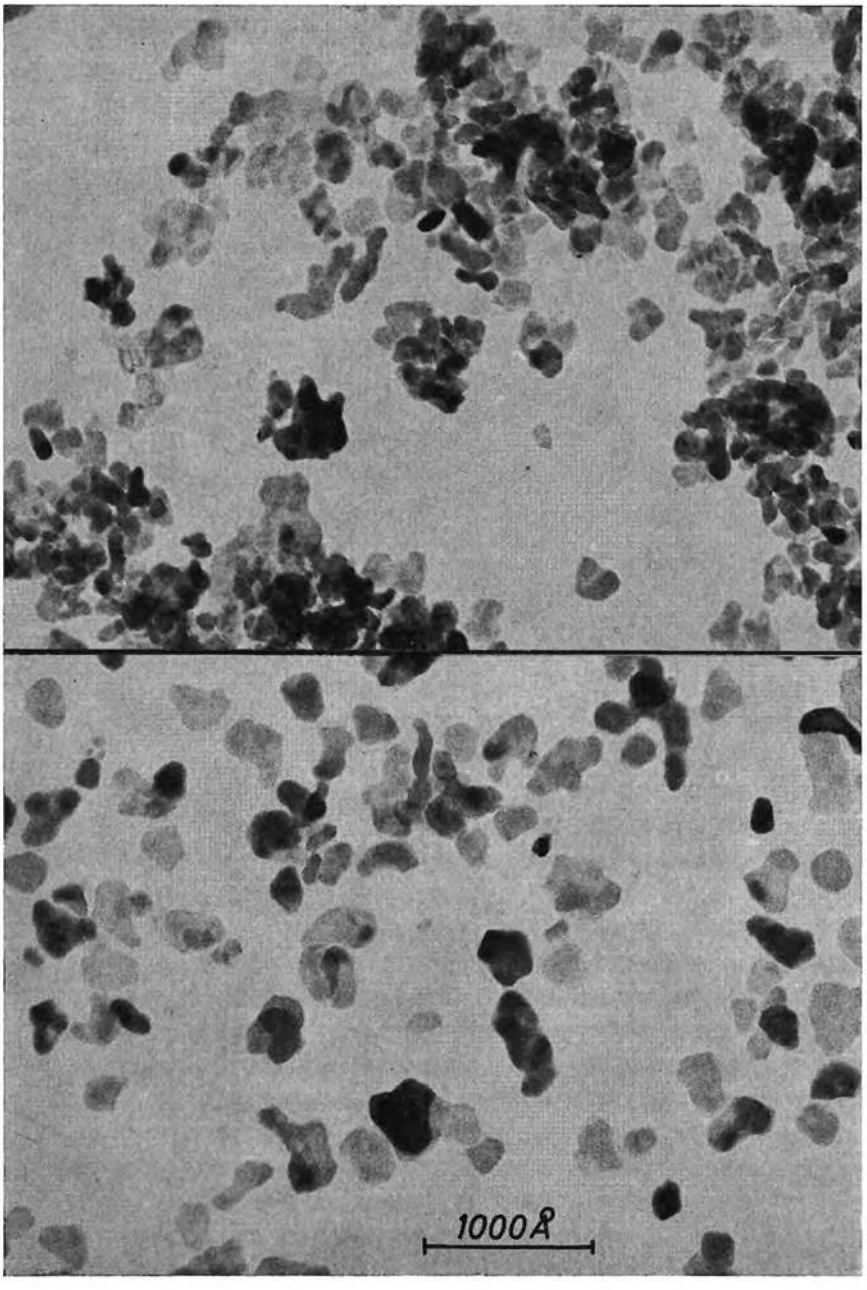

See caption on preceding page.

TABLE 7-III

Magnetic susceptibility χ and magnetization values (c.g.s. units) at 10 000 Oe of iron(III)-oxide hydrates prepared at 20 resp. 90 °C and dehydrated at various temperatures during two hours

iron(III)-oxide hydrate prepared at	20 °C		90 °C	
T (°C)	$\chi.10^6$	$\sigma.10^2$	$\chi.10^6$	$\sigma.10^2$
20	101	97	110	110
100	128	126	137	136
150	154	151	174	164
202	156	156	159	153
226	122	117	143	147
251	133	125	145	134
276	70	59	144	134
301	23	23	166	145
353	18	17	61	50
403	17	17	22	22

As shown by the table, the susceptibility is greatly dependent on the dehydration temperature; the χ measurements are represented graphically in fig. 7.4; clearly χ passes through a maximum for both series lying between 150 and 200 °C and there is a minimum at about 230 or 260 °C. These data once more demonstrate that the dehydration behaviour is dependent on the preparation history of the iron(III)-oxide hydrate. For a compound prepared at 20 °C, χ rapidly decreases above 250 °C; at 300 °C the limiting value of 17.10^{-6} is reached which is equal to the susceptibility of α-Fe_2O_3. Samples prepared at 90 °C are more stable; here the susceptibility falls to its limiting value only at about 350 °C.

As discussed in the preceding section the X-ray diffractions taken at the two maxima of the χ-T show that they are due to different compounds; for samples prepared at 90 °C and heated at 200 °C the initial structure is observed whereas at 300 °C this at least partially is converted into α-Fe_2O_3. When using oxide hydrates prepared at 20 °C the presence of α-Fe_2O_3 could also be established in samples heated at about 230 °C.

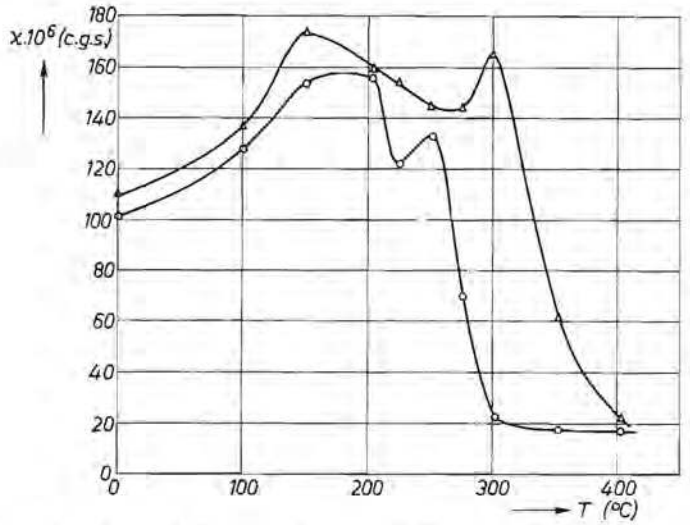

Fig. 7.4. The dependence of the magnetic susceptibility on the dehydration temperature. Circles: sample prepared at 20 °C, triangles: sample prepared at 90 °C.

Both from X-ray line broadening and from electron micrographs it appears that up to 250 °C hardly any growth of particles occurs. Therefore the increase of χ is explained as due to an increased disorder created in the lattice by the disappearance of H_2O originally present as OH or as hydrate water.

7.5. Mechanism of the dehydration

The dehydration behaviour can be described as follows. The iron(III)-oxide-hydrate particles have a large quantity of H_2O adsorbed on their surface. This water is given off on heating already at 60 °C. At higher temperatures, but still below 200 °C the dehydration goes further by the reaction of OH groups; the water molecules thus formed migrate to the surface and are released therefrom. The possibility of the dehydration of oxide hydrate at such low temperatures has been demonstrated for δ-FeOOH [7-14-17]). The fact that the Mössbauer spectrum remains unchanged upon dehydration up to 200 °C indicates that the surroundings of the iron ion have not changed, i.e. that after the removal of OH the vacancies thus created are more or less stabilized; hence the lattice does not collapse. This possibility has been discussed by Freund and is verified experimentally for β-FeOOH [7-14]).

In agreement therewith are the X-ray results and the electron micrographs which indicate that new compounds are not formed and the particles have preserved their original size.

There is some disordering in the original lattice as can be concluded from the increase of the magnetic susceptibility. At higher temperatures (250-350 °C)

the dehydration is nearly completed. Depending upon the preparation temperature of the starting material in our series, 20 or 90 °C, the susceptibility decreases considerably above 260 or 300 °C. Electron micrographs reveal that at the same time particle growth occurs leading to the formation of small particles which according to X-ray measurements have the α-Fe_2O_3 structure. Finally between 350 and 450 °C the surface energy is given off as shown by the D.T.A. measurements and rapid sintering occurs leading to well-crystallized α-Fe_2O_3 consisting of crystallites with a size mainly between 300 and 400 Å. The calorimetric and X-ray results of Fricke et al. mentioned in the introduction give a further support for the scheme outlined above.

7.6. Summary

(1) Iron-oxide hydrate looses the greater part of its water, present both as OH and H_2O, between 60 and 200 °C.

(2) Upon dehydration below 200 °C the iron-oxygen lattice is preserved; the particles keep their original size (20-30 Å). Only some disordering occurs leading to an increase of the magnetic susceptibility.

(3) In the temperature region 250-350 °C the dehydration is completed under the formation of α-Fe_2O_3. Simultaneously a slight particle growth occurs; the superparamagnetic character disappears but the particles remain small, < 100 Å. At 400-450 °C rapid sintering occurs under the formation of well-crystallized α-Fe_2O_3 with particles of 300 to 400 Å.

REFERENCES

7-1) A. Simon and Th. Schmidt, Kolloidz. **36**, 65, 1925.
7-2) V. Časlavska, V. Frei and A. Blažek, Coll. Czech. chem. Comm. **27**, 2168, 1962.
7-3) O. Glemser and G. Rieck, Z. anorg. allg. Chem. **297**, 175, 1958.
7-4) R. C. Mackenzie, Nature **164**, 244, 1949.
7-5) E. Wedekind and W. H. Albrecht, Ber. dt. chem. Ges. **60**, 2239, 1927.
7-6) E. Wedekind and W. H. Albrecht, Ber. dt. chem. Ges. **59**, 1726, 1926.
7-7) W. H. Albrecht, Ber. dt. chem. Ges. **62**, 1475, 1929.
7-8) W. H. Albrecht and E. Wedekind, Z. anorg. allg. Chem. **202**, 209, 1931.
7-9) W. Fricke and L. Klenk, Z. Elektr. **41**, 617, 1935.
7-10) R. Fricke and K. Meyring, Z. anorg. allg. Chem. **230**, 357, 1937.
7-11) C. Mazières, Anal. Chem. **36**, 602, 1964.
7-12) F. Freund, Ber. dt. ker. Ges. **42**, 23, 1965.
7-13) R. Fricke and P. Ackermann, Z. Elektr. **40**, 630, 1934.
7-14) J. Dézsi, L. Keszthelyi, D. Kulgawvzuk, B. Molnár and N. A. Eissa, Phys. Stat. sol. **22**, 617, 1967.
7-15) M. J. Ridge and G. R. Boell, Inorg. Phys. Theor. 1147, 1967.
7-16) J. D. Bernal ,D. R. Dasgupta and A. L. Mackay, Clay Minerals Bull. **4**, 15, 1959.
7-17) A. W. Simpson, J. appl. Phys. Suppl. **33**, 1203, 1962.

Acknowledgement

The investigations described in this thesis were carried out at the Philips Research Laboratories. I thank the directors of these laboratories for their permission to publish the results as a thesis.

The work has been accomplished in a close and highly appreciated co-operation with several colleagues. Many of the points investigated originated during stimulating discussions with Drs G. W. van Oosterhout. The analytical work has been done jointly with Mr J. Visser, the radio-tracer work with Mr P. N. Kuin, the Mössbauer spectroscopy with Dr J. S. van Wieringen, the X-ray work with Mr C. Langereis, the infrared spectroscopy with Dr J. Bakker, the N.M.R. experiments with Dr G. E. G. Hardeman and the D.T. and T.G. analysis with Drs P. J. L. Reynen. Thanks are also due to F. Huizinga for experimental assistance and to Mr J. M. Nieuwenhuizen and Mrs J. R. M. Gijsbers-Dekker for the electron micrographs.

Special thanks are due to Dr J. de Jonge for his criticisms of the manuscript.

Mrs A. Meyer-Huisman gave valuable assistance during the proof-reading stages.

Summary

On the neutralization of aqueous solutions of ferric salts a series of reactions takes place, the end product being a gelatinous precipitate. Hydrolysis of the $Fe(H_2O)_6^{3+}$ ions occurs as soon as OH^- ions are brought into the solution. Thereupon, at first no precipitate is formed; when the degree of hydrolysis, defined as the ratio of the number of equivalents of OH^- added to Fe^{3+}, exceeds the value of 2·5, the formation of a gel suddenly starts. There is no consensus of opinion in the literature regarding the nature of the processes that take place in the solution. Whereas in the older literature it is assumed that a continuous series of polynuclear species is formed, it is stated in the more recent literature that only dimers are formed, which in a short pH traject unite, with the formation of a gel.

From our investigations, carried out with solutions of ferric nitrate, it follows that hydrolysis of the ferric ions, even at low degree of hydrolysis, gives rise to the formation of colloidal particles. Upon further addition of OH^- ions when the point of electroneutrality is reached, flocculation occurs of these particles with the formation of a gel. This is derived partly from the fact that the ionic product $[Fe^{3+}][OH^-]^3$ is constant in a large concentration region. For a determination of this ionic product it is necessary to determine $[Fe^{3+}]$. This has been achieved by making use of a titration of the Fe^{3+} ions using EDTA with KCNS as an indicator. Ultracentrifugation experiments, carried out with the aid of tracer techniques, confirm the view that, upon the addition of OH^- ions, small discrete particles are formed instead of a continuous series of polymers. The precipitation processes occurring in solutions of Fe^{3+} ions differ from the precipitation reactions usually observed only in that the size of the particles is extremely small.

In order to isolate the particles from the gel a procedure has been used in which the gel is frozen at temperatures below 250 °K. During the subsequent thawing the gel disintegrates and a very fine powder is obtained, further indicated as iron(III)-oxide hydrate. The way in which the disintegration of the gel occurs has been studied with the aid of Mössbauer spectroscopy. Use has been made of the phenomenon that particles with a very small mass, when absorbing a γ quantum, acquire such a velocity that resonance is no longer possible. If the surroundings have a great rigidity, e.g. after freezing, these take up the impulse. In this way the freezing of the gel can be studied accurately. From these investigations it proved to be probable that during the freezing no essential changes take place within the particle.

The iron(III)-oxide hydrate, prepared in the way as described above, has been investigated with the aid of several methods:

(1) Electron microscopy shows that the particles have a size of 20-30 Å.

(2) Measurements of the magnetic susceptibility reveal that the material is super-

paramagnetic. From these measurements it can be concluded that the particles contain about 1000 iron ions, in good agreement with the electron-microscopic evidence.

(3) Crystallographic investigations using MoKα radiation demonstrate that the particles are crystalline, contrary to the prevailing assumption that the material should be amorphous. The crystallographic structure is different from that of the well-known iron oxides and oxide hydroxides.

These results which show that the particles may be considered as crystallites greatly support the mechanism of the hydrolysis outlined before. Due to the small size of the particles and consequently the considerable line broadening, it has not been possible to elucidate the crystallographic structure.

The preparation of larger crystals by recrystallization in solutions did not succeed; instead of growth of the crystallites originally present, recrystallization takes place with the formation of α-Fe_2O_3 or α-FeOOH. This recrystallization has been studied with the aid of magnetic measurements; a series of intermediate products is formed which have a high magnetic susceptibility. This can be explained on the basis of the superparamagnetic character of the particles: on increase of the particle size the moment per particle first increases, goes through a maximum value and decreases again due to a coupling of the magnetic vector with a preferred crystallographic direction ("blocking"). The chemical composition of the oxide hydrate is not constant. After having been dried on P_2O_5 the material contains about 15% H_2O. This corresponds to the formula $Fe_2O_3.1{\cdot}6\ H_2O$. Infrared spectroscopy has demonstrated that about half of the water is present as H_2O. This water is adsorbed on the particle surface as it can be removed at room temperature with dry nitrogen gas. The other half of the water is bonded in a different manner, probably in the form of OH, as the typical H_2O band at 1630 cm^{-1} is not observed in the spectrum. Investigations with nuclear-magnetic-resonance spectroscopy show that at least 50% of the water is bonded in a manner such as to give rise to a line broadening of about 1 Oe. This points to OH groups. In combination with the infrared investigations it seems most probable therefore that the material with composition $Fe_2O_3.1{\cdot}6H_2O$ may be indicated formally by $FeOOH.0{\cdot}3H_2O$, more generally $FeOOH.nH_2O$. Hence we are dealing with an oxide hydroxide with H_2O adsorbed on the surface of the particles.

On thermal dehydration up to 200 °C, nearly all the water is expelled, the composition then still being about $Fe_2O_3.0{\cdot}2H_2O$. Electron microscopy together with X-ray diffractometry confirm that, under these circumstances, neither particle growth nor recrystallization (for instance to α-Fe_2O_3) take place. The magnetic susceptibility increases, indicating an enhanced disorder. Mössbauer spectroscopy suggests that the coordination shell of the iron ion does not change. Apparently on the release of the OH groups the structure of the particle largely remains unchanged.

Upon heating to temperatures above 300 °C, recrystallization occurs with the formation of α-Fe_2O_3. The magnetic susceptibility decreases considerably due to the formation of comparatively large α-Fe_2O_3 crystals.

Samenvatting

Bij neutralisatie van waterige oplossingen van ferrizouten vindt een reeks reacties plaats met als eindproduct een gelatineus neerslag. Hydrolyse van het $Fe(H_2O)_6^{3+}$ ion treedt op zodra OH^- ionen in de oplossing gebracht worden. Daarbij wordt aanvankelijk geen neerslag gevormd; eerst wanneer de hydrolysegraad, uitgedrukt in de verhouding van het aantal toegevoegde equivalenten OH^- tot Fe^{3+}, de waarde 2·5 overschrijdt, zet plotseling de vorming van het gel in. Over de aard van de processen die zich in de oplossing afspelen bestaat geen overeenstemming. Terwijl in de oudere literatuur de vorming van een continue reeks polynucleaire producten aangenomen wordt, volgt uit meer recente onderzoekingen dat hoogstens dimeren worden gevormd waaruit dan in een kort pH traject het gel ontstaat.

Uit onze onderzoekingen uitgevoerd met oplossingen van ferrinitraat blijkt dat hydrolyse van het ferri ion reeds bij geringe hydrolysegraad leidt tot de vorming van colloidale deeltjes, die als bij verder toevoegen van OH^-ionen het ladingsnulpunt wordt bereikt aanleiding geven tot een gelatineus neerslag. Dit volgt o.a. uit het feit dat het ionenproduct $[Fe^{3+}]\,[OH^-]^3$ constant is over een zeer groot concentratietraject. Voor de bepaling hiervan is het noodzakelijk $[Fe^{3+}]$ te kennen. Daartoe is gebruik gemaakt van een titratie met behulp van EDTA met KCNS als indicator. Ultracentrifuge-experimenten, welke zijn uitgevoerd met behulp van tracer-technieken bevestigen de opvatting dat toevoegen van OH^- ionen leidt tot de vorming van discrete kleine deeltjes en niet tot een continue serie van polymeren. De hydrolyse van Fe^{3+} ionen verschilt dus slechts daarin van gewone precipitatiereacties dat de gevormde deeltjes uitzonderlijk klein zijn.

Om de deeltjes welke de bouwstenen van het gel vormen er uit te isoleren is een werkwijze toegepast waarbij het gel wordt bevroren tot temperaturen beneden 250 °K. Tijdens het daarop volgende ontdooien desintegreert het gel en wordt een zeer fijn poeder verkregen aangeduid met de term ijzeroxydehydraat. De wijze waarop de desintegratie van het gel plaats vindt is bestudeerd met behulp van Mössbauer-spectroscopie, waarbij gebruik gemaakt is van het verschijnsel dat, bij uitstraling van een γ-quantum (afkomstig van een energieovergang in de kern) aan deeltjes met een zeer kleine massa een zodanige snelheid wordt medegedeeld dat resonantie onmogelijk wordt. Bij grote stijfheid van de omgeving, zoals na bevriezen, is deze in staat om de impuls op te vangen; aldus kan het bevriezen van het gel nauwkeurig bestudeerd worden. Uit deze onderzoekingen is gebleken dat zeer waarschijnlijk geen essentiele veranderingen in het deeltje plaats vinden.

Het ijzer(III)-oxide-hydraat, met behulp van bovengenoemde werkwijze verkregen, is onderzocht met behulp van verschillende onderzoekmethodes:

(1) Electronenmicroscopie toont dat de deeltjes afmetingen hebben van 20 à 30 Å.
(2) Uit metingen van de magnetische susceptibiliteit van het zich superparamagnetisch gedragende materiaal kan worden afgeleid dat de deeltjes zijn opgebouwd uit circa 1000 Fe^{3+} ionen, in overeenstemming met de electronenmicroscopische gegevens.
(3) Kristallografisch onderzoek met behulp van MoKα-straling toont aan dat de deeltjes kristallijn zijn, in tegenstelling met de heersende opvatting dat het materiaal amorf zou zijn. De kristalstructuur verschilt van die van de bekende ijzeroxyden en oxyden-hydroxyden.

Het feit dat de deeltjes mogen worden opgevat als kristallieten is een krachtige ondersteuning voor het boven omschreven beeld van de hydrolyse. Als gevolg van de geringe afmetingen der deeltjes en de hiermede gepaard gaande zeer sterke lijnverbreding is het niet mogelijk gebleken de kristalstructuur te bepalen.

De bereiding van grotere kristallen door rekristallisatie in oplossing is niet gelukt; in plaats van groei der oorspronkelijk aanwezige kristallen vindt een omkristallisatie plaats tot α-Fe_2O_3 of α-FeOOH. Deze rekristallisatie is met behulp van magnetische metingen te volgen; er wordt een serie tussenproducten gevormd die een zeer hoge magnetische susceptibiliteit hebben. Deze kan worden verklaard uit het superparamagnetisch karakter der deeltjes: bij toenemende deeltjesgrootte neemt het moment per deeltje eerst toe, gaat door een maximum en neemt daarna weer af tengevolge van koppeling van de magnetische vector aan een kristallografische voorkeursrichting. De chemische samenstelling van het oxide-hydraat is niet constant. Het materiaal bevat na drogen boven P_2O_5 meestal ongeveer 15% water. Dit komt overeen met de samenstelling $Fe_2O_3 . 1{\cdot}6H_2O$. Uit onderzoekingen met behulp van infrarood-spectroscopie is gebleken dat ongeveer de helft van het gebonden water in de vorm van H_2O aanwezig is. Vermoedelijk is dit aan het oppervlak geadsorbeerd daar het door middel van droge stikstof bij kamertemperatuur is te verwijderen. De andere helft van het aanwezige water is op een andere manier gebonden, vermoedelijk in de vorm van OH, daar de typische H_2O band bij 1630 cm^{-1} ontbreekt in het spectrum. Onderzoek met behulp van kernspinresonantie toont aan dat ten minste 50% van het water op een manier gebonden is welke aanleiding geeft tot lijnverbredingen van circa 1 Oe, hetgeen wijst op hydroxylgroepen. In combinatie met de infraroodonderzoekingen lijkt het daarom het meest voor de hand liggend het materiaal met de samenstelling $Fe_2O_3 . 1{\cdot}6H_2O$ aan te duiden als $FeOOH . 0{\cdot}3H_2O$: in het algemeen dus als $FeOOH . nH_2O$. Het betreft hier dus een oxide-hydroxide met het H_2O geadsorbeerd aan het oppervlak der deeltjes.

Bij thermische dehydratie tot 200 °C wordt bijna al het gebonden water afgegeven, de samenstelling is dan nog ongeveer $Fe_2O_3 . 0{\cdot}2H_2O$. Hierbij treedt nog geen deeltjesgroei of rekristallisatie op (b.v. tot α-Fe_2O_3), zoals is vastgesteld

met behulp van electronenmicroscopie en röntgenopnamen. Er is een toename van de magnetische susceptibiliteit hetgeen wijst op een toegenomen wanorde. Uit het gelijk blijven van het Mössbauer-spectrum volgt dat de omgeving van het ijzer-ion niet merkbaar verandert. Blijkbaar blijft de structuur van het deeltje bij uittreden van OH groepen grotendeels behouden.

Bij verhitten tot boven 300 °C treedt rekristallisatie op tot α-Fe_2O_3. De magnetische susceptibiliteit neemt hierbij sterk af als gevolg van de vorming van relatief grote α-Fe_2O_3 kristallen.

STELLINGEN

A. A. van der GIESSEN

STELLINGEN

I

Het „angle of incidence" effect dat soms is waargenomen bij het opdampen van metaallagen op substraten in de beginstadia van de filmgroei, moet worden toegeschreven aan de impuls van de invallende atomen en niet aan een schaduweffect van reeds aanwezige kiemen.

D. O. Smith, M. S. Cohen en P. G. Weiss, J. appl. Phys. **31**, 1755, 1960.

V. Kambersky, S. Malek, Z. Frait en M. Ondris, Czech. J. Phys. **11**, 171, 1961.

J. G. W. van de Waterbeemd en G. W. van Oosterhout, Philips Res. Repts **22**, 375, 1967.

II

De bewering van Spiro c.s., dat in waterige oplossingen van ferrinitraat bij hydrolyse bolvormigedeeltjes worden gevormd met een diameter van 70 Å, wordt niet bevestigd door hun experimenten.

G. Spiro, S. E. Allerton, J. Renner, A. Terzis, R. Bils en P. Saltman, J. Am. chem. Soc. **88**, 2721, (1966).

III

Voor de analyse van kleine hoeveelheden koolstof in anorganische materialen verdient de conductometrische of titrimetrische methode de voorkeur boven de in enkele vooraanstaande normbladen voorgeschreven gravimetrische bepalingswijze.

A.S.T.M. Book 1966, part 32, pag. 12.
B.S. 1121, part 11, 1967.
N.E.N. 1033-1, 1966.
J. J. Engelsman, A. Meyer en J. Visser, Talanta **13**, 409, 1966.

IV

De door Indira en Doss gegeven verklaring van de wigvorming die optreedt bij het aanleggen van een spanning aan een kwik-water grensvlak is juist, maar wordt niet gesteund door hun experimenten.

K. S. Indira en K. S. G. Doss, Elektrochimica Acta **12**, 741, 1967.

V

Het is waarschijnlijk dat bij het glanzend galvanisch neerslaan van metalen op substraten de vorming van metaal oxy-hydroxyden een essentiële rol speelt.

VI

De bewering van Criscuoli en Turelli dat de reversibele veranderingen van de coercitiefkracht, bij cyclische warmtebehandelingen, van de legering met samenstelling $Fe_{0.50}Al_{0.24}Ni_{0.23}Cu_{0.03}$ moeten worden toegeschreven aan ordewanorde verschijnselen wordt niet bevestigd door hun experimenten.

R. Criscuoli en M. Turelli, Z.f. angew. Physik **23**, 219, 1967.

VII

De magnetische eigenschappen van de door Johnston, Heikes en Petrolo bereide zeer fijn verdeelde ijzerpoeders zijn vermoedelijk beter dan door deze onderzoekers in hun publicatie vermeld.

W. D. Johnston, R. R. Heikes en J. Petrolo, J. Am. chem. Soc. **79**, 5390, 1957.

VIII

De pyrophoriciteit van metaalpoeders wordt, behalve door de deeltjesgrootte en de reactiewarmte bij oxydatie, mede bepaald door de diffusiesnelheid van het metaalion in de op de deeltjes gevormde oxydhuid.

W. Feitknecht en A. Durtschi, Helv. chim. Acta **47**, 176, 1963.

IX

De verklaring van Kuhn c.s. betreffende de irreversibiliteit van het gedrag van gelen bij bevriezen en smelten is aanvechtbaar.

W. Kuhn, R. Bloch en P. Läuger, Kolloid Z. **193**, 1, 1963.

X

In de discussie van Piggot over het effect van de golflengte op diffractiediagrammen van kleine kristallieten is ten onrechte het facet van de signaal-ruis verhouding buiten beschouwing gelaten.

M. R. Piggot, J. appl. Phys. **37**, 2927, 1966.

XI

De door de overheid gesubsidieerde consumentenvoorlichting moet tot bredere lagen van de bevolking worden gericht dan thans het geval is.

A. A. van der Giessen 28 mei 1968